The effect of mutations in the envelope protein of Zika virus on cellular tropism.

PhD Candidate: Fernando Ruiz Jiménez

School of Life Sciences

W/A1316, Virus Research Group, Queen's Medical Centre, University of Nottingham, UK

Supervisors: Professor Jonathan Ball & Dr Patrick McClure

Thesis submitted to the University of Nottingham as a fulfilment of a Doctor of Philosophy (PhD)

Student Declaration:

I declare that the data presented is entirely my work, except where otherwise stated.

Table of Contents

Tables

Figures

Abbreviations

50% Tissue Culture Infectious Dose	(TCID50)
Amino Acids	(AA)
Annealing Temperature	(Ta)
Azithromycin	(AZ)
Baby Hamster Kidney	(BHK-21)
Bicinchoninic Acid	(BCA)
Biosafety Level	(BSL)
Blood-Brain Barrier	(BBB)
Bovine Growth Hormone	(BGH)
Capsid	(C)
Central Nervous System	(CNS)
Cerebrospinal Fluid	(CSF)
Chikungunya Virus	(CHIKV)
Circular Polymerase Extension Reaction	(CPER)
complementary DNA	(cDNA)
Congenital Zika Syndrome	(CZS)
Coronavirus Spike Protein	(S)
Cryo-Electron Microscopy	(Cryo-EM)
Cytomegalovirus	(CMV)
Cytoplasmatic Tail	(CT)
Cytoplasmic domain	(CY)
Dengue Virus	(DENV)
Deoxyribonucleic Acid	(DNA)
Dipeptidyl Peptidase IV	(DPP4)
Dulbecco's Modified Eagle Medium	(DMEM)
Ebola Virus	(EBOV)
Endoplasmic Reticulum	(ER)
Envelope	(Env) or (E)
Equilibration Buffer	(EQU)
Escherichia coli	(E. coli)
Escherichia coli promoters	(ECP)
Fetal Bovine Serum	(FBS)
Glycoprotein	(GP)
Green Fluorescence Protein	(GFP)
Guillain-Barre Syndrome	(GBS)
Heat-Shock Cognate Protein 70	(HSC70)
Heat-shock protein 70	(HSP70)

Hepatitis A virus Cellular Receptor 1	(HAVCR-1)
Hepatitis Delta virus ribozyme	(HDVR)
HIV Capsid protein	(CA)
HIV Matrix protein	(MA)
Horseradish Peroxidase	(HRP)
Human Bone Marrow Endothelial Cells	(HBMEC)
human cytomegalovirus	(hCMV)
Human Embryonic Kidney 293	(HEK293T)
Human Immunodeficiency Virus	(HIV)
Hygromycin Phosphotransferase Gene	(Hygr)
Immunofluorescence	(IF)
Infectious genome amplicons	(ISA)
Interferon	(IFN)
Interferon gamma	(IFN-γ)
Interferon-Inducible Transmembrane Protein	(IFITM)
interleukin 2	(IL-2)
Japanese Encephalitis Virus	(JEV)
Kinase, Ligase and DpnI	(KLD)
Leibovitz's-15	(L-15)
Lentiviral Vectors	(LV)
Lipid Nanoparticles	(LNPs)
long terminal repeat	(LTR)
Low-Density Lipoprotein Receptor	(LDLR)
Lysis Buffer	(LYS)
Mayor Histocompatibility Complex class 1	(MHC-I)
Membrane	(M)
Messenger Ribonucleic Acid	(mRNA)
Middle East Respiratory Syndrome Coronavirus	(MERS-CoV)
Modified Terrific broth	(TB)
Moloney Murine Leukemia Virus	(MoMLV)
Monoclonal antibody	(mAb)
Monocyte-Derived Macrophages	(MDM)
Murine Leukaemia Virus	(MLV)
Naphthol blue-black	(NBB)
Natural Killer	(NK)
Non-Essential Amino Acid	(NEAA)
Non-Structural Protein	(NS)
Nucleocapsid	(NC)
Open Reading Frame	(ORF)
Pattern Recognition Receptor	(PRR)

Peripheral Blood Mononuclear Cells	(PBMC)
Peripheral Nervous System	(PNS)
Phosphate Buffered Saline	(PBS)
Polyethyleneimine	(PEI)
Polymerase Chain Reaction	(PCR)
Polyvinylidene Difluoride	(PVDF)
Precursor of the Membrane	(PrM)
Pseudotypes	(PPs)
Radial Glial Progenitor	(RGP)
Real-Time Polymerase Chain Reaction	(RT-PCR)
Receptor Binding Domain	(RBD)
Resuspension Buffer	(RES)
Reticulum Retention	(ERR)
Rev response elements	(RRE)
Ribonucleic Acid	(RNA)
Rough Endoplasmic Reticulum	(RER)
SARS coronavirus	(SARS-CoV)
Severe acute respiratory syndrome	(SARS)
Signal Transducer and Activator of Transcription 1	(STAT 1)
Signal Transducer and Activator of Transcription 2	(STAT 2)
Simian Immunodeficiency Virus	(SIV)
Simian Vacuolating Virus 40	(SV40)
Site Directed Mutagenesis	(SDM)
Spike	(S)
Spondweni virus	(SPOV)
Subviral Particles	(SVPs)
Super Optimal broth with Catabolite repression	(SOC)
T helper 1	(Th1)
Tick-Borne Encephalitis	(TBE)
Toll-like receptor 3	(TLR3)
Trans Golgi Network	(TGN)
Trans Membranal Domains	(TMDs)
Transporters associated with antigen processing	(TAP)
Tryptose Phosphate Broth	(TPB)
Tumoral Necrosis Factor α	(TNF- α)
Untranslated Region	(UTR)
Vesicular stomatitis virus	(VSV)
Vesicular Stomatitis Virus Glycoprotein	(VSV-G)
West Nile Virus	(WNV)
Western Blot	(WB)

Wild Type	(WT)
Yellow Fever Virus	(YFV)
Zaire strain of EBOV	(EBOVZ)
Zika Virus	(ZIKV)

Abstract:

Zika virus infection arose as a public health issue during late 2015 and 2016 on the American continent. ZIKV epidemic was especially interesting since the previous report of patients infected by the virus only showed mild symptoms including fever, rash, and joint pain, however, the appearance of neurological symptoms including Guillain Barre syndrome in adults and microcephaly on new-borns and other clinical features that were grouped into Zika congenital syndrome. This change on the outcome of the infections resulted in many questions, what changed on the virus that favoured neuroinvasion? are these changes linked to mutations that suffered the virus? The envelope protein of the virus was the best candidate to try to explain the infection of neural cells and the later development of the reported syndromes since this is the first protein that interacts with the hosts' cells and changes in the amino acid sequence can lead to new interactions between the virus and the host.

In this study, experiments were designed to try to answer these questions, including identifying mutations on the envelope protein that had a direct impact on the cellular tropism. As a way to dissect the entry process and the interaction between the cells and the mutations on the glycoprotein, a pseudotype model was used. Different strategies were used to try to produce pseudotypes that incorporate the Zika protein including adjusting the amounts of backbone and heterologous glycoprotein, use different cell lines, and supplementing other viral proteins that could enhance particle production.

Other approaches were tested, including the generation of plasmids that contain the viral genome, viral production and harvest and the amplification of viral fragments to produce infectious viruses from PCR products. Altogether these experiments showed that the flaviviruses pose a challenge to the development of pseudo particles and other methodologies due to its replication cycle and the singularities of this viral family.

Acknowledgments. -

First and foremost, I would like to express my immense gratitude to Dr Jonathan Ball for his supervision, continual support, for his critical approach, and for pushing me to reach a higher level when it comes to thinking outside the box. I would also like to thank Dr Richard Urbanowicz, Dr Patrick McClure, Dr Barnabas King, Professor Will Irving and Alex Tarr for their guidance.

I am incredibly grateful to Chidinma Raymond for her continuous support, motivation, and her friendship and to Jayseree Day and Arwa Bagasi for their company, friendship and help over the project. Thanks are also well deserved for, Theocharis Tsoleridis, Christopher Mason, Joe Campbell, Jonathan Ball, Janet Daily and all members of the University of Nottingham Virus Research Group.

I would like to specifically thank Dr Barnabas King Dr Richard Urbanowicz, Dr Patrick McClure for the help during the generation of data and introduction to the methodologies.

I want to express my gratitude to Dr Andres Merits and Dr Jordan Clark for providing essential reagents, including the plasmids containing the Zika virus genome and the Hepatitis delta ribozyme. I would also like to thank Dr Jose Humberto Perez Olais for his friendship, support, experienced advice, and the help given to perform Immunofluorescences, Dr Bibiana Chavez Munguia for her service on the electron microscopy section and Dr Rosa Maria del Angel for her help and for welcoming me on her lab for me when I needed.

This study would not have been possible without the funding received from the national council of science and technology (CONACYT) scholarship number 438310 and the University of Nottingham life sciences school.

Lastly, I would like to express my eternal gratitude to grandparents, sister and family, without whom I wouldn't have gotten to where I am today and my friends Alan, Monica, Nicole, Fatima, Yareli, Salvador, Cecilia and Diego for their endless support.

1. Introduction:

1.1. ZIKV overview:

Zika virus (ZIKV) is a member of the *Flavivirus* genus of the *Flaviviridae* family. *Flaviviruses* are enveloped viruses with a single strand of positive-sense RNA with a size of ~10.8 kb. The genome is associated with the Capsid (C); this protein is surrounded by a lipid membrane associated with the Envelope (E) protein and the Membrane (M) protein in the mature viruses. The genome contains an ~100 nt 5′ untranslated region (UTR), a single open reading frame of ~10 kb, and an ~420 nt 3′ UTR. The only open reading frame (ORF) codifies for a single polyprotein that is cleaved by cellular or viral proteases to produce three structural proteins C, Precursor of the Membrane (PrM), E and seven non-structural (NS1, NS2A, NS2B, NS3, NS4A, NS4B, NS5) [1][2].

1.1.2. ZIKV expansion and epidemiology:

ZIKV has emerged as a new infection across the American continent, and it is slowly spreading across the globe. *Aedes Aegypti* is the primary vector of this virus but also can spread other flaviviruses such as Yellow Fever (YF), Dengue (DENV), Chikungunya (CHIKV) and West Nile (WNV). Other species of *Aedes* that are capable of efficiently spreading the virus are Aedes *albopictus, Aedes. hensilli* (Yap Islands)*, Aedes polyniensis* (French Polynesia) [3].

ZIKV was isolated in 1947 for the first time in the Zika forest near Entebbe, Uganda, from the serum of a sentinel macaque (strain known as MR766) [1]. The virus was recognized as a human disease-causing pathogen when three people fell ill in Nigeria [4]. After the discovery, ZIKV infections were occasionally reported across Africa, Malaysia, and Indonesia. [5] During 2007, there was an outbreak in the Yap Islands followed by a more significant outbreak in French Polynesia and the Easter Island during 2013-2014. The outbreak in French Polynesia had a pivotal role in the passage of the virus to the Americas because the seroprevalence of the ZIKV within the island increased dramatically from October of 2013 to December of 2014. Before the outbreak of October, the

seroprevalence for ZIKV was of 0.8% by the second half of the outbreak, it was 50%, and by the end, it was 66% [6]. The epidemic then spread to the Easter Island and the Cook Islands reaching the American continent in 2015.[3] Phylogenetic analyses suggest that the virus emerged in Uganda 1920 most probably between 1892 and 1943 with two independent ZIKV introductions into West Africa from the Eastern portion of the continent. The first introduction in Cote d'Ivoire and Senegal was related to the MR766 strain which continued its movement until it reached Sokal-Sobara in 1995. The second introduction was linked to a Nigerian cluster when the virus moved from Uganda to the Central African Republic and Nigeria in 1935. The analysis also suggests that the lineage of ZIKV that was introduced into Micronesia around 1960 was from Uganda that gave rise to the Asian Lineage [7]. However, there is still the possibility that the virus originated in a different geographical location since there were reports from patients with neutralizing antibodies against ZIKV on other places such as India, Philippines, Malaysia and Borneo, on the period between 1953-1958. geographical origin of ZIKV is still debatable, and samples from that locations and temporality are needed to create a more precise picture of the natural history [8][9][10][11]

The sequence analysis from different outbreaks across time has shown three major lineages: East African, West African, and Asian. The Asian lineage includes the strains from the older outbreaks (Malasya 1966) and contemporary Asia, Oceania, and America outbreaks. Even with all this lineages and strains, there is only one serotype in contrast with another related flavivirus such as DENV that has four serotypes [2].
Currently, there are 92 countries with either active transmission or that had the transmission in the past including South, Central, and North America, for example, Mexico, Micronesia, Palau, Brazil, Colombia, Ecuador, French Guiana, Guyana, Paraguay, Peru, Venezuela [12].

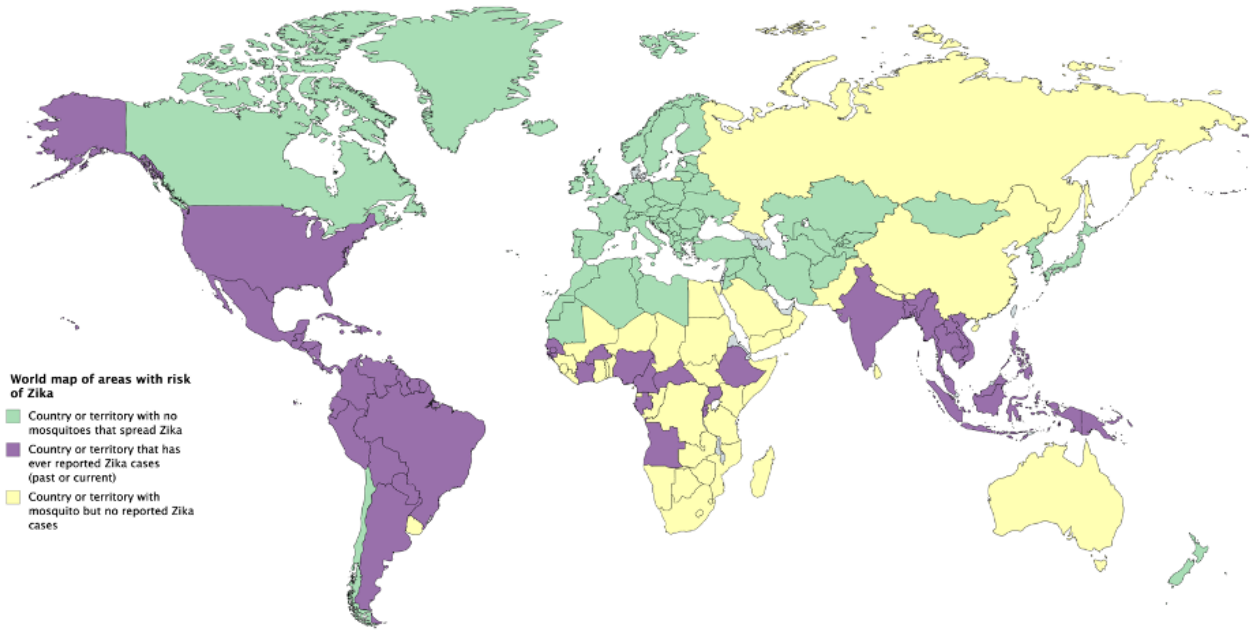

Figure 1.1 Countries with the presence of the vector and with a risk of ZIKV infection. The map depicts with colour coding the different circumstances that countries face during ZIKV epidemic. Purple territories have reported cases ZIKV infections either past or present. Yellow countries have the presence of the mosquito vector, but no reported infections. Finally, green countries had no presence of the vector (Figure modified from CDC 2020) [12][13].

1.2. ZIKV life cycle.

Much of the ZIKV is based upon presumed similarity to the related *Flavivirus* such as DENV, YF, and WNV. To infect a host cell the virus needs to attach to the cellular surface and be internalized to the cytoplasm with the help of specific proteins located on the outer face of the plasmatic membrane, this process is known as receptor-mediated endocytosis. Zika virus as part of the arbovirus category follows the path of other pathogens like DENV that infect the endothelial cells to gain access to the extravascular space and establish an infection in tissues and organs far from the inoculation spot. The

cellular receptors that are proposed as major contributors are the receptor tyrosine kinase bio which is part of the TAM family (AXL, TYRO 3, Mertk), the c-type lectin DC-SIGN (CD-209), TYRO3 and in a lesser extent TIM-1, it is worth noting that other cell receptors may confer different tropism to the virus [14][15][16]. However, although AXL has been proposed as one of the most important receptors, the deletion of this receptor does not protect brain organoids against the infection suggesting that the elimination of this protein is not sufficient to stop the infection, on the other hand, the overexpression of TYRO 3 render non-permissive cells the capability of being infected [17].

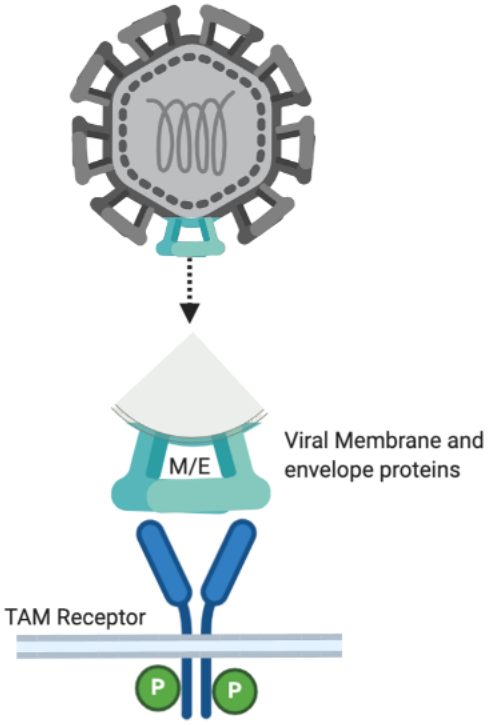

Figure 1.2. Interaction between the virus and the cellular receptor. Viral envelope protein interacts with the cellular receptor from the TAM family (AXL, TYRO 3, Mertk), allowing the internalization and the sub sequential release of the genetic material.

Once the virus is internalized, the endosome starts to mature, and the environment turns acidic, causing conformational changes in the E protein that expose the fusion domain. The membrane of the endosome and the viral membrane fuse and the genetic material and capsid protein is released into the cytoplasm [14].

As with other viruses from the same family, the ZIKV genome can be directly translated to proteins as if it was a cellular mRNA once it is uncoated from the capsid.
The genome produces a single polyprotein with 3000 residues that is cleaved by cellular proteases and by the viral (NS2B-NS3) protease. The polyprotein is processed co- and post-translationally, the resulting proteins contain signal peptides or transmembrane domains that direct their location in the membrane of the endoplasmic reticulum (ER). Once the viral proteins are processed, the structural proteins C, prM, and E that constitute the virion and the non-structural proteins NS1, NS2A, NS2B, NS3, NS4A, NS5 which participate in the RNA synthesis and modify the cellular environment to produce the new viral progeny (Figure 1.3).

Figure 1.3. Genomic organization of ZIKV. The positive-sense RNA with a size of ~10.8 kb produces a single polyprotein flanked by to UTRs. The structural genes C, PrM, E and the seven non-structural NS1, NS2A, NS2B, NS3, NS4A, NS5 are processed by cellular and viral proteases.

Replication starts when the viral RNA-dependent RNA polymerase (NS5) produces a negative-strand RNA intermediate using the positive strand viral genome [18]. The NS3 protein also participates in this process with its helicase activity while other viral proteins maintain the right environment for the replication favouring membranal structures known as replication complexes. In this complex, there is an increased concentration of the non-structural proteins; this characteristic is shared with other viruses such as DENV. The structural protein C is positively charged and can bind to the newly synthesized genome forming the nucleocapsid. This complex is then covered with a lipidic bilayer membrane derived from the host cell; this membrane contains the viral prM/M and E glycoproteins which are anchored to the membrane via hydrophobic trans membranal domains (TMDs). [19] The E protein is the receptor-binding molecule mediates the fusion between the virus

and the target cell. PrM proteins work as a molecular chaperone that inhibits the premature fusion of E protein. prM is cleaved by the Trans Golgi Network (TGN)-resident protease furin during transit across this membranous complex. The acidic changes of the TGN cause conformational changes of the membrane proteins and allow the action of the furin in the PrM protein; this cleavage produces the mature M protein and the Pr peptide. Finally, the virus (mature if it only contains M protein and immature if it contains PrM) is released to the extracellular space using the secretory pathway. [20] It is crucial to notice that during the viral assembly a different kind of particles are produced, subviral particles (SVPs) are generated due to the interaction between PrM, E and the lipidic bilayer of the ER. The SVP particles do not contain the nucleocapsid. Thus, they are not infective; this strategy may help to trick the immune system [21] [2].

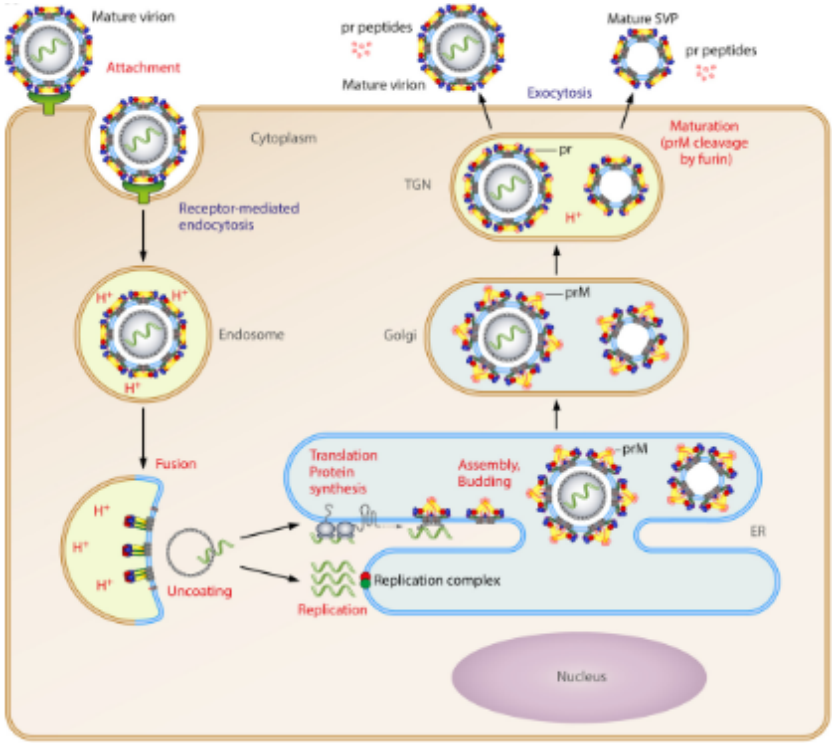

Figure 1.4. *Flavivirus* life cycle. The cycle starts when the virus attaches to the cell surface when it enters in contact with a receptor or receptors, triggering internalization of the particle by receptor-mediated endocytosis. The acidification of the endosome exposes the fusion domain of the E protein which fuses the endosomal and viral membranes

releasing the genome into the cytoplasm, the genetic material is translated, and the replication of the genome starts with the help of the non-structural proteins. The NS proteins reshape the membrane of the ER into the replication complex, also in the ER, the structural proteins assemble and form the viral progeny, which transit to the TGN where the terminal maturation steps take place before their release from the cell (Figure from Heinz, F. X., & Stiasny, K. (2017) [2].

1.2.1. ZIKV envelope and membrane proteins.

The E and M proteins are found on the viral surface, E glycoprotein is the major component in this location and is the primary target of neutralizing antibodies. This protein shares the general structure of the Arboviruses (Arthropod-borne viruses) with three different domains (D): DI, DIII, and DIII. The DI domain is located at the centre of the monomer and has a β-barrel structure; the DII contains the fusion loop composed of a hydrophobic glycine-rich structure. Finally, the DIII is the most variable region and has been implicated in the initial interaction with the cellular receptor. Typically, flaviviruses have two glycosylation sites, N153/154 of the DI, is highly conserved among the family while the DII site is DENV characteristic and so far, absent in ZIKV. isolates.[13] The amino acidic divergence in the E protein between strains oscillate between ~6% between lineages and ~2% within the lineages this means that it has a low level of variation.[2]
The sequence comparison of the E protein of ZIKV against other flaviviruses shown that they shared homology levels between 40 % and 58 %, meaning that they share some regions like the fusion binding domain. Between neurovirulent viruses such as (WNV), Japanese encephalitis virus (JEV), tick-borne encephalitis (TBE) and febrile-illness-causing viruses like (YFV) and DENV) there are distinct traits that allow them to infect specific targets, for example, deletions, insertions, and mutations of the E protein. However, their contribution to the resulting pathology is still elusive for example: when the cryo-electron microscopy (Cryo-EM) structure of ZIKV was super positioned onto the DENV2 Cryo-EM structure and the crystal structure of JEV and WNV E proteins this analysis showed structural similarities. ZIKV shared similarities with DENV at the hi-loop of DII, where both have an insertion of three residues compared with JEV, TBEV, and

WNV. Nevertheless, ZIKV was more like JEV and WNV in other areas, for example, ZIKV, JEV, and WNV share a mutation Asn67Asp compared to DENV indicating an absence of the glycosylation site. ZIKV E protein has only one Asn 154 glycosylation site in contrast with DENV that has two sites (Asn67 and Asn153). The Asn154 seems to play a role in the neurovirulence of WNV. However, this site is shared by DENV, but with an entirely different outcome, future studies are needed to determine if there is an association between this glycosylation site and the virulence of Zika [22].

DENV infection rarely results in neurovirulence; these symptoms appear in a small set of patients and seems to be related to the particular response of the host. Another difference between DENV and ZIKV is the insertion of a residue in the DIII of ZIKV compared with DENV; this addition may increase the overall stability of the virus allowing it to withstand the conditions of different biological fluids such urine, saliva, and semen where the virus has been isolated [23][24].

Table 1.1. Comparison between the cellular receptor between different flaviviruses. The table shows the receptors that use various members of the *Flavivirus* genus, the viruses listed are causal agents of febrile of neurological diseases, and some of them share common receptors. It's worth noting that proteins like Hepatitis A virus cellular receptor 1 (HAVCR-1) are used by different viruses no matter if the outcome is febrile or neurological. Viruses like DENV are promiscuous using a huge variety of receptors to enter the cells while other viruses are more restricted in the proteins that they use. Zika virus shares receptors with other flaviviruses but also seems to have specific receptors that may confer its capability to cause serious repercussions such as microcephaly.

In mosquito cells, DENV has been shown to interact with heat-shock protein 70 (HSP70), R80, R67 and a 45-kDa protein Heat shock cognate protein 70(HSC70) as a penetration receptor may mediate JEV entry into the C6/36 cells [15] [18] [25].

*More evidence is needed to confirm this protein as cellular receptors for the virus.

Receptor	High affinity laminin receptor	HSP 70	HSP 90	GRP 78	DC-SIGN	CD14	AXL	TYRO-3	DC-SIGN-R	HAVCR1 (TIM 1)	Mannose receptor	37/64 kDa high affinity laminin receptor	Prohibitin	Claudin
Virus														
DENV	X	X	X	X	X				X	X	X	X		
JEV	X	X	X	X	X	X						X	X	X*
YFV										X				
WNV	X				X				X	X	X	X*		
ZIKV					X*		X	X		X	X*	X*		X*

1.2.2. ZIKV targets and susceptibility.

During its life cycle Zika is capable of infect different cells from a variety of systems such as fibroblasts, keratinocytes, and immature dendritic cells and cells present in the placenta and the chorionic villi like placental macrophages (called Hofbauer cells); trophoblasts; umbilical cord mesenchymal stem cell and endothelial cells all these cells act as a pathway that leads to the vertical transmission of the virus. It is worth noting that the infection to the vascular endothelial cells has implications in the invasion of the virus to the mature central nervous system (CNS) by crossing the Blood-Brain Barrier (BBB). Finally, ZIKV can also infect the male reproductive system cells preferentially: spermatogonia, primary spermatocytes and Sertoli cells which lead to the destruction of the seminiferous tubules and cell death [19] [26].

In the following table are listed the cells lines that have been tested for susceptibility to the ZIKV infection.

Table 1.2. Susceptibility of common cell lines to ZIKV infection. -The table shows different cell lines and their permissibility to the viral infection, in the first column susceptible human cell lines are listed, in the second column list, the non-human cell lines that are capable of sustaining the infection in the final column are listed the cells that are not permissive to the ZIKV infection [27].

Human Cell lines that are Highly susceptible to ZIKV infection.	**Non-Human Cell lines that are Highly susceptible to ZIKV infection.**	**Cell lines that are not permissive to ZIKV infection**
1. JEG-3 (Placenta choriocarcinoma) 2. HEK (Human fetal kidney) 3. HeLa (Cervical adenocarcinoma) 4. HOSE6-3 (0varian surface epithelium) 5. LNCaP (Metastatic prostatic adenocarcinoma) 6. 833KE (Testicular germ cell tumor) 7. SF268 (Anaplastic astrocytoma) 8. RD (Rhabdomyosarcoma) 9. ARPE19 (Retinal pigment epithelium) 10. Hep2 (Laryngeal epidermoid carcinoma) 11. Calu-3 (lung adenocarcinoma) 12. HFL (embryonic lung fibroblasts) 13. Caco-2 (Colorectal carcinoma) 14. Huh7 (Hepatocellular carcinoma)	1. VERO (African green monkey kidney) 2. LLC-MK2 (Rhesus monkey kidney) 3. PK-15 (Porcine Kidney) 4. BHK-21 (Baby Hamster Kidney) 5. DF-21(Chicken fibroblasts) 6. C6/36 (Mosquito /Aedes albopictus)	1. U937 cells (Monocyte /Macrophages) 2. THP 1 cells (Monocyte /Macrophages) 3. H9 cells (T lymphocyte)

1.2.3. Pathogenesis and immune response.

During the development of the foetus, the cortical neurons and most of the glial cells are generated either by a direct or indirect manner by the radial glial progenitor (RGP) cells. These cells are highly polarised and elongated, covering all the layers of the newly formed neocortex. The apical region of the RGP cells is in contact with the ventricular surface and the cerebrospinal fluid (CSF), while the basal region is in contact with the pial surface and works as a pathway for the neuronal migration. Currently, it is known that the genetic alterations that affect the survival or the proliferation of the RGP lead to microcephaly. It was observed that the infection by ZIKV in the developing brains it is mainly focused on the RGP cells and actively diminish their proliferation, this phenomenon is suggested as the main route for the development of the microcephaly [28].

The infection by ZIKV is sensed by the Pattern Recognition Receptor (PRR) Toll-like receptor 3 (TLR3) in human fibroblasts and human brain organoids leading to type 1 and type 2 interferon (IFN) response. To establish a productive infection the virus must overcome the host type 1 interferon immune response, ZIKV it can block the IFN response in primate and human cells but not in mouse cells making harder to develop models for Zika exposure in these mammals. The blockage of the interferon signalling involves the degradation of the interferon-regulated transcriptional factor Signal Transducer and Activator of Transcription 2 (STAT 2); this degradation leads to the inhibition of the induction of Interferon-stimulated genes. As with other *Flavivirus* ZIKV may share similar strategies to counteract the action of the Interferon response like the reduction of the Phosphorylation of the Signal Transducer and Activator of Transcription 1 (STAT 1) signal transduction pathway with the help of the NS proteins NS2A, NS4A and NS4B. Other of the proposed targets of the virus to shut down the immune response is TANK-binding kinase 1 (TBK1), a multi-functional protein involved in innate immunity, cell proliferation, and apoptosis [1][29][30].

The Major Histocompatibility Complex class 1 (MHC-I), a significant component of the innate immune response plays a role in the activation of Natural Killer (NK) cells that target the infected cells. The NK cells respond to the excitatory and inhibitory stimuli;

within these stimuli, the MHC-1 works as an inhibitory molecule when its present on the cell surface. Many viruses downregulate this receptor to escape the T cytotoxic lymphocytes, another set of immune cells that destroy infected cells but by doing this, the NK cells recognise the absence or the low concentration of it and kill the infected cells. To bypass this issue viruses like ZIKV (*Flaviviruses*) upregulate the MHC-1, they do this by either increasing the expression of this receptor by activating the NF-κB transcriptional activity or enhancing the activity the transporters associated with antigen processing (TAP) [31].

To counteract the infection, the cell, boost the productions of IFN-stimulated proteins such as the Interferon-Inducible Transmembrane Protein(IFITM) which blocks the attachment and entry of the virus to the target cell.[18] In case that the host is pregnant, when the virus reaches the trophoblasts in the placenta, the barrier that protects the foetus against infections and supports its nutrition, these cells activate as part of their response the transcription of a cluster of micro RNAs known as miR19 that can diminish the viral replication [31].

Besides to the activation of the interferon signalling the ZIKV infection activates the autophagy pathway, a complex intracellular degradation process where the cytoplasmic content is directed to a lysosome for degradation, as in other viral infections ZIKV can activate and trick this process into benefiting its replication [32].

The adaptive immune response also targets ZIKV either by the production of highly specific neutralising antibodies or by the activation of T cytotoxic and T helper lymphocytes. During the infection populations of plasmatic and memory B cells that are in charge of the production of antibodies that can block the entry of the virus into the cells. As established before the E protein is the primary target of the neutralisation when peripheric blood B cells were purified using Soluble E protein as an antigen. It was observed that the region within E that is the main target for the neutralisation is the fusion loop of the DII, besides neutralisation these antibodies can activate another phenomenon that contains viral replication such as, antibody-dependent cellular cytotoxicity, complement-dependent cytotoxicity. The other set of lymphocytes activated during the

Zika infection are the TCD4, who orchestrate the immune response. During the infection, the TCD4 are polarised to the T helper 1 (Th1) subset, characterised by the production of IFN-γ, Tumoral Necrosis Factor α (TNF- α) and interleukin 2 (IL-2). TCD8 cells are also activated during the infection and populations of these cells target specifically a region of the E protein comprising the 294-302 residues, the activation of this cells responds to the typical antiviral response expected from these cells [33].

1.2.4. ZIKV and Spondweni virus (SPOV) immunological and pathogenic resemblance.

ZIKV is a member of the *Flaviviridae* family that resembles other members, such as the already mentioned DENV and YFV. However, it has been reported that Spondweni virus (SPOV) shares similar tropism with ZIKA on mice treated with anti-Ifnar1 monoclonal antibody (mAb), which can spread to different organs and tissues, including the CNS, testes, and placenta in pregnant subjects. However, these viruses nt only share similar pathological outcomes when tested in the lab; antibodies isolated from patients against ZIKV and DENV were evaluated in their capability to protect against SPOV infection. Interestingly, both groups of anti- DENV and anti-ZIKV mAb were able to confer some degree of protection, but not only that, in some cases, they were able to neutralize the virus efficiently. This evidence shows not only that ZIKV and SPOV share tropism under specific circumstances but that they are recognized by the immune system on specific common epitopes. This resemblance has fired suspicions that SPOV may cause similar symptomatology and pathogenesis to ZIKV in humans under the right circumstances [34] [35]

1.3. Symptoms, diagnosis, and treatment.

ZIKV infection shares similar symptoms to other viruses such as DENV and CHIKV such as fever, maculopapular rash, arthralgia, myalgia, retro-orbital pain, and conjunctival hyperaemia. The incubation period is 3-14 days, and associated symptoms usually disappear after 3-7 days [5][36].

During the first week after the appearance of the symptoms the virus can be diagnosed by the detection of ZIKV RNA using Real-Time Polymerase Chain Reaction (RT-PCR) in blood samples, but the viable virus can also be detected in other samples like urine, saliva, semen, and vaginal secretions up to for 30 days. Serological detection present difficulties in countries where there is cocirculation of Zika with other flaviviruses since because the antibodies against other viruses cross-react with Zika producing false-positive reactions [5].

The ZIKV lack of specific treatments but individual recommendations can be followed to improve the condition of the patients. Rest, drinking fluids to prevent dehydration, take paracetamol to reduce the fever and the pain. [37] A recent study showed that the treatment with the antibiotic azithromycin (AZ) rescued cells with ZIKV-induced cytopathic effect; this compound is safe during pregnancy and can be used with little risk. The treatment with AZ also recovered the cell viability and decreased the viral production in u87 cells (glioblastoma cell line), it was also found that AZ was effective in reducing the infection in Hematopoietic progenitor cells (HPCs)-derived astrocytes without toxicity. These results open the door to research and design a treatment scheme for pregnant women and prevent the neurological manifestations in the new-borns [30].

1.3.1. Neurological disorders

The infection with this virus usually courses as a self-limited benign febrile disease, however, in some cases, other manifestations can take place, for example, Neurological syndromes such as Microcephaly, Guillain-Barre syndrome (GBS), meningoencephalitis and myelitis.

One of the main concerns raised after the outbreak of ZIKV was the increasing numbers of new-borns with microcephaly during the months after the expansion of the disease within America. Microcephaly, as its name indicates it is the shrinking of the head circumference at birth with ≤31.7 cm for boys and ≤31.5 for girls and before the outbreak in French Polynesia and Brazil it was not reported as part of the symptomatology for Zika

infection. The association with ZIKV was based on a positive test for Zika either by serological tests or RT-PCR.

It was estimated that the riskiest stage for developing microcephaly during gestation was the first trimester with a risk of 1% that may seem small. However, it can be very representative when it the parentage of infection in the general population is very high, like in the French Polynesia or Island of Yap outbreaks (66% and 73% respectively). This contrast with other viruses that generate congenital abnormalities like cytomegalovirus (CMV) that has a risk of 13% of causing defects but only about 1-4 of % pregnant women are infected with CMV. [5] However, other reports suggest that the microcephaly can appear after birth even if the infant born with regular cranial radio due to the destruction of the neural progenitor or other neural cells in utero because of persistent immune activation. [38]

1.3.2. Guillain–Barré syndrome (GBS)

The GBS is an autoimmune disease where the immune system attacks the peripheral nervous System (PNS) it was observed an increase in patients with this syndrome after Zika infection in French Polynesia causing weakness, facial palsy, inability to walk and about 30% of the patients needed respiratory help. Although this pathology can be life-threatening, the patients can fully recover after the proper treatment. It has been suggested that during the ZIKV infection, a mechanism of molecular mimicry with ganglioside 1 (G1); however, no evidence of cross-reactivity has been produced. [37]

1.3.3. Acute myelitis

A case of acute myelitis was reported in January of 2016 when a 15 years-old girl with no antecedent of neurological problems was admitted in Pointee-a-Pitre, Guadaloupe with hemiparesis. The lab results only showed raised leucocytes and polymorphonuclear leucocytes. The images of the nuclear magnetic resonance of the brain were typical. Polymerase Chain Reaction (PCR) detected high levels of ZIKV in serum, urine, and

cerebrospinal fluid of the patient. In this case, the treatment with methylprednisolone improved the neurological condition. The presence of ZIKV in the cerebrospinal liquid suggest the neurotropic capability of the virus in vivo. [38]

1.3.4. Congenital Zika syndrome.

Congenital Zika Syndrome (CZS) comprise a series of clinical features that are a direct result of the neurological damage caused by ZIKV infection. The affection can be divided into structural and functional anomalies. The structural components include changes in cranial morphology, brain anomalies, ocular anomalies, and congenital contractures. Functional anomalies are related to the impairment of neurological functions. Severe microcephaly (head circumference ≥ 2 standard deviations below the mean for sex and gestational age at birth) is the extreme manifestation of CZS, and it is observed after intrauterine ZIKV infection, it is followed by craniofacial disproportion with depression of the frontal bones and severe neurologic impairment. Brain abnormalities associated with ZIKV infection resemble the neuropathology associated with CMV congenital infection [39][40]. Other features included in the CZS are low birthweight, redundant scalp skin, anasarca, apolyhydramnios, and arthrogryposis. Within the neurological abnormalities, they can be divided into the ones that affect the brain such as, cerebral lesions, polymalformative syndromes, brainstem dysfunction and the cause ophthalmological defects like cataract, asymmetrical eye sizes, intraocular calcifications and macular atrophy, optic nerve hypoplasia, iris colombam and lens subluxation.[41] Finally, the impact in the motor development of the patients still needs to be evaluated, however, the lack of typical behaviours such as rollover, sit or even hold their heads suggests that they will not be able to be ambulatory.[42]

1.3.5. Reproductive concerns.

Recent studies showed that ZIKV is capable of infect testes and epididymis of mice but not prostate and seminal vesicle this shed some light into the reports of Zika virus in the semen of convalescent men. The long-term infection in the testes may cause infertility in

immunocompetent males raising new concerns about the reproductive health of the people within the outbreak areas [43]

1.4. Vaccines.

Given the rapid expansion of ZIKV across the American continent due to the extensive presence of the vector and the appearance of a new variety of neurological symptoms associated with the infection, the production of a vaccine to prevent the spreading and the transmission from the mother to the foetus it is imperative. As established before the DII fusion loop is one of the primary targets for neutralisation in purified peripheral blood B cells from patients. However, this epitope is partially blocked during the in vivo infection, and the antibodies targeting this epitope require the Fc fraction of the antibody to carry out the proper biological action. DIII, the domain of the protein in charge of the receptor-binding activity is also the target of antibodies with potent neutralising activity this because by interfering with the binding ability of this domain the interaction between the host's cell and the virus blocked. [44]

Different strategies are being tested to produce a suitable vaccine that can prevent from both the acute phase disease and the neurological symptoms, among the candidates proved we can find DNA vaccines, inactivated the whole virus, modified mRNA, and a viral vector. Animal trials were a modified mRNA vaccine strategy encoding PrM-E was used showed that this vaccine was able to produce stable titers of neutralising antibodies in both mice and rhesus monkeys. DNA vaccines composed of PrM and E had also been tested, with this vaccine, the host produces the secreted form of E and subviral particles. However, this strategy is safer than the inactivated or attenuated viral vaccines it also has its disadvantage; the DNA must be delivered to cell for the protein production and the immune activation so another agent must be added like lipid nanoparticles (LNPs). Finally, the viral vector-based vaccines use Adenovirus as a carrier for the antigen, this virus can be produced in high titres, and since it has a broad cellular tropism, the infection and delivery of the product is secured. however, since there are occurring natural infections of Adenoviruses during the lifetime of the human host, the immune system can

recognise the vaccine and clear it with better efficiency before it can trigger a proper immune response against Zika.[44][45]

Due to the neurotropism exhibited by the ZIKV during the epidemics described before, the similarities between the American sequences and the ones recovered from French Polynesia, the variety of receptors that the virus can use to enter different cell types further research is needed to elucidate all the mechanisms involved in the pathogenesis altogether [41]. A useful technology that has been used before to dissect the entry steps on other viruses is the pseudotypes or pseudo particles approach. With this methodology a retroviral backbone is used as a delivery system to introduce a reporter gene into recipient cells, the critical piece of this approach is the incorporation of a heterologous glycoprotein to modify the tropism of the particle. This technology allows to study the early stages of the infection and introduce modifications into the glycoprotein without the possible off-target mutations across the viral genome. It is worth reviewing the basis of the technology due to the plasticity of the system and the multiple applications.

1.5. Development of the lentiviral vectors.

One of the many tools used within virology labs to study how does an enveloped virus interact with the host cells is the pseudotypes. These particles are often used to study gene expression, regulation, gene therapy and host-virus interplay. Pseudotypes (PPs) are viral particles that are comprised by a vector (the most commonly used are the Lentiviral Vectors (LV)) and a heterologous viral glycoprotein. Lentiviral vectors have several advantages over other backbones such as Vesicular stomatitis virus (VSV) based pseudotypes:

1. Lentiviral vectors have low antigenicity due to the lack of virally encoded genes.
2. They can integrate the gene of interest to the host's genome irreversibly.
3. They can deliver relatively large genes due to its engineered packaging signals and specialised machinery.
4. New generations of these vectors have enhanced biosafety thanks to multi plasmid systems.

5. They are quite flexible in terms of the number of different glycoproteins that they can incorporate into the particle.

During the development of this technology, several species of retroviruses have been used. The original vectors were based on the Moloney Murine Leukemia Virus (MoMLV) that had the disadvantage of being replicative competent and were susceptible to being silenced, are incapable of infect nondividing cells or promote oncogenesis, however, as the methodology progressed other members of the retroviruses family were tested such as HIV (Human immunodeficiency virus). [46]

MoMLV has restricted tropism dampening its ability to infect different cells, to try to solve this issue viral gag and pol genes were stability transfected into cells and supplemented with a plasmid that encoded Vesicular stomatitis virus glycoprotein (VSV-G), after nine days of selection 90.9% of the transfected cells expressed the Glycoprotein (GP). The supernatants produced by these cells were then collected and titered. To analyse the changes in the host-cell infectivity capabilities of the vector, several different cell lines were tested including Baby hamster kidney (BHK-21), zebrafish, chum salmon and rainbow trout. When the particles collected from both MoMLV wt glycoprotein and MoMLV VSV-G+ were compared in its ability to transduce the cells with the G418 resistance gene. The vectors that expressed the VSV-G produced 418 resistant colonies, whereas the MoMLV wt produced none [43]. VSV envelope protein has exhibit the same broad tropism as the full virus. Since it possesses pantropic qualities, it leads to suggest that a ubiquitous receptor play a role in its life cycle, later it was described that Low-Density Lipoprotein Receptor (LDLR) and other members of this family are responsible for viral internalisation. [47]

With the previous knowledge of the disadvantages of using MoMLV, HIV vectors were developed, the wild type virus possesses a precursor envelope glycoprotein GP 160 that is cleaved into two subunits, the outer membranal protein GP 120 and the inner GP 41. The cleaved proteins then arrange as heterodimers that bind to the cellular receptor CD4 and coreceptors CXCR4 and CCR5[1]. During the first approaches of the pseudotypes, it was necessary to express the CD4 receptor into the recipient cells in order to be infected, however, using the same model as with MoMLV heterologous glycoproteins were used.

To construct the new generation of vectors a three plasmids system was implemented, the packaging plasmid added sequences such as the human cytomegalovirus (hCMV) promoter who directs the expression of viral proteins in trans. To further improve the security of the system, the envelope genes, and the accessory protein Vpu were removed from the plasmid. The packaging signal (Ψ) was deleted from the 5' untranslated regions. However, the 5' splice donor site was preserved. An insulin gene polyadenylation signal substituted the 3'long terminal repeat (LTR) at the end of the Nef reading frame. Cis-acting sequences required for reverse transcription and integration were eliminated as well. The second plasmid contains a heterologous glycoprotein either the MLV or VSV envelope protein. The third plasmid known as the transducing plasmid contains sequences required for packaging, transcription, and integration. This plasmid contains the Rev response elements (RRE) and a reporter gene like firefly luciferase or β-galactosidase. Using this system, *Naldini et al.* were able to transduce terminal differentiated neural cells of adult female rats [48]. A similar strategy was used [49] were an HIV based plasmid was modified to delete the nucleotides 294 to 314 of the packaging signal (Ψ), in addition to this the *nef* gene and the 3'LTR were replaced with the hygromycin phosphotransferase gene (Hygr) gene and a synthetic polyadenylation signal. In this case, the plasmid was designed to be transfected and produce stable HIV-1 packaging cell lines; these cells, in return, will produce transducing units that could be used on other cell lines. The supernatant of the stable cells was tested to assess its transducing capability with modest but positive results.

1.5.2. Pseudotyping using Vesicular stomatitis virus.

An alternative to lentiviral pseudotyping is the VSV based system. Vesicular stomatitis virus is a non-segmented, negative-stranded RNA virus that belongs to the family *Rhabdoviridae*, genus *Vesiculovirus*. It expresses a broad tropism infecting different mammals such as horses and swine. Early experiments showed that coinfection of VSV and other viruses produced VSV chimeric particles that displayed a heterologous mixture of GP on their surface; this cemented the idea for pseudotyping using VSV as the core and swapping the envelope depending on the purpose of the assay. The approach used was to design a DG-VSV virus with a reporter gene that would infect cells that

already expressed the GP of interest; the VSV will indistinctly include the heterologous GP into the virion after a round of replication. The particles then could be harvested and used to test infectivity. The main disadvantage of this methodology is the need to produce and harvest the first round of VSV particles that will be used for pseudotyping; the process also depends on the production of the heterologous GP on the transfected cells [50]. In this project, a Lentiviral approach was selected due to the safety that working with plasmids offers against the need to generate a viral stock and perform the first round of infection previous to the pseudotyping collection and harvest. Lentiviral pseudotyping also has a substantial body of evidence that supports their use with GP from different families.

1.5.3. Examples of successful using lentiviral-based pseudotyping.

Once the basic system was mounted, modifications could be done either in the retroviral component or in heterologous glycoprotein that was added [51[52].

As discussed before, pseudotypes allow the study of different viral glycoproteins in a safe environment without a Biosafety Level 3 (BSL3) or BSL4 facility. In practice, the PPs requires just a single round of infection, and it is possible to dissect the tropism and entry process of a virus. In the following paragraphs, we are going to discuss some examples of glycoproteins.

1.5.4. Severe acute respiratory syndrome (SARS) or SARS coronavirus (SARS-CoV).

This member of the *Coronaviridae* family was efficiently pseudotyped by *Giroglou et al.* when a portion of the cytoplasmic tail of the glycoprotein sequence was truncated. The vector of choice for this experiment was MLV; full Spike (S) protein was detected from the pp preparation indicating that the cleavage by trypsin that is observed in the full virus is not necessary for the proper incorporation of the glycoprotein. Furthermore, the treatment with exogenous trypsin decreased the infectivity of the pseudoparticles. In this case, the authors propose that the truncation of the glycoprotein may affect 1) incorporation of the S protein in the viral particles, 2) receptor binding or 3) Fusion/entry process. Finally, both

the SARS virus and the PPs have the same tropism, proving that the model can replicate the receptor binding process as the full virus [53].

1.5.5. CHIKV.

Viral Glycoprotein E1-E2 was pseudotyped using and HIV based lentiviral vector. Several cell lines were in their capability to support viral infection. Human Embryonic Kidney 293 (HEK293T), HeLa, Human Bone Marrow Endothelial Cells (HBMEC), HEPG2 were the most permissive, whereas lymphocyte originated cell lines showed low levels of infection. In this case, by identifying the non-permissive cells, different putative cellular receptors can be transfected to identify which one has a role in the natural infection [54].

1.5.6. DENV.

DENV PP's were produced using an HIV-1 backbone in co-transfection with a plasmid containing and the 3′ 42-nucleotides of C (amino acid residues 101 to 114), PrM and E proteins from DENV2, during this study, the transmembrane domain (TM) of E protein with the TM and cytoplasmic domain (CY) of VSV-G protein, this addition targeted the DENV glycoprotein to the plasmatic membrane. This addition did not have any impact on protein production since the western blot analysis showed similar amounts of PrM and E proteins when compared with the wild type (WT) protein. The PPs produced with either the VSV-G TM-CY signal and de DENV WT were comparable in infectivity showing no significative difference between PPs produced using the constructs. However, the results point out to some level of endoplasmic reticulum retention (ERR) that seemed to be stronger than the VSV plasmatic membrane targeting signal. Finally, when Bafilomycin A and ammonium chloride were tested, the activity of the luciferase reporter gene was completely inhibited mirroring the results reported for full DENV [55][56].

1.5.7. ZIKV.

Recent attempts had been made to pseudotype Zika virus prME protein, a novel report the retroviral backbone strategy shed some light about the viability of pseudotype flaviviruses using this system. Two plasmid backbones were tested, pNL4-3-R−E− which

efficiently different viruses from different families and the *nef* +viral vector pNL Luc AM. It is worth noting that overthought pNL4-3-R−E− works for different kinds of GP; it was highly inefficient on prME-pseudotype production. When the *nef* + plasmid was used as a backbone, significant amounts of pseudotype particles were detected in the cell culture supernatant. Detection of particles indicated that *nef* directly impacted the delivery of the genetic material and the incorporation of the viral GP on the pseudotypes. Pseudotypes produced with this approach were used to infect U87 and 86HG39 glioblastoma cell lines with positive results, *Chavali et al., 2017* reported the production of infectious ZIKV PP using pNL4-3-R−E− and MoMLV backbones which contrast with the reports from *Kretschmer et al., 2020* [57].

1.5.8. Filovirus.

Ebola virus GP (EBOV) was pseudotyped using HIV-1 backbone; the results showed that the PPs had similar behaviour compared to the full virus in terms of, the dependency of the cholesterol on the lipid rafts for the proper internalisation and entry kinetics. Similar to the phenomenon described before for DENV, EBOV GP mediated entry and fusion steps require the acidification of the endosome. The inhibition of the vacuolar ATPase resulted in the impaired entry of the PPs [58]. EBOV PPs had been used before to test the impact of mutations on the tropism for human cells [59]. Biomedical applications of EBOV PPs are under development; when the glycoprotein of the Zaire strain of EBOV (EBOVZ) was added to HIV-based backbone; the PPs were able to efficiently transduce mice and human airway epithelia of trachea and lung as well as in submucosal glands [60].

1.5.9. Vesicular stomatitis virus.

VSV-G was one of the first heterologous proteins introduced into PPs [61]. As mentioned before, the addition of this GP broadened the tropism that the PPs had, allowing the transfection of different cell lines and the development of possible new therapies. However, the cytotoxicity of the protein on most mammalian cells makes it difficult the widespread application [62]. VSV-G pseudotyped on lentiviral backbones demonstrated to be highly efficient in transducing alveolar epithelium cells highlighting its capability to

target polarized cells, especially the basolateral surface [55]. Studies had been carried to assess the safety of this system in vivo, injection of the particles in mice demonstrated a high frequency of Green Fluorescence Protein (GFP) transgene in the liver (up to 59%) and spleen (up to 54%) 4 days after injection and decreased dramatically to a maximum of only 1.3% in liver and 0.38% in spleen from mice 40 days after injection [63]. The main disadvantage for the widespread use of VSV-G as the heterologous GP for the PPs applied on gene therapy is its susceptibility to being neutralized by human sera [64].

The viral proteins listed before are just a few examples of how the PP system can be modified to target different biological questions such as receptor usage, gene therapy, the impact of the different mutations on the cellular tropism. Nevertheless, not all the viral GPs have been pseudotyped raising the question of which factors influence the PP formation.

1.5.10. Influence of HIV capsid and matrix protein in glycoprotein incorporation.

Different viral proteins have different cellular localization during viral replication, for example, HIV Gag protein (composed of matrix protein (MA), capsid (CA), nucleocapsid (NC),p6 and two short peptides SP1 and SP2) is responsible of the assembly and locates in the cytoplasmic compartment, it then interacts with the plasmatic membrane mediated by MA specifically via a binding site for phosphatidylinositol-4-5-biphosphate (PI[4,5]P2, considered a significant landmark for proteins that need to associate with the PM) that also increases Gag oligomerization [65]. In the natural replication of HIV, the envelope protein (env) is translated in the rough endoplasmic reticulum (RER) as a precursor protein gp160 which contains an ER membrane signal. This signal is cleaved during transcription by the cellular signal peptidases. Additionally, TMD of the gp41 contains a hydrophobic stop-transfer signal (membrane anchor) that increases ER retention [66]. The GP is then glycosylated with N-linked and some O-linked oligosaccharide side chains. During the trafficking of the protein between the ER and the Golgi apparatus, it

suffers different modifications that conclude with cleavage of the gp160 precursor into gp120 and gp41 by furin and furin-like proteases (corroborated by the inhibition of this proteases) [667.

To favour the incorporation of env into the virion the components need to be sorted appropriately, and the obstacles must be bypassed for example, both proteins are located in different cellular compartments which means that cellular trafficking guides this process. To try to explain how does the incorporation process occurs, four possible mechanisms have been proposed. First, a passive mechanism where virion buds from the PM carrying with it any Env protein that happens to be there during the event. The second model involves the selective co-targeting of Gag and Env to a specific site of the PM; by doing this, it creates an enriched area of the membrane where both components can adequately interact. Both Gag and Env are known to be targeted to lipid rafts; this phenomenon favours this hypothesis [67]. The third explanation proposes the specific protein-protein interaction between Env and Gag, supported by the interactions between MA and Env mentioned before. Finally, the recruitment of the cellular proteins to the ensemble site to bride the interaction between Env and Gag.

It is fundamental to understand the characteristics of Env and MA to explain the virion formation further. One of the features that characterize the lentiviral Env protein is the length of the CY Usually, this domain is 130 amino acids (aa) long, whereas other retroviruses are shorter than 60 aa. The CD of gp41 has attracted a significant amount of attention due to their interactions that it has with a variety of cellular factors. Experiments have shown that the gp41CD is cell type-specific when it comes to replication, the truncation of this domain blocks replication of the virus in most cell types including peripheral blood mononuclear cells (PBMC) and monocyte-derived macrophages (MDM). MA and Env interact through gp41CD. However, the details of this interaction still need to be elucidated [69]. The amino-terminal domain of HIV-MA is essential for the interaction of Gag with Env, small in-frame deletions or missense mutations within the last 100 aa of the N-terminal region results in lower Env incorporation into the virion comparable to background levels [68].

Mutations within MA that interfere with the interaction with Env did not have any impact with the virion formation. Hydrophobic amino acid substitutions at Simian Immunodeficiency Virus (SIV) MA residues 22 and 24 (R22A/G24V, R22L, G24L, and R22L/G24L) increase the levels that Env is incorporated into virions and enhance virus infectivity relative to the wild-type virus [64]. Modelling studies carried on SIV MA showed that similar to HIV, mutations on the N-terminal region of MA that prevents the incorporation of Env are located on the tip of the molecule, in the vicinity of the charged region. The formation of the trimer brings together this N-terminal residue which forms a rim around a saucer-like depression where can hold the cytoplasmatic tail (CT)of the glycoprotein [69].

Based on the mechanisms described before, the interaction between MA protein and the glycoprotein is dependent of the location of the components, the residues on MA that facilitate the interaction and the topography of the trimers that allow the accommodation of the CT into the spaces that appear during the assembly of the mature virion. Understandably, foreign glycoproteins must fulfil similar requirements to be properly incorporated into the pseudotype. It is important to remark that not all viral glycoproteins can be incorporated into pseudotypes; the reasons still need to be elucidated. Other strategies can be used to study the influence of modifications in viral glycoproteins into the infectivity and tropism. Reverse genetic systems like cloning cassettes and stitching fragments of the viral genome together are safe alternatives to work with genomes and swap viral genes at convenience.

1.5.10. Flavivirus pseudotyping is it possible?

As described before, pseudotyping requires three essential steps to work: selection of the backbone, glycoprotein selection and the cells that are going to be challenged for infection **(Figure 1.5).** Unlike the cases of other viruses that were pseudotyped, the evidence presented above does not seem as robust as it should be. Previous attempts to pseudotype flaviviruses either depend on a replicon system that produces some of the

viral proteins to efficiently generate the infective particle or the use of enormous amounts of retroviral backbone plasmid to force the system into the direction needed for the experiment. The replicon model has been used to test the neutralizing ability of antibodies against YFV, ZIKV and DENV; notably, some texts in the literature use the word pseudotyping indistinctly of the method of production either by retroviral backbones or replicon systems, and this may arise questioning about the feasibility of the process.

These discrepancies had led to questioning the possibility of true pseudotyping for *the Flavivirus* genus. Several factors may play a pivotal role in the efficiency of particle generation, including the effect of the backbone, the interaction of the backbone and the heterologous GP, the presence of intrinsic cellular factors that may either favour or impair particle production and several more that may not even be described yet. [70][71][72].

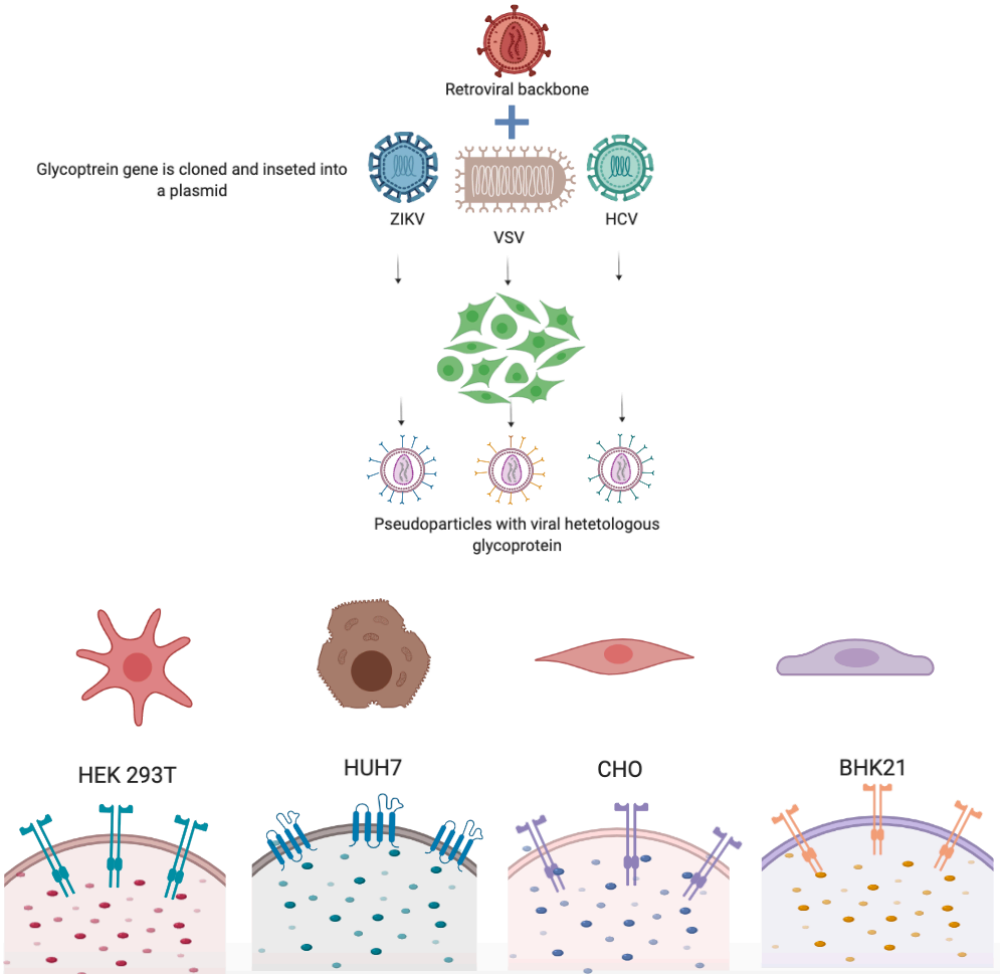

Figure 1.5. General scheme of pseudotyping. As described before most of the approaches to produce pseudoparticles are based on a retroviral backbone and a heterologous glycoprotein cloned into an expression plasmid, these elements are then transfected into HEK293T cells. The transfected cells then produce the infectious particles that are going to be tested on different cell lines.

1.6. Infectious clones of different viruses.

For a long time, the infectious clones have been a useful tool to maintain viral genomes into stable plasmids. Viruses from different families and with a different type of genetic material (DNA and RNA) have been introduced into plasmids to study different life cycle events. Sometimes during the cloning process problems arise that diminish the efficiency of the virus production either the length of the sequence, the cis-elements that are required or even the plasmid where the genome is maintained. Viruses such as Foot to mouth disease virus had technical difficulties before the successful cloning of the 5´ UTR, the main difficulty was the presence of long cytidyl polymeric sequences which needed to be addressed in order to produce high titres of an infectious virus similar to a wt sample [66]. Coronaviruses are the largest positive single-stranded RNA virus with around 30 Kb, to efficiently clone these sequences, it was useful to amplify fragments and join them together into a bacterial artificial chromosome [67]. When it comes to flaviviruses, the instability that the genomes show when they are inserted into a plasmid has been reported in different occasions. When JEV was cloned into a cassette the stability of the construct was influenced by the CMV promoter, modifications of the eukaryotic promoter to reduce its spurious transcription in *Escherichia coli* (E. coli) was an approach that increased the viability of the system. However, the viral genome still contains prokaryotic promoter-like elements that play a major role in the maintenance of these plasmids into the bacterial host [73].

The instability of the cloned genomes of flaviviruses such as DENV and JEV in bacteria is due to the toxicity of the cryptic expression of viral proteins by multiple presences of *Escherichia coli* promoters (ECP) within the sequences. Silent mutations that disrupt the ECPs stabilized the full-length DENV2 and JEV cDNA clones in E. coli. It is important

to note that these promoters are located in both the translated and the untranslated regions of the genome hindering the design of simple approaches to study viral replication [74][75].

In recent years the development of new cloning strategies has facilitated the production of artificial viruses from sequences isolated not only from cell culture but also from clinical and field samples.

1.7. Infectious genome amplicons (ISA)

One of the many advantages of working with positive-sense single-stranded RNA viruses is the ease in the isolation process, along with the simplicity of cloning the genome. ISA methodology where the genome is amplified as fragments that are inserted into transit vectors that serve as templates for a successive amplification where the products are fused to form the full-length genome with the difference that CMV promoter is added into the 5´terminal region upstream the 5ÚTR of the virus, the Hepatitis Delta virus ribozyme (HDVR) and the polyadenylation signal of the simian vacuolating virus 40 (SV40) are also added downstream the 3´UTR. Once the full sequence is obtained, it can follow two experimental routes, the transfection into mammalian cells of this linear molecule or a secondary circular polymerase extension reaction (CPER) where an untranslated linking sequence forms a circular product similar to a plasmid that is then transfected into cells [76][77].

When this approach was used to generate viruses from the sequences of two JEVs, genotype I (JEV I) and genotype III (JEV III), one genotype 2 WNV, one serotype-4 DENV, one WT strain of YFV and one Far- Eastern subtype TBEV the genome was divided into three fragments of approximately 4 Kb during the cloning step; each fragment had 70 to 100 bp overlapping regions, the CMV promoter and the HDVR/SV40pA sequences were also added. The fragments were then transfected into permissive cell lines (human adrenal carcinoma (SW13) and BHK-21) where a recombination event occurs allowing the formation of a single-stranded molecule and the subsequential production of viral particles [78].

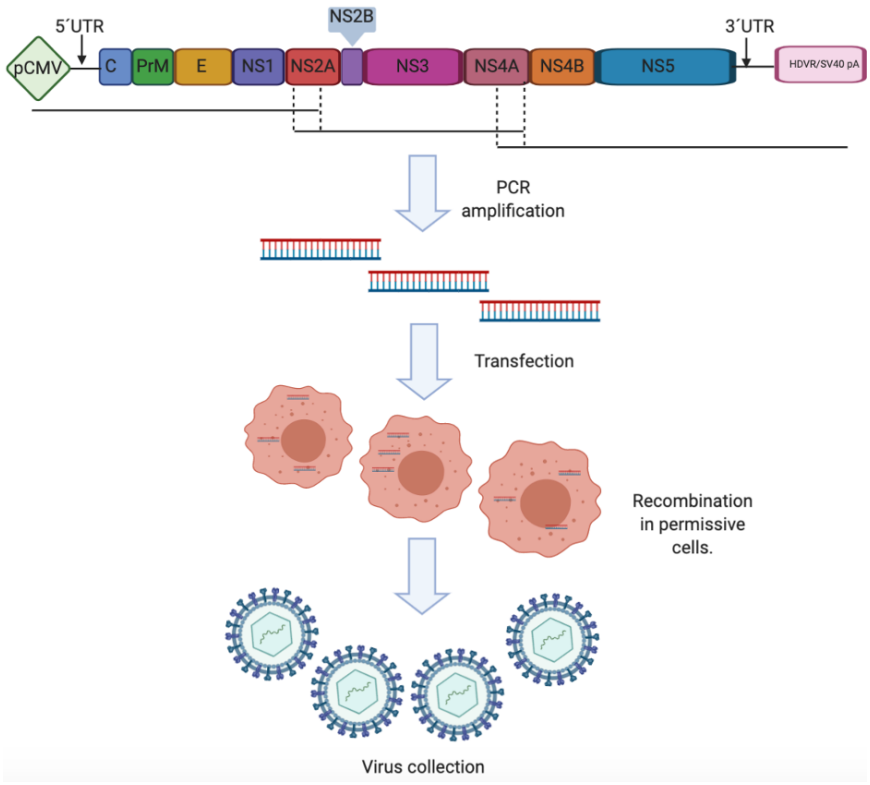

Figure 1.6. Amplification of genomic fragments and virus production. The flaviviral genome was divided into three different fragments during amplification; each fragment contained an overlap sequence to induce the *in cellulo* recombination event that fuses the fragments once that it is transfected. The single linear fragment product of the recombination is then used as a template to produce infectious viruses. The addition of the CMV promoter drives the translation of the product, whereas the HDVR/SV40pA help with the RNA processing of the template (Figure modified from Aubrey et al. 2014).

With this process, the researcher has the flexibility design smaller amplicons of the genome to cover specific regions and modify them without the need of working with the whole sequence, which could be problematic.

ZIKV RNA isolated from brain tissue was used as a template to produce viruses without the need of tissue culture passaging. The genome was divided into smaller fragments that were then fused into a circular structure using CPER, the virus produced with this methodology had the similar sequence (3 nucleotide changes were observed in the CPER

produced genomes) as viruses isolated from the conventional culture methods. Moreover, the collected ZIKV was able to infect cells the same way as the WT; this model allows the rapid production of infectious viruses from publicly available sequence data without the need for international transport of infectious samples [79].

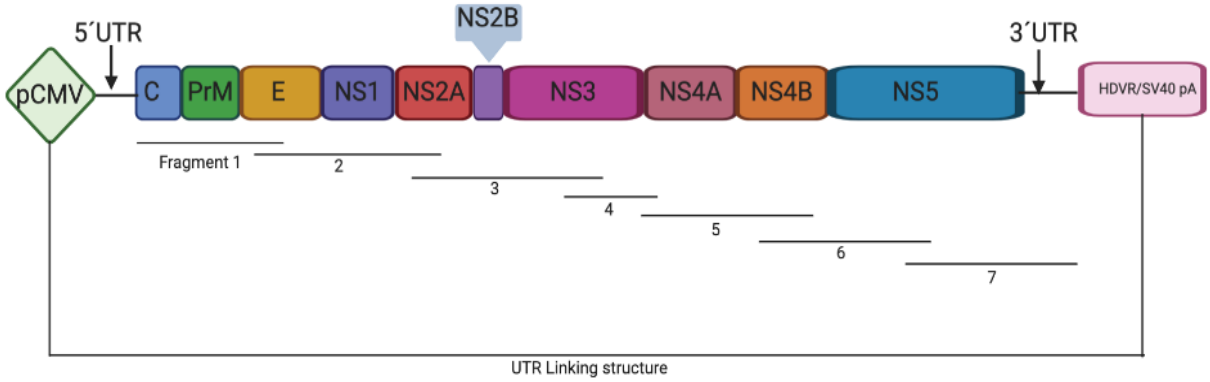

Figure 1.7. Diagram of ZIKV genome assembled using CPER from synthetic fragments. The viral genome was divided into 7 fragments with a 22nt overlap, CMV promoter and HDVR/SV40pA sequences were also added to enhance viral production. The construct was stitched into a circular structure using a UTR linker region (modified from Setoh et al 2017).

2. Hypothesis

- The sequence changes in the Surface proteins of the Zika virus during its passage from Asia to America granted the ability to infect new cell types and produce new clinical manifestations.

3. Main aim

- To determine if the mutations in the surface proteins M and E between strains of ZIKV modify the cellular tropism.

3.2. Particular aims

- To generate a set of mutants that mimic the sequences from the isolates across Latin and North America.

- To produce viable pseudotypes and full viruses to analyse the infectivity of the different mutant constructs.

- To infect different mammal and insect cell lines with the mutant viruses and the constructs to analyse the effectivity of the infection.

4. Material and methods.

4.1. Cell culture

Huh7, BHK-21, VERO and HEK 293T cells were grown at 37°C with 5% of $C0_2$ in Dulbecco's Modified Eagle Medium (DMEM) medium with 5% of Non-Essential Amino Acid (NEAA) (Gibco, Thermofisher) and 10% of inactivated Fetal Bovine Serum (FBS) (Gibco, Thermofisher) no antibiotics were added to the media. The cells were seeded and passage into T 75 or T 175 flasks respectively every 72 hours. Briefly, the cell layer was washed with either 8 or 4 ml of room temperature Phosphate Buffered Saline (PBS) buffer 1x (Sigma-Aldrich), the PBS was discarded and was followed by the addition of the same volume of Trypsin (Gibco, Thermofisher) and incubation until the cells completely detached from the flask surface. The incubation was followed by the addition of (1:1) volume of DMEM medium topped up to 25 or 50 ml, the cells were counted in the cell haemocytometer and centrifuged at 300 G for 7 minutes. Pelleted cells were resuspended in 10 ml of DMEM medium, 2 million Huh7 cells were seeded, and between 5-7 million of HEK293T cells, the flasks were filled with 25 or 35 ml of DMEM media.
The cells for the transfection were prepared to seed 1.5 million HEK293T cells in Primaria dishes (Corning, ThermoFisher) with 10 ml of DMEM media and grown overnight.

C6/36 and Aag2 cells were incubated at 28ºC in an air incubator, Leibovitz's-15 (L-15) medium with 2mM L-Glutamine supplemented with 5% heat-inactivated FBS, 1% MEM non-essential amino acids (100x), 2% tryptose phosphate broth (TPB) without antibiotics. The cells were passaged when 80% confluence was reached. Briefly, cells were detached using a scrapper followed by a centrifugation step of 5 minutes at 200G; the cell pellet was washed using 1X PBS. The cells were then spun at 200G again for 5 minutes, the supernatant was discarded, and 1.2 million cells were seeded on a T25 flask on a volume of 10 ml of L-15 medium.

4.1.2. MG-132 proteosome inhibitor treatment.

A 100 mM stock solution of the proteasomal inhibitor MG-132 (Sigma-Aldrich) was prepared on cell culture suitable DMSO (Sigma-Aldrich), working solutions of 0.1 µM,1 µM, 10 µM, 25 µM, 50 µM were prepared toping up the volume with supplemented DMEM. 10,000 HEK293T cells were seeded on clear bottom 96 well plates, the cells were treated for 72 hours with the different concentrations of the proteasomal inhibitor and incubated at 37ºC, likewise, HEK293T cells transfected with the ZIKV GP plasmid were treated with the inhibitor during the pseudotype production.

4.1.3. Viability assay

The metabolic activity of HEK293T cells that were treated with the proteasomal inhibitor was measured using the CellTiter-Blue® Assay (Promega). Different controls were used during the assay, no cell fluorescence control, untreated cells control, positive control for cytotoxicity, after the test time for the compound concluded 20 µl of CellTiter-Blue® reagent was added for each 100 µl of conditioned media, the plate was then shaken for 15 seconds on a plate shaker. The plate was then incubated at 37ºC for 1 to 4 hours, the plate was then shaken for 10 seconds and fluorescence at 560/590nm was recorded using the plate reader Fluorostar Omega (BMG, lab tech).

4.2. Zika virus sequence selection and alignments

Zika virus sequence was retrieved from Genbank with the following criteria: isolates from clinical samples (not those passaged prior to sequencing), samples from South America and North America but also the outbreaks that occurred in the Pacific before the outbreak in America. The Clustal W sequence alignment was carried out using MEGA7: Molecular Evolutionary Genetics Analysis version 7.0 for bigger datasets (Kumar, Stecher, and Tamura 2015), suggested parameters (Gap opening penalty 15, Gap extension penalty

6.66) for pairwise and multiple alignment were used. The phylogenetic threes were constructed using the maximum like hood method, the test of phylogeny selected was the Boothstrapmethod using a No of boothstrap replication of 1000 with the standard parameters recommended by the program, Jones-Taylor-Thornton substitution model was used for the analysis.

4.3. Zika C-PrM-E and C-GFP-PrM-E cloning.

Dr Andres Merits kindly provided the template used for the cloning of the protein sequences. The C-PrM-E sequence of the two different plasmids (PCCI-SP6-ZIKV-EGFP and PCCI-SP6-ZIKV) were cloned using the primers: Forward caccATGCTGAGAATAATCAATGCtagg and Reverse CTAAGAGACGGCTGTGGATA. The templates were diluted (1:100) and (1:1000) and the standard protocol for the Q5 Hot Start High-Fidelity DNA Polymerase PCR (New England Biolabs Inc) was followed, (98°Cor 30 seconds, 25 cycles of 98°C for 10 seconds, 63°C for 20 seconds, 72° C for 1-minute 72°C for 1 minute) the products were loaded onto a 1% agarose gel and electrophoresed for 42 minutes at 90 volts.

4.4. Insertion of the product into pcDNA3.1D/V5-His-TOPO.

Before carrying out the TOPO reaction, the PCR products were treated with Dpn I enzyme (New England Biolabs Inc). The products were incubated for 15 minutes with 1µl of the enzyme at 37°C followed by another incubation for 5 minutes at 80°c. The treated PCR products were introduced into the vector following the instructions of the manufacturer (ThermoFisher Scientific) briefly, the TOPO vector and the product were mixed along with the salt solution and water gently and incubated for 30 minutes at room temperature. 2 µl of the TOPO cloning reaction were mixed with 50 µl of chemically competent *E.coli* Stellar cells and incubated on ice for 30 minutes, once the time concluded cells were heat-shocked at 42°C for 45 seconds and incubated on ice for 5 minutes, then 250 µl of Super Optimal broth with Catabolite repression (SOC) SOC media was added. An additional 1

hour of incubation was performed at 37°C under shaking (200 rpm). Finally, the cells were spread on an agar plate with ampicillin as a selection agent (1 µl of 100mg/ml solution per ml of agar). The plate was incubated overnight, and the colonies were screened using T7 and Bovine Growth Hormone (BGH) primers.

4.5. Colony screening.

To perform the colony screening Hotstart Taq polymerase (Qiagen) was used, a heat activation step of 95ºC for 15 minutes was performed. To prepare 15 µl of master mix, 1.5 µl of 10X Qiagen PCR buffer, 0.3 µl of 10 µM Forward Primer, 0.3 µl of 10 µM Reverse Primer, 0.6 µl of 10 mM DNTPs, 0.075 µl Qiagen Hotstart Taq (5 units/ µl) and 12.225 of water were mixed.

For each of the products transformed into the cells, 10 bacterial colonies were tested. 15 µl aliquots of the master mix were placed into each PCR tube, a sample of each colony was taken and mixed with the master mix, then it was stabbed on to the corresponding box on 4X8 gridded LB+ AMP agar plate. The plate was incubated overnight 37ºC and the PCR was carried out as following.

Table 4.1. Temperature cycles for colony screening.

Temperature	Time	Number of cycles
95ºC	15 minutes	
95ºC	20 seconds	30 cycles
55ºC	20 seconds	
72ºC	1 min/kb	
72ºC	2 minutes	
8ºC	Infinite hold	

The PCR product were loaded into a 2% agarose gel and electrophoresed for 42 minutes at 90 volts.

The plasmid was purified using GenElute Plasmid Miniprep kit (Sigma-Aldrich), briefly, overnight cultured cells were pelleted at 12,000 g for 1 minute, the supernatant was discarded, and the cells were resuspended in 200 µl of resuspension buffer and pipetted up and down followed by the addition of 200 µl of lysis buffer and incubation at room temperature for 5 minutes, once the incubation concluded 350 µl of Neutralization solution was added. The mixture was centrifuged at 12,000 g for 10 minutes. In another tube, the column was simultaneously prepared using column preparation solution. The lysate was then transferred into the column and spun at 12,000 g for 1 minute, the flow-through was discarded, and the washing steps with wash solution one and wash solution two were carried out. Finally, the plasmid was eluted from the column using 50 µl of elution buffer and quantified using the Nanodrop 1000 (Nanodrop, Thermofisher)

4.6. Site directed mutagenesis (SDM)

The mutants of the membrane and envelope protein were produced using the Q5 site-directed mutagenesis kit (98°C for 30 seconds, 25 cycles of 98°C for 10 seconds, 63°C for 20 seconds, 72°C for 3 minutes, 72°C for 4 minute) (New England Biolabs Inc).
The protocol was followed as directed by the manufacturer. Briefly, the template was amplified with the chosen primer (Table 4), the annealing temperature (Ta) used was determined by the primer design software (NEBaseChanger.neb.com), and the extension time used was 5 minutes. Once the PCR was performed, the product was treated with the Kinase, Ligase and DpnI (KLD) Enzyme mix (New England Biolabs Inc) using 0.5 µl of PCR product, 2.5 µl of the 2X KLD Reaction buffer, 0.5 µl of the 10X KLD Enzyme mix AND 1.5 µl of Nuclease-free water. The mix was incubated at 22°C for 5 minutes, and all the volume was mixed with 50 µl of chemically competent cells then incubated on ice for 30 minutes and heat-shocked for 45 seconds followed by a 5-minute incubation on ice. Once the incubation has concluded 250 µl of SOC media was added, and the mixture was shaken gently at 37°C for 1 hour. Finally, the media was spread onto a selection plate and incubated overnight. The colonies were screened using PCR with T7 and BGH primers, the product was sent for Sanger sequencing (Source BioScience service), and the electropherogram trace files were compared against the wild-type sequence.

Table 4.2. Primers used during the site mutagenesis.

ZIKV GFP SDM 1	
GCG->GTG[A^{123}->V]	
ZIKV_GFP_SDM1 Forward	GCCATGGCCGtGGAGGTCACT
ZIKV_GFP_SDM1 Reverse	TGTGGTCAGCAGCAGTCCC
ZIKV SDM 1	
GCG->GTG[A^{123}->V]	
ZIKV_SDM1 Forward	GCTATGGCAGtGGAGGTCACTAG
ZIKV_SDM1 Reverse	TGTGGTCAGCAGCAGTCCC
ZIKV SDM 2	
AAC->AGC [N^{139}->S]	
ZIKV_SDM2 Forward	TTGGACAGAAgCGATGCTGGG
ZIKV_SDM2 Reverse	GTACATATAGTATGCACTCCC
ZIKV SDM 3	
TTC->CTC [F^{257}->L]	
ZIKV_SDM3 Forward	GAACCCTGGCcTCGCGTTAGC
ZIKV_SDM3 Reverse	CTGAATATCCAATTTTCGACTCTAATCAAGTGC
ZIKV SDM 4	
ACT->GCT [T^{300}->A]	
ZIKV_SDM4 Forward	GGACAAACCGgCTGTCGACAT
ZIKV_SDM4 Reverse	TGTGCCATTACGGTGACAC
ZIKV SDM 5	
AGT->ACT [S^{550}->T]	
ZIKV_SDM5 Forward	GTTCTAGGGAcTCAAGAAAGGAGC
ZIKV_SDM5 Reverse	CACGACAGTTTGCCTTTTG
ZIKV SDM 6	

CAC->TAC[H^{691}->Y]	
ZIKV_SDM6 Forward	CCCACCACTGGtACAGGAGTGG
ZIKV_SDM6 Reverse	GTGATCTTCTTCTCCCCAC
ZIKV SDM 7	
ATG->GTG [M^{691}->V]	
ZIKV_SDM7 Forward	AACGTTGCTGgTGTGGTTGGG
ZIKV_SDM7 Reverse	CCAATGAGAATTTGTGAGAACCAG
ZIKV SDM 8	
ATG->AGG [M^{777}->T]	
ZIKV_SDM8 Forward	ATTTCCCTTAcGTGCTTGGCC
ZIKV_SDM8 Reverse	AGATCCATTCTTTGTGTTCAG

4.7. Pseudotype production.

293T cells were co-transfected with plasmids contain the HIV-1 based backbone and the glycoprotein to produce pseudotypes. Briefly: for plasmid transfection, 2 µg of lentiviral vector pNL4.3 and the glycoprotein of interest was mixed with Opti-MEM media (ThermoFisher Scientific) to a final volume of 300 µl. Alternatively, for cells under division, we use 2 µg of lentiviral vector Murine Leukaemia Virus (MLV) plasmid using the same protocol.

In another tube, a mixture of 276 µl of Opti-MEM with 24 µl of Polyethyleneimine (PEI) was prepared and mixed with the plasmid solution and incubated for 1 hour at RT. Later, the mixture was added to the 293T dishes with 7ml of fresh Opti-MEM and incubated for 6 hours at 37°C. Finally, the media was poured out and replaced with fresh supplemented DMEM (10% FBS 1%NEAA), and the cells were incubated for 72 hours at 37°C.

After the 72-hour incubation period, the cell culture media was harvested and filtered through a 0.22 µm membrane filter and the flow-through containing the pseudo particles was collected and stored at 4°C for future assays.

4.7.2. Luciferase assay.

96-well plates of Huh7 cells were seeded for the luciferase assay, 15,000 cells per well were seeded and incubated overnight. The cells were treated with 150 µl of the filtered cell culture media of the transfected HEK 293 T cells and incubated for 6 hours at 37°C followed by the addition of 150 µl of DMEM media and incubation for 72 hours. Once the incubation time was completed the cells were lysed using the lysis buffer from luciferase assay system (Promega) following the instructions of the kit, the plate was incubated for 15 minutes at room temperature on a shaker followed by 15 seconds on the vortex. The chemiluminescence was measured using the plate reader Fluorostar Omega (BMG, lab tech) adding 50 µl of luciferase assay substrate.

4.8. RNA extraction and receptor screening.

The RNA from the cells (HEL 293 T and HuH7) was extracted using GenElute Mammalian Total RNA Miniprep Kit (Sigma-Aldrich). The pelleted cells were lysed with 250 µl of lysis solution (mixed with 2-mercaptoethanol ,10 µL of 2-ME for each 1 mL of Lysis Solution.) and homogenized in the Hybrid Ribolyser; the lysate was then transferred into a filtration column and spun at 16000 g for 2 minutes; an equal volume of 70% ethanol was added to the flow-through. The lysate/ ethanol was transferred into the binding column and spun for 15 seconds at 16000 g (also for subsequent steps) discarding the flow-through, 500 µl of wash solution one was added to the column and spun for 15 seconds followed by the addition of 500 µl of wash solution, the column was again spun for 15 seconds, and another washing step was performed. Finally, the column was transferred to another tube, and 50 µl of the elution buffer was added, and the column was centrifuged for 1 min, the Flow-through was quantified using the Nanodrop 1000 (ThermoFisher Scientific).
The mRNA was used as a template to produce cDNA using RNA to cDNA Eco Dry Premix (Random Hexamers) (Takara, Clontech). 1-5 µg of total RNA was diluted to a final volume of 20 µl and added into the tube with the Eco dry Premix, once the pellet was dissolved, the tubes were incubated at 42°C for 60 minutes and then heated to 70°C for 10 minutes. The cDNA produced was then used as a template for PCR.

4.9. Analysis of the cytoplasmic domains of the viral glycoproteins.

Sequences of 32 different glycoproteins from viruses that were efficiently pseudotyped were retrieved from genbank, sequence analysis to predict the conformation of the cytoplasmic tail was performed using Network Protein Sequence Analysis (NPS) [74].

4.10. Improving the yield of the PCCl SP6 Zika plasmid.

The Plasmid PCCL SP6 Zika that was kindly donated by Dr Andres Merits was designed as a single copy plasmid that contained a stable version of the ZIKV genome, this plasmid presented difficulties during its harvest and purification, and therefore an alternative method to the standard LB *E.coli* growth protocol was designed. 350 ng of the plasmid PCCl SP6 Zika wt were used as the material for transformation of an aliquot of 50µL of NEB Stable Competent *E.coli* (High Efficiency), with cells thawed on ice for 10 minutes. The plasmid was then mixed with the cells by gently flicking the tube and the mixture was then incubated on ice for 30 minutes the cells were then heat-shocked at 42ºC for 30 seconds. The heat-shocked cells were then immediately returned to ice for 5 minutes taking care of not mixing the cells. 350 µl of NEB 10-Beta/Stable Outgrowth Media was added to the mixture; then the tube was incubated on a shaker for 60 minutes at 30ºC at 250 RPM. Luria Broth (LB) plates were prepared with chloramphenicol at different concentrations. Then the plates were warmed at 30ºC prior to plating the cells. The plates were then incubated at 30ºC overnight, although if the colonies were smaller thand the usual size observed for standard cloning, an additional 24 hours incubation was carried out.

The colonies selected after the first overnight incubation were sub seeded by streaking. After the incubation of 48 hours at 30°C, a PCR reaction for the whole genome was carried out. The colonies positive for the PCR were then incubated on Terrific Broth.

4.11. Overnight culture of positive colonies on Terrific broth.

Modified Terrific (Sigma-Aldrich) broth (TB) was selected to increase the plasmid yield, TB was prepared as follows. 47.6 g of Terrific powder was dissolved in 1 L of distilled water and supplemented with 8ml of glycerol. When the broth was prepared, the colour was light brown, after the sterilization on the autoclave it turned dark brown.

The selected colonies were incubated overnight on 50 ml of Terrific broth with 50µl of chloramphenicol (25µg/ml) at 30°C and 150 rpm on a baffled bottom flask. After overnight incubation, another 50 µl of chloramphenicol was added, and another overnight incubation was carried out.

4.12. NucleoBond Xtra midi plasmid purification.

The genome containing plasmids were purified using the NucleoBond Xtra Midi kit (Macherey-Nagel). Briefly, the cells were grown for 48 hours on 50 ml of TB with chloramphenicol, the cells were pelleted by centrifugation at 4500 g for 10 minutes at 4ºC, and the supernatant was discarded completely. The cell pellet was resuspended in 16 ml of Resuspension Buffer (RES)+ RNase A by pipetting up and down. Once the cells pellet was completely scattered (taking care that all the clumps are disincorporated) 16 ml of Lysis Buffer (LYS) was added. The suspension was mixed gently by inverting the tube five times. Vortexing the cells was avoided due to the possible release of chromosomal DNA. The mixture was incubated at room temperature for 5 minutes; in the meantime, the NucleoBond Xtra column with the column filter was equilibrated using 12 ml of Equilibration Buffer (EQU).

The buffer was applied onto the rim of the column, the column was emptied by gravity, and the follow-through was discarded. 16 ml of Neutralization buffer (NEU) was added to the lysis suspension, and the lysate was mixed gently by inversion until a colour change from blue to colourless occurs. The precipitate was removed by centrifugation at 4500 g for 10 minutes. The lysate was loaded onto the column until it was emptied by gravity, the column and the filter were washed using 5 ml of EQU. The filter was removed by pulling the filter out of the column. The column was then washed with Wash Buffer (WASH). The

plasmid was eluted with 5 ml of preheated (50ºC) Elution Buffer (ELU), the eluate was collected on a set of 1.7 ml Eppendorf tubes. The DNA was precipitated using 3.5 ml of room temperature isopropanol (the final volume needs to be divided depending on the number of tubes using during the collection), the mixture was then vortexed thoroughly and centrifuged at 15000 g for 30 min at 4ºC. The supernatant was discarded carefully, 2ml of room temperature 70% ethanol was added to the pellet. The pellet was then centrifuged at 15000 g for 5 minutes at room temperature, the ethanol was removed completely using a micropipette tip, and the pellet was dried at room temperature. The DNA was then dissolved TBE and quantified using a Nanodrop (Thermo Fisher).

4.13. ZIKV genome amplification and Puc19 Cloning.

Primers were designed to clone the full Zika Virus genome including the UTR regions into the pUC19 plasmid. Auxiliary features were added including EcoRI restriction site, T7 and SP6 binding sites, a 15bp overhand of the pUC19 sequence was added during primer design to facilitate subsequent In-fusion cloning. **Table 4.3** shows the sequences used during the design and the full-length primer.

Table 4.3. Primer design for ZIKV genome cloning. The primers were designed including additional sequences to improve the performance of the plasmid, T7 and Sp6 polymerases binding sites were included for in vitro transcription.

Name	Sequence
5´Primer Design	
Upstream Sequence of **pUC19** Linearised At EcoRI Site With 5´In-fusion Digest Overhang	5´AACGACGGCCAGTGAATT
T7 Binding Site	5´TAATACGACTCACTATAGGGAGA
SP6 Binding Site:	5´ATTTAGGTGACACTATAGAAGAG
5´Of Zika Sequence	5´AGTTGTTGATCTGTGTGAATC
Full Primer	Full Primer Sequence
Forward Primer(T7)	5´AACGACGGCCAGTGAATTTAATACGACTCACTATAGGGAGAAGTTGTTGATCTGTGTGAATC
Forward Primer (SP6)	5´AACGACGGCCAGTGAATTATTTAGGTGACACTATAGAAGAGAGTTGTTGATCTGTGTGAATC
3´Primer Design	
Downstream Sequence of Puc19 Linearised At EcoRI Site With 5´In-fusion Digest Overhang (Positive Strand Sequence)	5´AATTCGAGCTCGGTACCC
3´ End of Zika Sequence	5´ GGGGAAATCCATGGGTCT (Positive Strand Sequence)
Reverse Primer (Positive Strand Sequence)	5´ GGGGAAATCCATGGGTCTAATTCGAGCTCGGTACCC
Reverse Primer (Reverse Complement)	5´ GGGTACCGAGCTCGAATTAGACCCATGGATTTCCCC

4.14. CloneAmp Hi-Fi PCR protocol for ZIKV genome amplification.

CloneAmp master mix was prepared by adding 12.5 µl of CloneAmp HiFi PCR Premix (Takara, Clontech), 5 pmol of Forward and Reverse primers,and 100 ng of template Zika Genome plasmid to a final volume of 25 µl in sterilized distilled water. The mixture was homogenized by tapping the tube. The cycling conditions are listed below:

Table 4.4. Temperature cycles for CloneAmp Hi-Fi PCR.

Temperature	Time	Number of cycles
98ºC	10 seconds	35 cycles
55ºC	15 seconds	
72ºC	2 minutes	
4ºC	Infinite hold	

.

The PCR product was purified using either Sodium acetate/ethanol or purification column.

4.15. LongAmp PCR ZIKV genome amplification.

LongAmp Taq Polymerase (New England Biolabs Inc) was used as an alternative to CloneAmp Hi-Fi protocol. Briefly. 5 µl of 5x LongAmp Taq reaction buffer, 0.75 µl of 10 mM dNTPs, 1 µl of 10 µM of each Forward and Reverse primers and 1 µl of the template (10-20 ng of genetic material), 1 µl of LongAmp Hotstart Taq DNA Polymerase and 15.25 of nuclease-free water.

Table 4.5. Temperature cycles for Long Amp PCR.

Temperature	Time	Number of cycles
94ºC	30 seconds	
94ºC	30 seconds	30 cycles
50-70ºC	15 seconds	
65ºC	13 minutes	
65ºC	10 minutes	
4ºC	Infinite hold	

5µl of the LongAmp PCR product were treated with 5µl 2X Q5 Hi-Fi Master Mix and then incubated at 72ºC for 15 minutes. Alternatively, the products were treated with KLD mix. Briefly, 1 µl of 10X KLD enzyme, 5 µl of 2x KLD buffer, 2 µl of PCR product and 3 µl of nuclease-free water were mixed and incubated at room temperature for 15 minutes. Products from both reactions were used for bacterial transformation, and colonies were counted after 24- or 48-hours incubation.

4.16. PCR clean-up using sodium acetate and ethanol.

PCR products from Q5 amplification were treated with a mixture of 40 µl of chilled absolute ethanol and 2 µl of 3M sodium acetate pH 4.5 (Thermo Fisher) for each 20 µl of PCR product. The PCR products were transferred into a tube containing the mixture, the tube was vortexed and then stored at -20ºC for 30 to 50 minutes (overnight incubation was carried out when small amounts of products were used). The tube was spun for 30 minutes at maximum speed (14,000 rpm). The supernatant was removed carefully without disturbing the pellet. The pellet was washed with 70% ethanol. The tube was spun at maximum speed for 5 minutes. Finally, the supernatant was removed using a micropipette tip, and the pellet was air-dried at room temperature. The pellet was resuspended on TBE, and the concentration was quantified using a Nanodrop (Thermo Fisher).

4.17. Monarch PCR clean-up Kit.

PCR products were mixed with the binding buffer on a (2:1) ratio (Binding buffer: sample) if the size was above 2 Kb or (5:1) if it was below this size. The sample then was loaded onto a column and spun for 1 minute at 16,000 g, the flow-through was discarded, and 200 µl of wash buffer was added to the column, the column was centrifuged 1 minute at 16,000 g. The washing step was repeated one more time, the column was then transferred into a new collection tube, and 20 µl of Elution buffer were added and centrifuged again for 1 minute. The DNA concentration was determined using a Nanodrop (Thermo Fisher).

4.18. In-Fusion cloning.

Alternative strategies were tested to clone the viral genome. In-Fusion HD Cloning kit (Takara, Clontech) was used due to its compatibility with other methods that were considered during primers design. Briefly, 5 µl of PCR product was treated with 2 µl of Cloning Enhancer. The mixture was incubated at 37ºC for 15 minutes, then 80ºC for 15 minutes in a thermocycler. Once the Cloning Enhancer-treated product was ready the infusion reaction was assembled with 2 µl of 5x In-Fusion HD Enzyme premix,2 µl of Cloning enhancer-treated product and 50 ng of linearized vector with 15bp ends complementary to PCR product ends, nuclease free water was added to complete the volume of 10 µl. The In-Fusion mixture was then incubated at 50ºC for 15 minutes then placed on ice. 25 µl of *E. coli* Stellar cells were mixed with the product and incubated on ice for 30 minutes, once the time concluded, cells were heat-shocked at 42°C for 45 seconds and incubated on ice for 5 minutes, then 250 µl of SOC media was added. An additional 1 hour of incubation was performed at 37°C with shaking (200 rpm). Finally, the cells were spread on an agar plate with ampicillin as a selection agent (1 µl of 100mg/ml per ml of agar).

4.19. Gibson assembly

Gibson assembly master mix (New England Biolabs Inc) was also used to fuse the PCR fragments together. Briefly, for 2-3 fragment assembly 0.02–0.5 pmols of each PCR product were mixed with 10 µl Gibson Assembly Master Mix (2X) and the volume was completed up to 20 µl using deionized water. The mixture was then incubated in a thermocycler at 50ºC for 15 minutes and then placed on ice for subsequent transformation as per section Insertion of the product into pcDNA3.1D/V5-His-TOPO.

4.20. ZIKV sequencing.

A primer walk strategy was used to sequence the viral genome; thirteen primers were designed (**Table 4.6**) to sequence the genome inserted into the Puc19 plasmid. The plasmids were sent for sanger sequencing.

Table 4.6. Primers for genome sequencing.

ZIKV sequencing primers

Primer Name	Sequence
ZIKV genome sequencing 1/13	AACGACGGCCAGTGAATT
ZIKV genome sequencing 2/13	CGGAACCTGCCATCACAA
ZIKV genome sequencing 3/13	GATGAGAATAGAGCGAAAGT
ZIKV genome sequencing 4/13	TGAAGCCACTGTGAGAGG
ZIKV genome sequencing 5/13	CAAGCAAGCCTGGGAAGATGGTAT
ZIKV genome sequencing 6/13	CCACTGTCGTTCCGGGCTAAGAT
ZIKV genome sequencing 7/13	TCATGGCCCTGGGACTAACC
ZIKV genome sequencing 8/13	CTAGACAAGTGTGGGAGAGTGATA
ZIKV genome sequencing 9/13	GGGGGCGCATAGGCAGGAATC
ZIKV genome sequencing 10/13	TGTGTCCTCATTGTTGTGTTCCTA
ZIKV genome sequencing 11/13	CAAGAGACGTGGGGGTGGAACAGG
ZIKV genome sequencing 12/13	CAGTGAAATATGAGGAGGATGTGA
ZIKV genome sequencing 13/13	GAGTCGTATACCAGGAGGAAGGAT

4.21. ZIKV culture.

Doctor Janet Ramshaw kindly donated the Brazil 2015 ZIKV strain. The virus was passaged on HEK293T cells. Briefly, the cells were infected with the virus aliquot and incubated for 96 hours using DMEM as maintenance media, then the supernatants were collected and filtered through a 0.22 µm membrane filter. The supernatant was later aliquoted and stored at 4ºC or -70ºC for long-term periods.
The virus was titred on 96 well plates using Reed and Muench assay.

4.21.2. ZIKV titration.

The viral titre of the supernatants was calculated using a Reed and Muench assay. Briefly, a 96 well plate was seeded with 20,000 BHK cells per well; after 24 hours, the cells were treated either with serial dilutions of the viral sample or with control mock media (supernatant harvested from cells that were not infected with virus). 10 wells were used per dilution; the volume used to treat each well was 200 µl (composed of Viral sample + DMEM). Ten wells were treated with each dilution, and 16 wells were used as control. The cells were incubated for 5 days, after the incubation time passed wells were checked for morphological changes or the detachment of the cells from the well´s bottom, the supernatant was removed, and 100 µl of Naphthol blue-black (NBB) solution (Merck) was used for fixing and staining. The solution contained 0.05% NBB in 9% of acetic acid with 0.1 M of sodium acetate (0.5 gr of NBB, 90 ml of glacial acetic acid, 8.2 gr of sodium acetate) and was taken to 1 litre with distilled water. The cells with the NBB solution were incubated two hours at room temperature; the dye was removed by flipping the plate over, followed by the submersion of the plate in water to wash the remaining NBB.

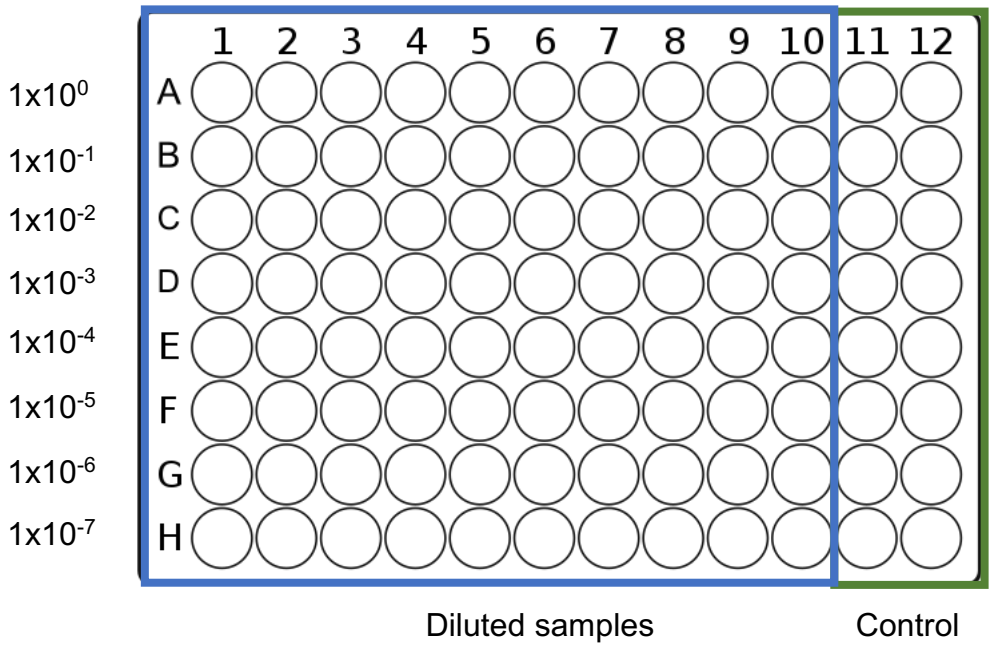

Figure 4.1. 96 well plate dilution distribution. The 96 well plate was divided into two groups to determine the viral titre, 10-fold dilutions were carried out using the supernatant of Hek293T cells used to cultivate the ZIKV.

4.21.3. Calculation of viral titre.

The positive wells were counted, and the data was inputted on the TCID50 calculator designed by Marco Binder, Dept. Infectious Diseases, Molecular Virology, Heidelberg University based on the Spearman & Kärber algorithm of 50% Tissue Culture Infectious Dose (TCID50) calculation described in Hierholzer & Killington (1996), virology methods Manual, p 374.

4.22. Western blot (WB).

Cells of the line of interest were detached from the 10cm dishes using cold PBS; the cells were centrifuged at 300 G for 7 minutes; the pelleted cells were then lysed using the following buffer adding the protease inhibitor Complete (Roche) when needed.

The protein concentration from the cell lysates was measured using the Pierce™ Bicinchoninic Acid (BCA) Protein Assay Kit. Briefly, a standard curve of albumin is used as reference ranging from 2000 µg/ml to 0 µg/ml, the curve and the samples are incubated in 96 well plates with a mixture of 50 parts of Reagent A and 1 part of Reagent B for 30 minutes at 37°C. After the incubation time has passed the plate was then read at 562nm on the plate reader Fluorostar Omega (BMG, lab tech). The data from the standard curve was plotted, and the samples were interpolated within the data set. The equivalent of 15 µg of protein are loaded into 10% Mini-PROTEAN TGX Precast Gels under either reducing or non-reducing conditions. The gels were run for 35 minutes at 180 volts; once the electrophoresis is completed, the gels were transferred into 0.45µm polyvinylidene difluoride (PVDF) membrane that was previously activated with methanol. Transfer was carried out using the Trans-Blot Turbo system from Bio-Rad using the standard protocol (1.0 A ;25 Volts constant for 30 minutes). The membranes were blocked using 10% Non-Fat-Dried Milk (domestic grade) in 1X PBS 0.1% Tween at room temperature for 2 hours. Once the blocking time concluded the blocked membranes were incubated overnight at 4°C with the primary antibody of interest. After the incubation time passed the membranes were washed with PBS tween 0.1% 150 mM of NaCl, the secondary Horseradish Peroxidase (HRP) antibody was incubated for 2 hours at room temperature. The membrane was revealed using the Radiance HRP substrate for CCD imaging (Azure Biosystems), the GBOX chemo XX6 (Syngene) was used as an imaging acquisition system.

4.22.2. Western blot membrane stripping.

Mild stripping buffer was used when needed. Briefly, 1 litre of stripping buffer was prepared using 15 grams of glycine (Invitrogen, Life technologies), 1 gram of SDS (Invitrogen, Life technologies), 10 ml of Tween 20 (Sigma), the components were dissolved in 800 ml of distilled water. The pH was adjusted to 2.2, and the volume was taken to 1 litre with distilled water. The membrane was placed on a container, and the volume of buffer required to cover it was poured, the membrane was incubated at room temperature for 10 minutes. The used buffer was discarded and replaced with fresh

stripping buffer followed by another incubation step of 10 minutes. The buffer was discarded, and the membrane was washed with PBS twice at room temperature. Then the membrane was washed twice with TBS-Tween, the membrane then was blocked again.

4.23. Immunofluorescence (IF).

Cells seeded on slides were fixed using a solution of 2% Paraformaldehyde for 20 min at 4°C without shaking. The cells were washed twice with 1X PBS buffer for 3 to 5 minutes under constant shaking. After the washing step, the cells were dried for 20 minutes or stored at -20°C (up to 7 days) or -70°C (for long-term storage). Drying the cells prevents damage caused by crystallisation of water in the freezing process. The cells were then permeabilised with cold acetone or saponin solution (0.2%) for 3 minutes. When using acetone, it is essential to accurately measure the time of permeabilisation because it may cause severe damage to the cell structure. After the permeabilisation step finished, the cells were washed with 1X PBS solution and then with distilled water.

After the washing steps, the cells were blocked using blocking solution for 45 minutes at 37°C within a humid chamber. After this incubation step, the cells were washed using 1X PBS for 4-5 times for 5 minutes under slow but constant shaking. Once the cells were washed, they were incubated overnight at 4°C with the primary antibody and were stored within the humid chamber.

After the overnight incubation, the cells were washed with PBS 1X for 4-5 times under constant shaking; then the secondary antibody was diluted in a diluent solution. The slides then were incubated with this mixture for 2 hrs at room temperature within the humid chamber without movement. The cells were then washed with 1X PBS 3 times for 5 minutes under constant shaking, after this, the cells were washed with 50 mM ammonium chloride for 3 minutes and finally with distilled water to remove possible excess of buffers. Before mounting the coverslips, the slides were washed for 20 minutes in absolute ethanol and then dried vertically with absorbing paper.

Once the coverslips were ready to be mounted four µL of Vectashield + DAPI were added to the slide for each coverslip. The slides were then immobilised using small drops of nail

polish surrounding the coverslip and were dried for 5 minutes at room temperature. The slides were then observed using the Confocal microscope Leica TCS SP8.
The images were analysed using the LAX Software suite (Leica).

4.23.2. Antibodies

The primary antibodies [α-NS3 GTX12452(1:200) α-E s4G2 clone Hb119 (1:200)], and the secondary antibodies [(Alexa 555, rabbit α-mouse A-21427, Invitrogen), (Alexa 594 goat α-rabbit, A-11012, Invitrogen)] were diluted in a PermWash solution. Primary antibodies α-GAPDH (1:4000) (Genescript, A01622), α-flavivirus Glycoprotein (1:1500) (Abcam, Ab214336), α-p24 (1:1000) (Abcam, ab9044), α-VSV-Glycoprotein (VSV-G) (1:1000) (Sigma, V-5507) and secondary α-goat IgG HRP (1:4000) (Sigma, A8919), α-mouse immunoglobulins HRP (Dako, P0260) were diluted on 10% Non-fat-Dried Milk in 1X PBS 0.1% Tween.

4.24. CPER PCR (Circular polymerase extension reaction).

To create the circular structure required for the CPER sequences of the CMV promoter and an additional 200bp linking region was subcloned from pCDNA 3.1 plasmid (CACTCTCAGTACAATCTGCTCTGATGCCGCATAGTTAAGCCAGTATCTGCTCCCTG
CTTGTGTGTTGGAGGTCGCTGAGTAGTGCGCGAGCAAAATTTAAGCTACAACAAG
GCAAGGCTTGACCGACAATTGCATGAAGAATCTGCTTAGGGTTAGGCGTTTTGCG
CTGCTTCGCGATGTACGGGCCAGATATACGCGTTGACATTGATTATTGACTAGTTA
TTAATAGTAATCAATTACGGGGTCATTAGTTCATAGCCCATATATGGAGTTCCGCGT
TACATAACTTACGGTAAATGGCCCGCCTGGCTGACCGCCCAACGACCCCCGCCCA
TTGACGTCAATAATGACGTATGTTCCCATAGTAACGCCAATAGGGACTTTCCATTGA
CGTCAATGGGTGGACTATTTACGGTAAACTGCCCACTTGGCAGTACATCAAGTGTA
TCATATGCCAAGTACGCCCCCTATTGACGTCAATGACGGTAAATGGCCCGCCTGG
CATTATGCCCAGTACATGACCTTATGGGACTTTCCTACTTGGCAGTACATCTACGTA
TTAGTCATCGCTATTACCATGGTGATGCGGTTTTGGCAGTACATCAATGGGCGTGG
ATAGCGGTTTGACTCACGGGGATTTCCAAGTCTCCACCCCATTGACGTCAATGGGA

GTTTGTTTTGGCACCAAAATCAACGGGACTTTCCAAAATGTCGTAACAACTCCGCC CCATTGACGCAAATGGGCGGTAGGCGTGTACGGTGGGAGGTCTATATAAGCAGAG CT), Hepatitis Delta Rybozyme sequence was kindly donated by Dr Jordan Clark from Glasgow university and was subcloned from a propietary plasmid (GGGTCGGCATGGCATCTCCACCTCCTCGCGGTCCGACCTGGGCATCCGAAGGAG GACGCACGTCCACTCGGATGGCTAAGGGAGAGCCACTTTTCTCTCGATTCTCTATC GGAA), the Simian vacuolating virus 40(SV40) Poly adenilation signal was subcloned from pCDNA 3.1 plasmid (AACTTGTTTATTGCAGCTTATAATGGTTACAAATAAAGCAATAGCATCACAAATTTC ACAAATAAAGCATTTTTTTCACTGCATTCTAGTTGTGGTTTGTCCAAACTCATCAATG TATCTTA) in addition to the ZIKV genome divided into different fragments were cloned, primers displayed on Table 7.

Table 4.7. CPER primer design.

CPER Primer design 200 bp Linker region

Primer name	Sequence
5´upstream CMV Overlap Sv40pA Forward	TGTCCAAACTCATCAATGTATCTTACACTCTCAGTACAATCTGCTCTGAT
5´upstream CMV Overlap Sv40pA Reverse	CACACAGATCAACAACTAGCTCTGCTTATATAGACCTCCCACC
CMVP-C-96 Overlap Forward	GGTGGGAGGTCTATATAAGCAGAGCTAGTTGTTGATCTGTGTG
CMV C-96 Overlap Reverse	CCGACACTAGTATCTGCGCCTCGT
C-96 PrM/E Overlap Forward	GGCTGCCATGCTGAGAATAATCAATGCTAG
C-96 PrM/E Overlap Reverse	CACCCCACATCAGCAGAGACGGCTGTGGAT
NS1-F1 Overlap Forward	CCTTAGGGGGGGTGTTGATCT
NS1-F1 Overlap Reverse	CCTCTTGCTGCTATACTTGAGGG
F1-F2 Overlap Forward	GATGAGGCCCACTTCACAGA
F1-F2 End Overlap Reverse	CACGTTTCCGCGTGCTCACTGC
F2-End Overlap Forward	CTGAAGCTCCCAACATGAAG
Zika Genome end HDVR Overlap Reverse	AGGTGGAGATGCCATGCCGACCCAGACCCATGGATTTCCCCACAC
HDVR Overlap Forward	GGTGTGGGGAAATCCATGGGTCTGGGTCGGCATGGCATCTCCACCT
hDVR SV40 pA Overlap Forward	CCACTTTTCTCTCGATTCTCTATCGGAAAACTTGTTTATTGCAGCTTATA
sv40pA with 5´CMV Reverse	ATCAGAGCAGATTGTACTGAGAGTGTAAGATACATTGATGAGTTTGGACA

PCR fragments were generated with high- fidelity Q5 DNA polymerase and primer pairs that have complementary ends with 24- to 30- nucleotide overlap. The resulting eight DNA fragments were then mixed in equimolar amounts (0.1 pmol each) and subjected to CPER with Q5 DNA Polymerase (an initial 3 min of incubation at 98ºC; 2 cycles of 30 seconds at 98ºC,30 seconds at 55ºC, and 6 minutes at 72ºC and 10 cycles of 30 s at 98ºC, 30 seconds at 55ºC and 72ºC for 8 minutes) to generate circular DNA.

Table 4.8. Temperature cycles for CPER.

Temperature	Time	Cycles
98ºC	3 minutes	
98ºC	30 seconds	2 cycles
55ºC	30 seconds	
72ºC	6 minutes	
98ºC	30 seconds	10 cycles
55ºC	30 seconds	
72ºC	8 minutes	
4ªC	Infinite hold	

4.25. Infectious sub genomic amplicons or Haiku.

Similar to the strategy designed for the CPER structure, the design was focused on the amplification of the ZIKV genome into different fragments with overlapping sequences, however, in this case no linking region was needed. CMV enhancer and promoter sequences were cloned from pCDNA3.1 (GACATTGATTATTGACTAGTTATTAATAGTAATCAATTACGGGGTCATTAGTTCATA GCCCATATATGGAGTTCCGCGTTACATAACTTACGGTAAATGGCCCGCCTGGCTGA CCGCCCAACGACCCCCGCCCATTGACGTCAATAATGACGTATGTTCCCATAGTAAC GCCAATAGGGACTTTCCATTGACGTCAATGGGTGGACTATTTACGGTAAACTGCCC ACTTGGCAGTACATCAAGTGTATCATATGCCAAGTACGCCCCCTATTGACGTCAAT GACGGTAAATGGCCCGCCTGGCATTATGCCCAGTACATGACCTTATGGGACTTTCC TACTTGGCAGTACATCTACGTATTAGTCATCGCTATTACCATGGTGATGCGGTTTTG GCAGTACATCAATGGGCGTGGATAGCGGTTTGACTCACGGGGATTTCCAAGTCTC CACCCCATTGACGTCAATGGGAGTTTGTTTTGGCACCAAAATCAACGGGACTTTCC AAAATGTCGTAACAACTCCGCCCCATTGACGCAAATGGGCGGTAGGCGTGTACGG TGGGAGGTCTATATAAGCAGAGCT), two different variants of the HDVR sequences were used. Variant 1: Chain R, Precursor Form of The Hepatitis Delta Virus Ribozyme (GATGGCCGGCATGGTCCCAGCCTCCTCGCTGGCGCCGGCTGGGCAACACCATTG CACTCCGGTGGTGAATGGGACT) and Variant 2 (GGGTCGGCATGGCATCTCCACCTCCTCGCGGTCCGACCTGGGCATCCGAAGGAG GACGCACGTCCACTCGGATGGCTAAGGGAGAGCCACTTTTCTCTCGATTCTCTATC GGAA). Primers are displayed on tables 9 and 10. The products from the PCRs were then purified and transfected either by electroporation or by polymer-based methods.

Table 4.9. Primers for Haiku strategy using HDVR variant 1.

Haiku Primer design Rybozyme sequence 1

Primer name	Sequence
CMV Enhancer and promoter Forward	GACATTGATTATTGACTAGTTATTAATAGT
CMV Enhancer and promoter Reverse	CACACAGATCAACAACTAGCTCTGCTTATATAGACCTCCCACC
CMV+C-96 Forward	GGTGGGAGGTCTATATAAGCAGAGCTAGTTGTTGATCTGTGTG
CMV+C-96 Reverse	CCGACACTAGTATCTGCGCCTCGT
Pr/M/E Forward	GGCTGCCATGCTGAGAATAATCAATGCTAGG
Pr/M/E Reverse	CACCCCACATCAGCAGAGACGGCTGTGGATAAGAAG
NS1-F1 Forward	CCTTAGGGGGGGTGTTGATCT
NS1-F1 Reverse	CCTCTTGCTGCTATACTTGAGGG
F1-F2 Forward	GATGAGGCCCACTTCACAGA
F1-F2 Reverse	CACGTTTCCGCGTGCTCACTGC
F2-END+HDVR Forward	CTGAAGCTCCCAACATGAAG
F2-END-HDVR-R-TAG Reverse	AGGCTGGGACCATGCCGGCCTGGATTTCCCCACACCGGCC
HDVR- SV40 pA Forward	GGCCGGTGTGGGGAAATCCAGGCCGGCATGGTCCCAGCCT
HDVR-SV40 pA Reverse	TAAGATACATTGATGAGTTTGGAC

Table 4.10. Primers for Haiku strategy using HDVR variant 2.

Haiku Primer design Rybozyme sequence 2

Primer name	Sequence
CMV Enhancer and promoter Forward	GACATTGATTATTGACTAGTTATTAATAGT
CMV Enhancer and promoter Reverse	CACACAGATCAACAACTAGCTCTGCTTATATAGACCTCCCACC
CMV+C-96 Forward	GGTGGGAGGTCTATATAAGCAGAGCTAGTTGTTGATCTGTGTG
CMV+C-96 Reverse	CCGACACTAGTATCTGCGCCTCGT
PrME Forward	GGCTGCCATGCTGAGAATAATCAATGCTAGG
PrME Reverse	CACCCCACATCAGCAGAGACGGCTGTGGATAAGAAG
NS1-F1 Forward	CCTTAGGGGGGGTGTTGATCT
NS1-F1 Reverse	CCTCTTGCTGCTATACTTGAGGG
F1-F2 Forward	GATGAGGCCCACTTCACAGA
F1-F2 Reverse	CACGTTTCCGCGTGCTCACTGC
F2-END+HDVR JRDN Forward	GGCCGGTGTGGGGAAATCCAGGGTCGGCATGGCATCTCCACCT
F2-END-HDVR-JRDN Reverse	ATTATAAGCTGCAATAAACAAGTTTTCCGATAGAGAATCGAGAGAAAAGTGG
HDVR pA SV40 Forward	CCACTTTTCTCTCGATTCTCTATCGGAAAACTTGTTTATTGCAGCTTATAAT
HDVR-pA SV40 Reverse	TAAGATACATTGATGAGTTTGGACAA

4.26. Electroporation of BHK-21 cells.

BHK-21 cells were prepared for electroporation of the subgenomic amplicons. Briefly, a flask of T175 BHK21 cells were washed once with room temperature 1X PBS. Then they were incubated with trypsin for 3 to 5 minutes. The trypsin was inactivated with 20 ml of DMEM media. Cells were counted and then spun down for 7 min at 300g, the cell pellet was resuspended in 10 ml of ice-cold PBS and spun down again for 7 min at 300g. $3x10^6$ cells per ml were resuspended in ice-cold Diethyl pyro carbonate (DEPC) PBS, 200 µl of the cell suspension were mixed with either 5 µg of RNA or the amount of DNA required after the equimolar calculation of the PCR products, the mixture was placed on the 2 mm electroporation cuvette (Gene Pulser/MicroPulser Electroporation Cuvettes). The electroporation was carried out in duplicate following the settings showed in table 11

Table 4.11. Settings used for electroporation of BHK-21 cells.

Setting	Condition
Voltage	260
Ms	25
No	1
Sec	0
Mm	2 or 4

The electroporated cells were resuspended in 10 ml of complete media, and the cuvettes were washed gently using the 200 µl pipette. The cells were then seeded into T25 flasks. Depending on the experiment, the cells were incubated for either 24, 48 or 72-hours prior virus harvest.

4.27. TransIT-LT1 and TransIT 293T transfection.

2.0 x10^5 293T cells/ml were plated in 2ml of complete DMEM medium on each well of a six-well plate and incubated overnight. Cells were between 60 and 70% confluent at the time of transfection. The TransIT-LT1 and TransIT 293T were warmed to room temperature and vortexed prior transfection. 250 µl of OptiMEM Reduced-Serum Medium were placed in a sterile tube, 10 µl of either the control plasmid, the PCR fragments or the CPER structure were mixed with the OptiMEM by pipetting. 7.5 µl of TransIT reagent were added without touching the tube walls and were mixed gently by pipetting. The mixture was then incubated for 30 minutes at room temperature.

The TransIT-DNA complex was added to the well drop by drop to different areas of the well, 2.5 ml of complete media were added after rocking the plate to distribute the complexes evenly. The cells were incubated for up to 96 hours with regular observation under a fluorescence microscope when the cytopathic effect was observed the cells were harvested for WB.

4.28. Electron microscopy

To image the viral particles within the cell during the replicative cycle, transmission electron microscopy was performed. Mock-treated and ZIKV-infected HEK293T cells were trypsinized and washed three times with room tempered 1X PBS and spun at 300 G for seven minutes. The cells were fixed using a 2.5% glutaraldehyde, 5mM calcium chloride and 0.1M sodium cacodylate, and then washed three times with 1X PBS. Subsequently at 300 G for four minutes. Subsequently. The cells were treated with a solution of 1% Osmium tetraoxide (OsO4), 1.5% potassium ferrocyanide and 0.1 M sodium cacodylate for 25 minutes. The cells were washed two times with distilled water and three times with 1X PBS at the speed and times used before. The next step was the sample dehydration using increasing concentrations of ethanol, starting with 50%, followed by 70% and finally 90% for 10 minutes each time and then two times with 100% ethanol for 10 minutes. The alcohol was removed, and then propylene oxide was added to get rid the remaining traces of ethanol, a preinclusion on a 1:1 polybed-alcohol was carried out for 90 minutes. Finally, two inclusion on pure resin were performed, the cells

were polymerized on BEEM capsules at 60ºC overnight and contrasted using 5% uranyl acetate prepared on 50% methanol for 18 minutes, followed by a final treatment with Reynolds lead for 2 minutes. Once the cells were stained, they were observed using an electron microscope (JEOL JEM 1011, JEOL Ltd Tokio), Dra. Bibiana Chavez Munguia carried out this procedure on the Center for Research and Advanced Studies of the National Polytechnic Institute, Mexico City, Mexico.

5. Results.

5.1. ZIKV sequences alignment and identification of mutants.

ZIKV outbreak in the Americas can be easily tracked using the reported sequences from the continent. However, little sequences are available from Asia before the 2015 outbreak. During the sequence analysis, samples from America, Asia and Africa were also included due to the passage of the virus across the globe during previous outbreaks that preceded its arrival to Brazil. In the first place, we selected the strains of Zika that would be subjected to bioinformatic analysis. The criteria for selection were the following: Being ex vivo samples, being collected during the Pacific outbreak that preceded the American outbreak, being representative of the region (Asia, America, Africa, and the pacific) the samples were isolated from different sources or biological fluids without cellular passage **(Figure 5.1)**.This last criterion was especially crucial since previous reports have identified the presence of the virus in a wide variety of organs and fluids, demonstrating its extensive tropism.

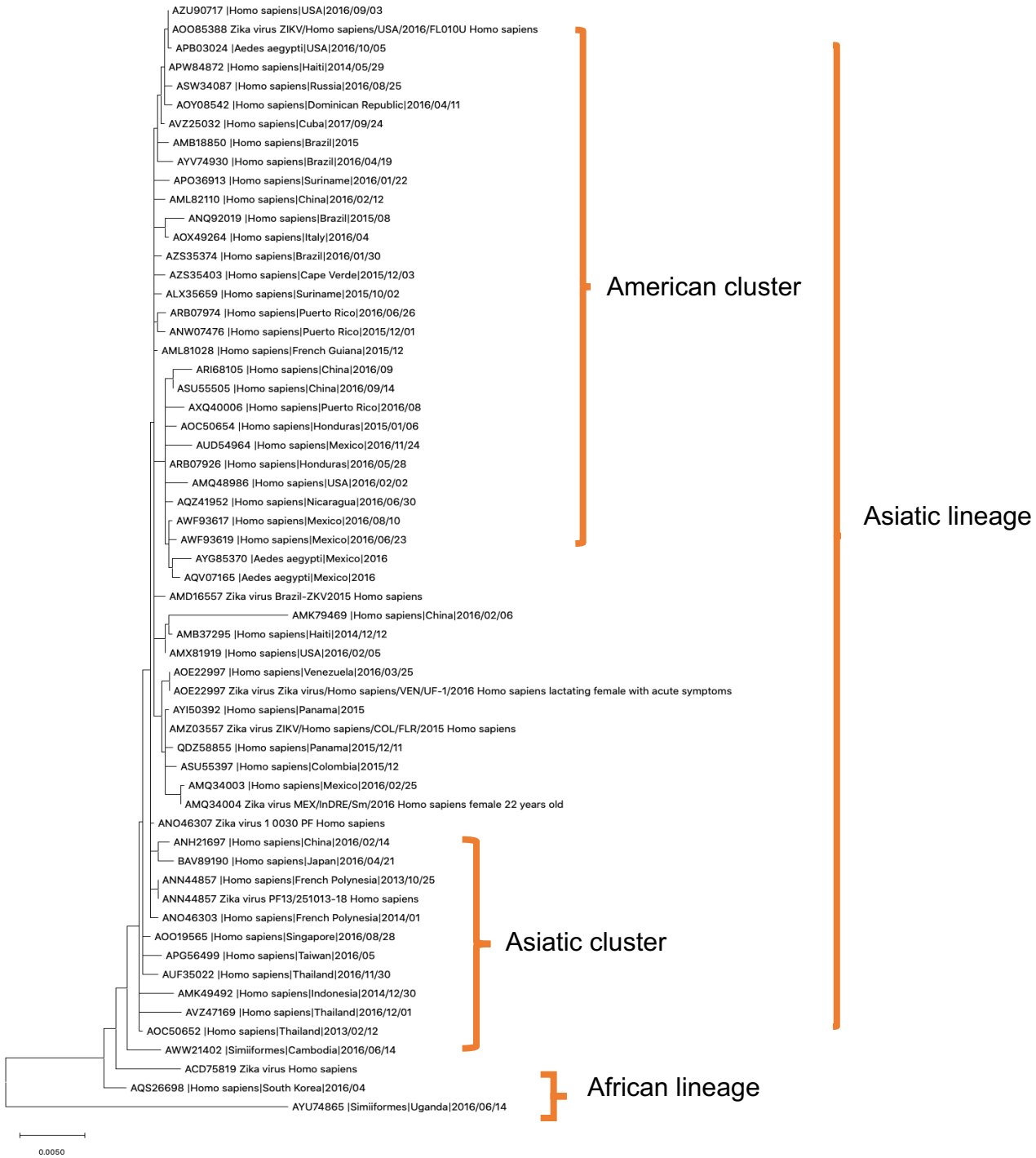

Figure 5.1. Phylogenetic tree of 59 ZIKV sequences from America, Asia, and Africa. The tree shows that the African lineage and the Asiatic lineage are

distinguishable, the American samples are also contained within the Asiatic lineage. (Cladogram elaborated with MEGA X software).

Eight samples were selected from the sequences above **(Table 5.1)**. The samples were picked from the outbreaks that preceded the Brazilian outbreak, the sequences from Micronesia and French Polynesia are the closest in time and geographically. Within these locations, the first cases of microcephaly were reported, from this time point onward the sequences were selected from different countries representatives of the cases within the continent.

Table 5.1. ZIKV strains retrieved from GenBank. Within the table, the characteristics of the samples are listed, including the country, the year of collection, the identification, the host, and the source of isolation.

City/Country	Date	Identification Number	Host	Isolation source
Yap Islands, Micronesia	2007	EU545988	Homo Sapiens	N. A
French Polynesia	25/10/13	KX369547	Homo Sapiens	Serum
French Polynesia	2013-2014	KX447515	Homo Sapiens	Serum
Brazil	2015	KU497555	Homo Sapiens	Amniotic Fluid
Colombia	2015	KU646827	Homo Sapiens	N. A
Barranquilla, Colombia	2015	KX087102	Homo Sapiens	Aedes albopictus cells
Venezuela	2016	KX702400	Homo Sapiens lactating female	Whole breast milk
Chiapas, Mexico	2016	KU922960	Homo Sapiens female	Saliva
Florida, U.S. A	2016	KX842449	Homo Sapiens	Urine

The sequences were then aligned to construct the three displayed below **(Figure 5.2).** This alignment was used to identify mutants within the Pr, M and E protein. As the three shows, two different clusters are formed, one comprising the American samples and one that is constituted with the samples that proceed from Micronesia and French Polynesia.

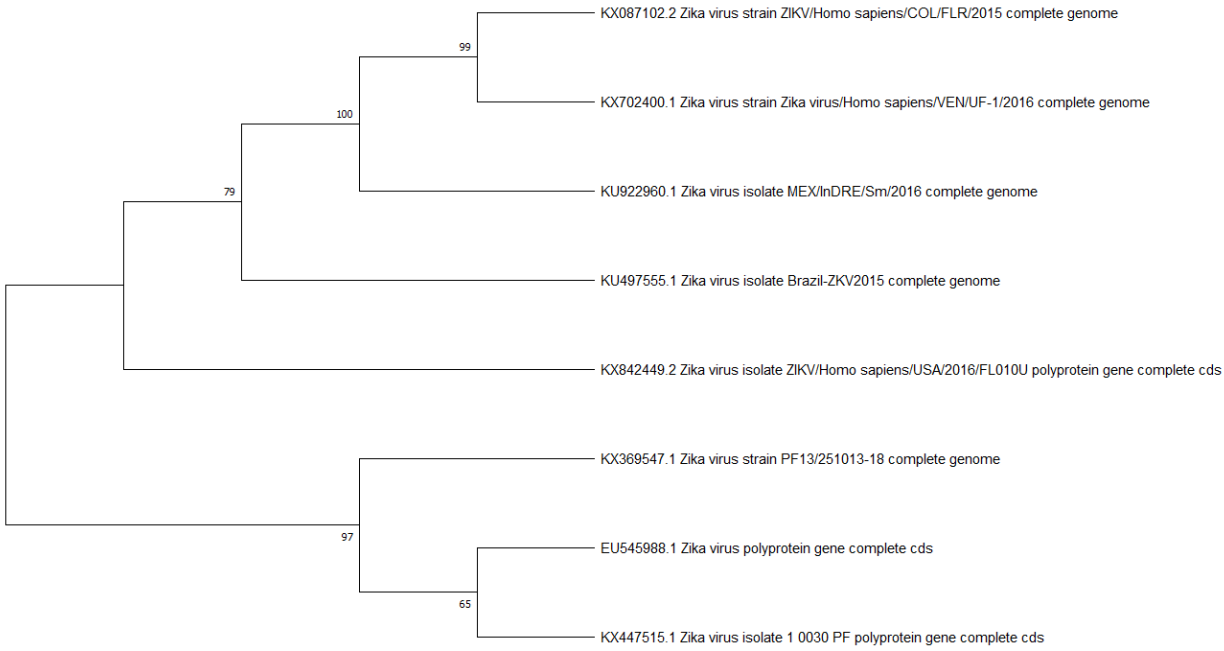

Figure 5.2. Phylogenetic tree of nine ZIKV sequences comprising samples from before and during the American outbreak. The analysis shows that even with the American and Asiatic lineage, the sequences can be distinguished from a temporal and geographic perspective (Cladogram elaborated with MEGA X software using the bootstrap method as stated in methods section).

5.1.2. Identification of the mutants within the membrane and envelope proteins.

Once the sequences were appropriately selected and identified, a multiple alignment analysis (Clustal W) was carried out to determine the changes in both nucleotide and amino acid sequences. Almost 50-point mutations across the strains were analysed, but only eight mutations were significant. These mutations were either within groups or across them, for example from alanine to valine or from histidine to tyrosine. (Appendix)

These mutations were found either in the Pr/M protein or in the domains DI, DII or the DIII of E protein. However, no mutations were found within the fusion loop of DII of the E protein.

In **tables 5.2.** and **5.3.** are listed the mutations that were selected for further experiments (**Figure 5.3)**. These mutations represent the natural changes that occurred during the passaging from Asia to America. The mutations selected were planned to be introduced into the templates derived from PCCI-SP6-ZIKV-EGFP and PCCI-SP6-ZIKV plasmids. Most of the changes observed during the comparison of the isolates against the base sequence are found in the Yap Island Isolates, which corresponds to one of the most recent outbreaks (2007) of the virus and a crucial step in its travel from Asia to America.

Table 5.2 Substitutions in the PrM-E (DI) used in the mutagenesis of the template.

Amino acid changes in PrM-E DI between the isolates

Base a.a	Changed to	Isolate
Alanine ^{123} (A)	Valine (V)	Yap Islands 2007 (EU545988)
Asparagine^{139}(N)	Serine (S)	Yap Islands 2007 (EU545988)
Phenylalanine^{257} (F)	Leucine (L)	French Polynesia 2013 (KX369547)
Threonine^{300} (T)	Alanine (A)	Yap Islands 2007 (EU545988)
Serine^{550} (S)	Threonine (T)	Brazil 2015 (KU49755)

Table 5.3 Substitutions in the DIII of E used in the mutagenesis of the template.

Base a.a	Changed to	Isolate
Histidine ^{691} (H)	Tyrosine (Y)	French Polynesia 2013 (KX447515)
Methionine ^{763}(M)	Valine (V)	Yap Islands 2007 (EU545988)

Methionine ^{777} (M)	Threonine (T)	Yap Islands 2007 (EU545988)

Due to the differences that appeared in the clinical landscape produced by the ZIKV infection, including neuroinvasion, it is possible that the mutations occurred within the glycoprotein sequence conferred a broader ability to infect new tissues and cell types.

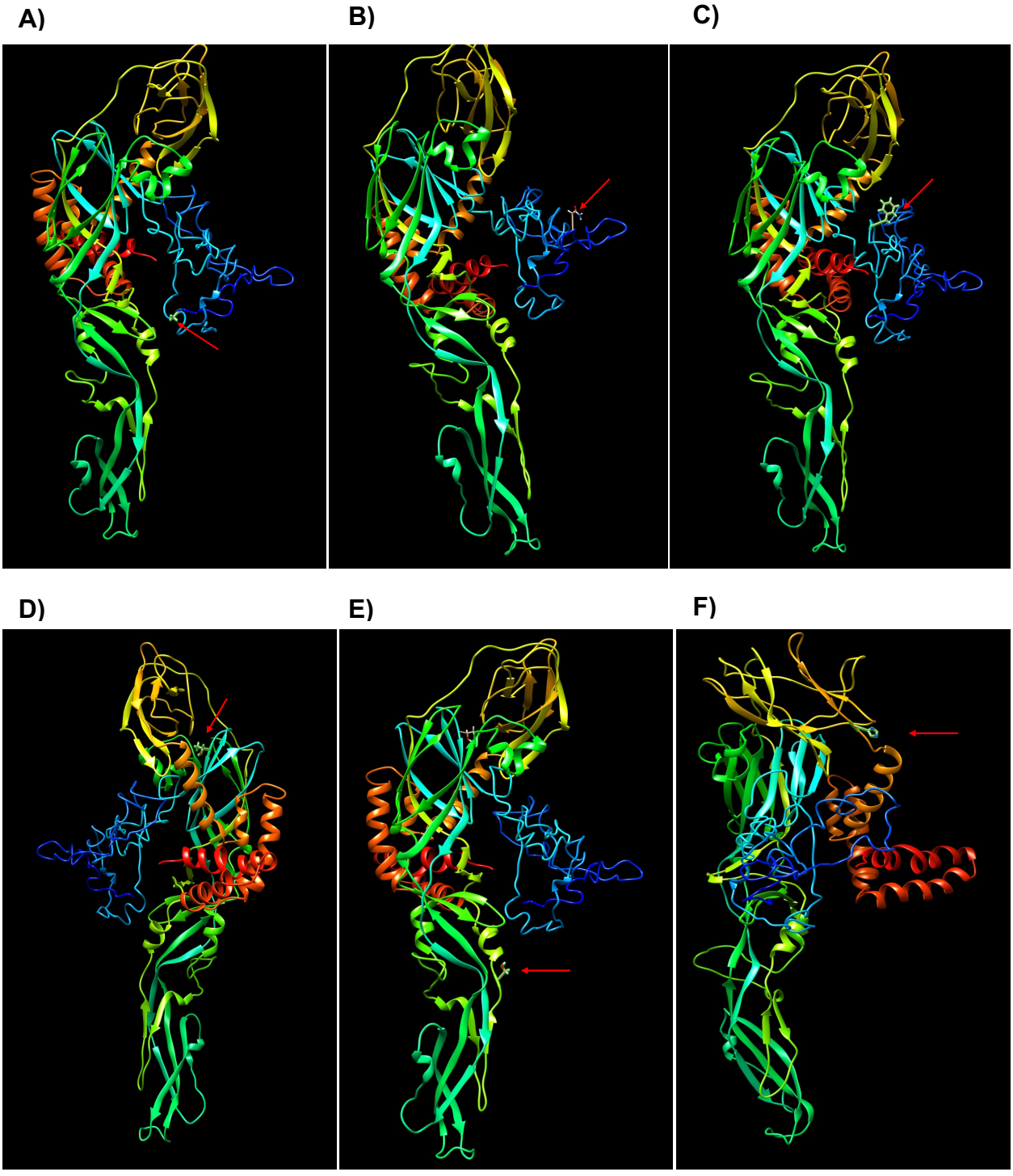

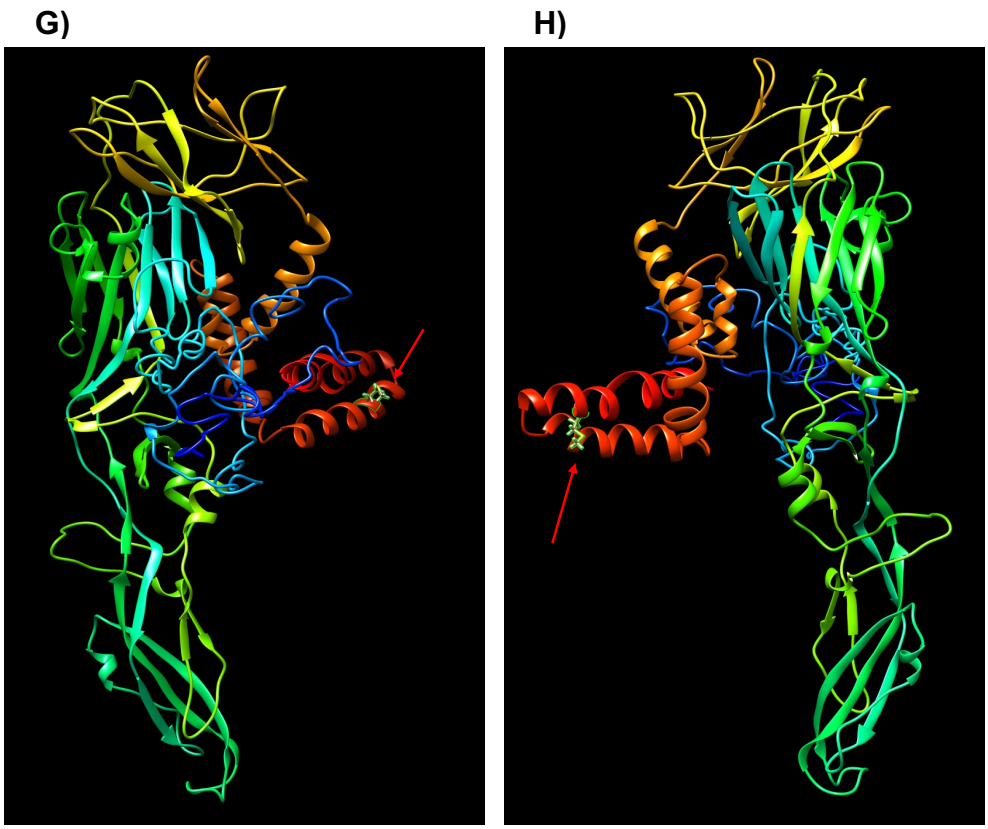

Figure 5.3. Schematic representation of the mutants and their location on PrM/E protein. The aminoacidic changes were highlighted on the protein structure of ZIKV PrM/E model (constructed homology modelling using KU97555 reference sequence) A) [A^{123}->V], B) [N^{139}->S],C) [F^{257}->L],D) [T^{300}->A],E) [S^{550}->T], F) [H^{691}->Y],G) [M^{691}->V] ,H) [M^{777}->T] red arrows are used to mark the position of the mutation.

5.2. ZIKV glycoprotein cloning.

Once the mutations were selected, plasmids PCCI-SP6-ZIKV-EGFP and PCCI-SP6-ZIKV plasmids were used as templates for cloning two versions of the ZIKV glycoprotein. From the PCCI-SP6-ZIKV plasmid, a PCR product containing the 3′ 96-nucleotide region of the C gene (corresponding to amino acid residues 101 to 114, which encode the signal peptide) and full-length PrM/E genes were obtained, this fragment had an expected size of approximately 2 Kbp. A second PCR product was created using the PCCI-SP6-ZIKV-EGFP template; this product contained the 3′ 96-nucleotide region of the C gene, GFP,

Foot-and-mouth disease virus 2A protease full-length C/PrM/E genes. The expected size of this product was around 3 Kbp **(Figure 5.4.)**

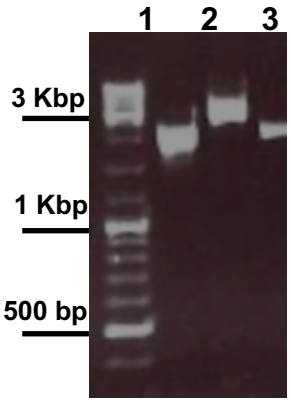

Figure 5.4. ZIKV Pr/M/E and C/GFP/PrM/E cloning standardisation. The bands represent the products of the ZIKV Glycoprotein cloning with or without the GFP reporter gene, as expected the band with the reporter has a size of more than 3000 base pair (3 Kbp) whereas the non-GFP version has a size of 2000 bp (2 Kbp). The first row shows the dilution of the non-GFP version of the product (using a 1:1000 dilution of the template). The second row shows the GFP version of the product; (using a 1:1000 dilution of the template). The third row shows the dilution (1:10,000) of a second non-GFP version of the product; this product was not used in further experiments.

A second PCR was carried out again using the dilutions described before; these products were introduced into pcDNA™3.1/V5-His TOPO plasmid **(Figure 5.5.)**.

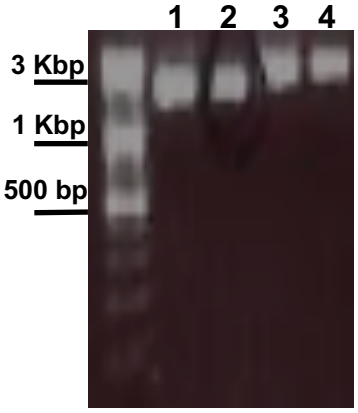

Figure 5.5. ZIKV PrM/E and C/GFP/PrM/ E cloning. A series of duplicates of the PCRs from the glycoprotein were carried out. Row one and two shows the products of the **ZIKV PrM/E** whereas rows three and four, shows the products of the **ZIKV C/GFP/PrM/ E cloning**.

Moving forward after products were identified, was the transformation using heat shock of *E. coli* with the products of the plasmid insertion. The colonies from the transformed cells were screened, a total of sixteen colonies were tested using T7 forward, and BGH reverse primers (**Figure 5.6).**

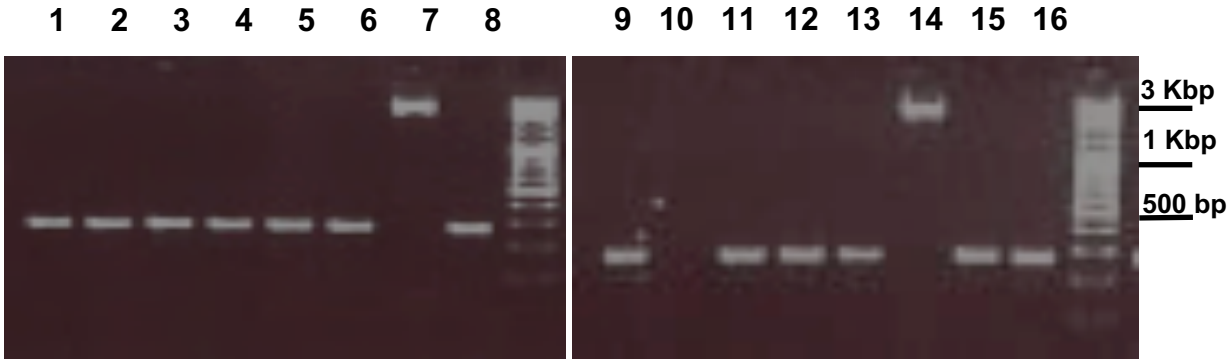

Figure 5.6. Colony screening for the pcDNA3.1 ZIKV C/GFP/PrM/E plasmid. Bacterial colonies grown overnight were screened using primers from sequences that flank the products. Colonies seven and fourteen were positives.

The same methodology was applied for the colonies from the transformation of the pcDNA3.1 ZIKV PrM/E plasmid **(Figure 5.7.).**

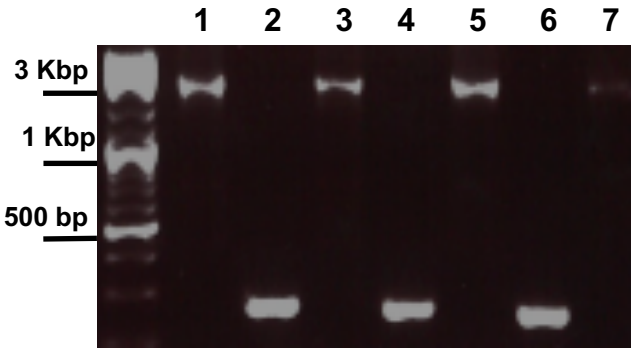

Figure 5.7. Colony screening for the pcDNA3.1 PrM/E plasmid. Bacterial colonies were screened for the ZIKV GP plasmid, positive colonies one, three and five can be seen in the agarose gel.

The positive colonies were then seeded on tubes containing five millilitres of LB media and incubated overnight at 37ºC under shaking. The cells were harvested, and the plasmids were isolated. The identity of the insert was corroborated using Sanger sequencing; the plasmids were named pcDNA3.1 ZIKV C/GFP/PrM/E and pcDNA3.1 ZIKV PrM/E.

Having cloned the wild-type glycoprotein and the GFP version on plasmids the next stage was to introduce the mutations using a single step site-directed mutagenesis kit.

5.2.2. Site-directed mutagenesis.

Once the pcDNA3.1 ZIKV C/GFP/PrM/E and pcDNA3.1 PrM/E constructions were fully identified and propagated, following with the workflow the addition of the mutations from tables 5 and 6 to the glycoprotein sequence was carried out. The mutagenesis was carried out on ZIKV C/GFP/PrM/E with the full set of primers described in the methods chapter. The products of the Q5® Site-Directed Mutagenesis Kit were transformed in E.

coli cells followed by the colony screening. **Figure 5.8** shows a representative gel of the colony screening performed to the mutant panel.

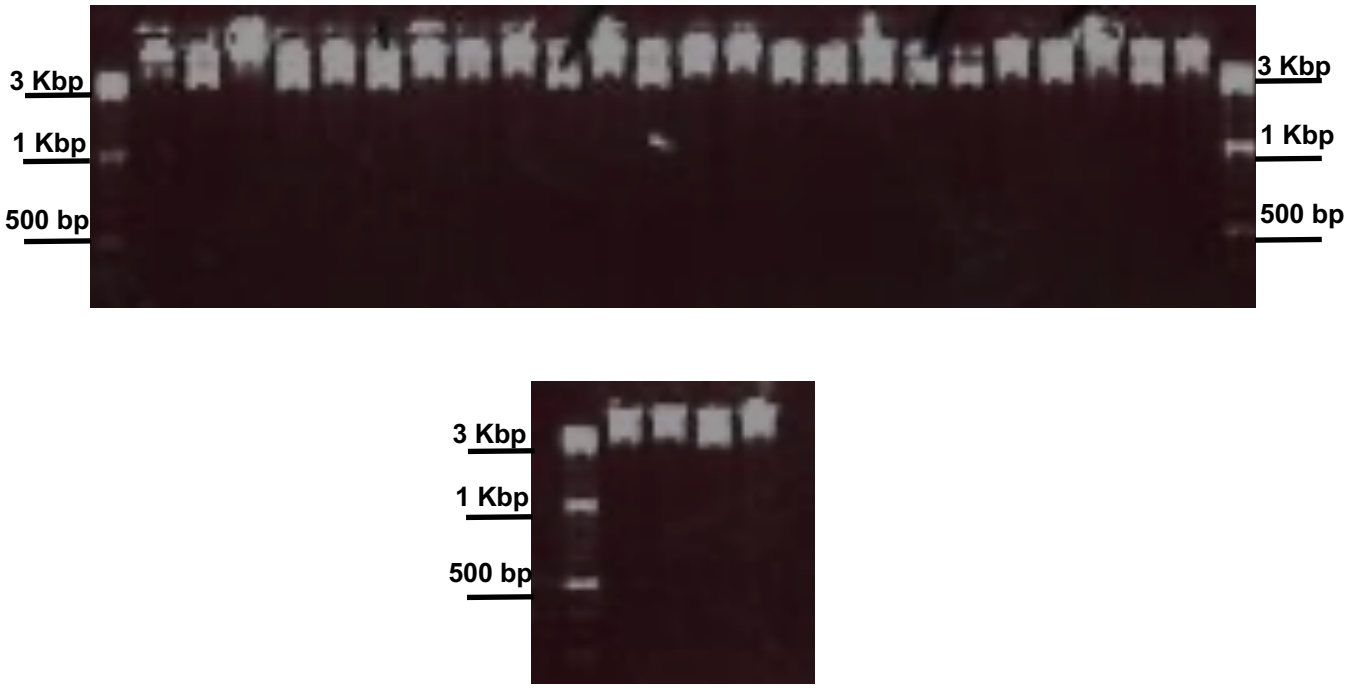

Figure 5.8. Mutant selection for the plasmid ZIKV C/GFP/PrM/E. The plasmids isolated from the colonies were screened for the mutants; the products were amplified using T7 and BgH primers. The mutations were identified using Sanger sequencing since there are no specific traits nor size difference is noticeable.

Almost all the colonies screened were considered wild type (WT), or without the mutation, only two colonies were positively verified by Sanger sequencing. The positive colonies for the mutations were then seeded in LB media and incubated overnight at 37ºC on a shaker. The cells were then either stored on glycerol stocks or harvested for plasmid purification.

Once the genes were cloned and the mutations introduced into the plasmids, a pseudotype assay was carried out supplementing the ZIKV PrM/E as a heterologous Glycoprotein.

5.3. Receptor screening on HEK293T and HUH7

Before testing infectivity of the mutants using the pseudotyping model, abundance of the messenger RNA of the proposed ZIKV cellular receptors (CD299, AXL, TYRO3, HAVCR1) was evaluated **(Figure 5.9.)** The cDNA was produced using reverse transcription of the mRNA, serial dilutions of the cDNA were electrophered on a 2% agarose gel.

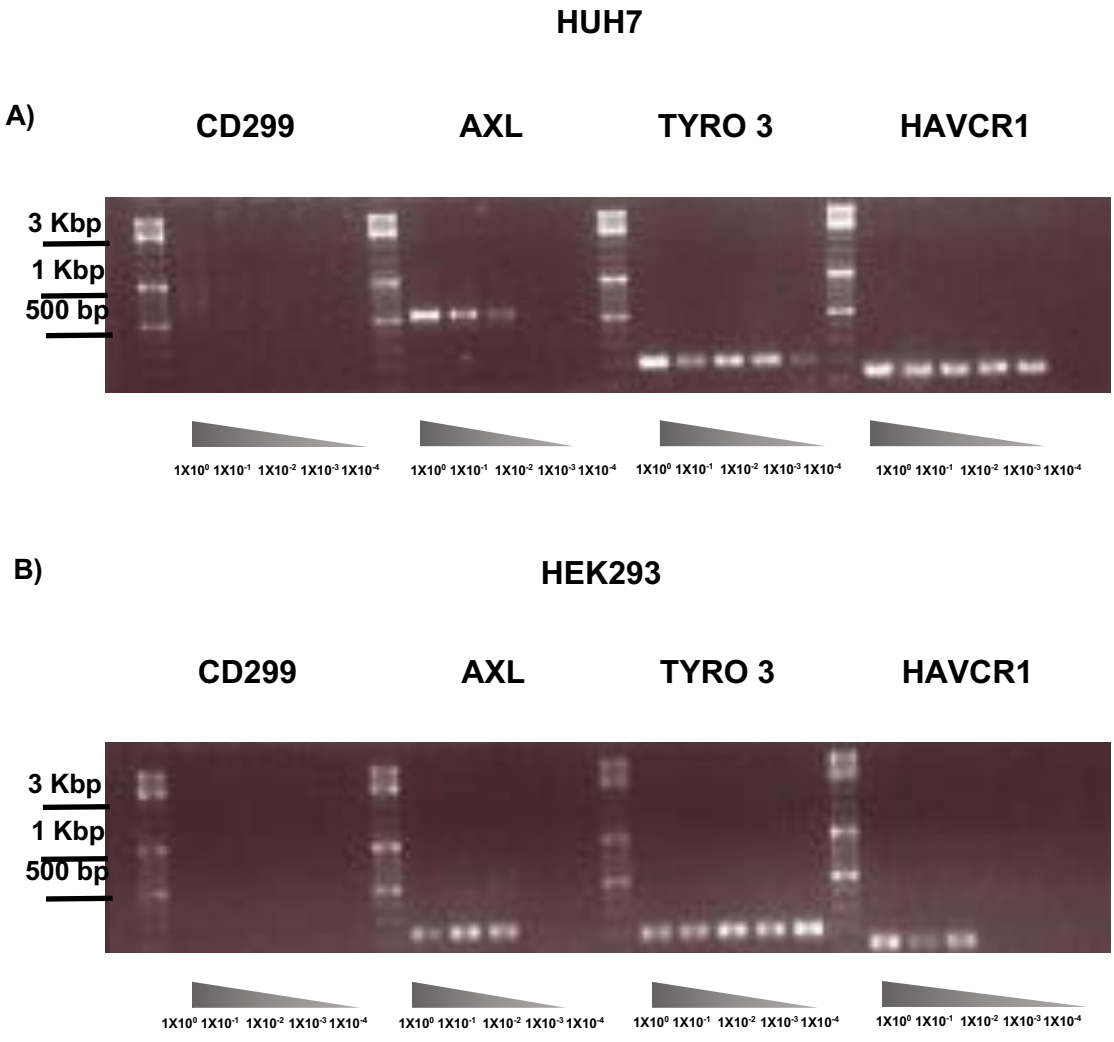

Figure 5.9. Receptor screening in Huh7 and 293T. PCR products from the different receptors screened as receptors for ZIKV, the base ten dilutions of the cDNA give a

perspective of the abundance of the receptor in the cells. **A)** three out of the four receptors were present in the HUH7 cells cells (AXL-TYRO-HAVCR1). **B)** PCR products from the different receptors in 239T cells, 3 out of the four receptors were present in the cells. (AXL-TYRO-HAVCR1).

These results should be taken with caution due the fact that presence of messenger RNA doesn't always translates to presence of the protein an additional step of protein identification may be required to validate these results, additionally a control of positive expression of CD299 is required to verify that the cells are not actually expressing this gene and it is not a design fault of the primers. The results regarding AXL, TYRO 3 and HVCR1 expression help to support the observations that HUH7 and HEK293T are permissive to ZIKV infection and may be due the fact that the proposed cellular receptor is present. Interestingly, AXL was observed on HUH7 cells with bigger size than the expected for the product this might be due the presence of contaminating genomic DNA on the samples used for amplification, it will be worth treating the samples with DNAse to get rid of non-desired genetic material.

5.4. Pseudotype production and infectivity.

The pseudotyping assays are based on using a retroviral backbone based on HIV-1 or other retroviruses supplemented with the glycoprotein of other viruses, thus assessing the impact in the infectivity of the wild-type protein or the mutants. The backbone also includes a reporter gene to help to measure the infectivity of the pseudoparticles. pNL4.3 HIV-1 based retroviral backbone was used for the experiments below; the plasmid encodes for the components necessary to assemble the virion and the signal to incorporate the reporter gene (luciferase) into the treated cells. However, the gp160 is truncated and requires the supplementation with the GP of interest, for example, ZIKV glycoprotein as a problematic sample and VSV-G as control. VSV-G is a standard protein with a broad tropism among cell types and species which is helpful in cases like this since different cell lines from different mammals were tested to try to standardise the plasmid concentrations and ratios.

Since little information is available about pseudotyping flaviviruses such as Dengue, Yellow Fever or Zika, a standardization process was carried out to try to find the proper concentration of viral GP needed to produce infectious PPs. The cell line chosen for the first experiments was HEK293T due its permissibility to the ZIKV infection. Two controls were used to secure that the chemiluminescence recorded during the luciferase assay was due to the infection process and not background noise or unspecific interactions between the particle and the cell. In **Figure 5.10**, graphs are displayed showing the luciferase assays using both constructions GFP (+) and GFP (-) plasmids (**Figure 5.10.A** displays the protein composition within the plasmids). Mock treated cells were treated the same way as the transfected cells; however, during the transfection protocol, no plasmids were used only PEI and Optimem. The Δ-Env control consists in the transfection of the pNL4.3 retroviral backbone plasmid without the heterologous GP; this control allowed the detection of the noise produced by the unspecific internalization of the particle into the cells, in the case of luciferase activity detection it would be due to incorporation of the PP that was not mediated by a cellular receptor. Finally, the positive control for the system consists on the addition of a plasmid that encodes a standard GP that is known to work on the cell line or species that is going to be tested, due to its broad tropism and the reproducibility of the results VSV-G was used. Increasing amounts of both ZIKV PrM/E GFP (-) and ZIKV PrM/E GFP (+) plasmids were tested, previous studies conducted in the lab standardized a concentration of 2 µg of plasmids. A fixed concentration of 2 µg of pNL4.3 backbone was added for all the samples, but the mock, 2 µg of VSV-G were added to the positive control.

The lowest amount of plasmid used for transfection was 1 µg, and it was increased microgram by microgram until reaching 5 µg. HEK293T cells were used to produce the particles; since the PPs are secreted to the extracellular media, the supernatants were harvested and filtered after 72 hours. In the first instance, the luciferase activity was measured on the producer cells. The producer cells produce both the viral proteins (HIV and ZIKV) and the luciferase reporter gene, by measuring the enzymatic activity at the end of the production time, just after the medium harvesting it gives information about the

expression of the pNL4.3 plasmid proteins. On the other hand, when the treated HEK293T cells are exposed to the PPs, the efficacy of the infection is measured by the enzymatic activity on the infected cells. **Figure 5.10.B** shows the enzymatic activity in both the producer and the infected cells when the luciferase activity is compared between these two groups of cells it clearly shows that the activity in the producer cells is orders of magnitude higher than the infected cells when it comes to the cells treated with PPs of the ZIKV GP. When the positive and negative control were analysed, they behave accordingly showing enzymatic activity in the producer cells but not in the infected cells in the case of the negative control (Δ-env) and activity in both the producer and infected cells when treated with VSV-G particles. However, when the activity of the infected cells has been measured no difference was observed when compared to the negative control (**Figure 5.10. B and C**), neither on GFP (+) or GFP (-) construct. It is worth noting, that as the plasmid amount increases in the producer cells during transfection the luciferase activity decreases, this effect is accumulative.

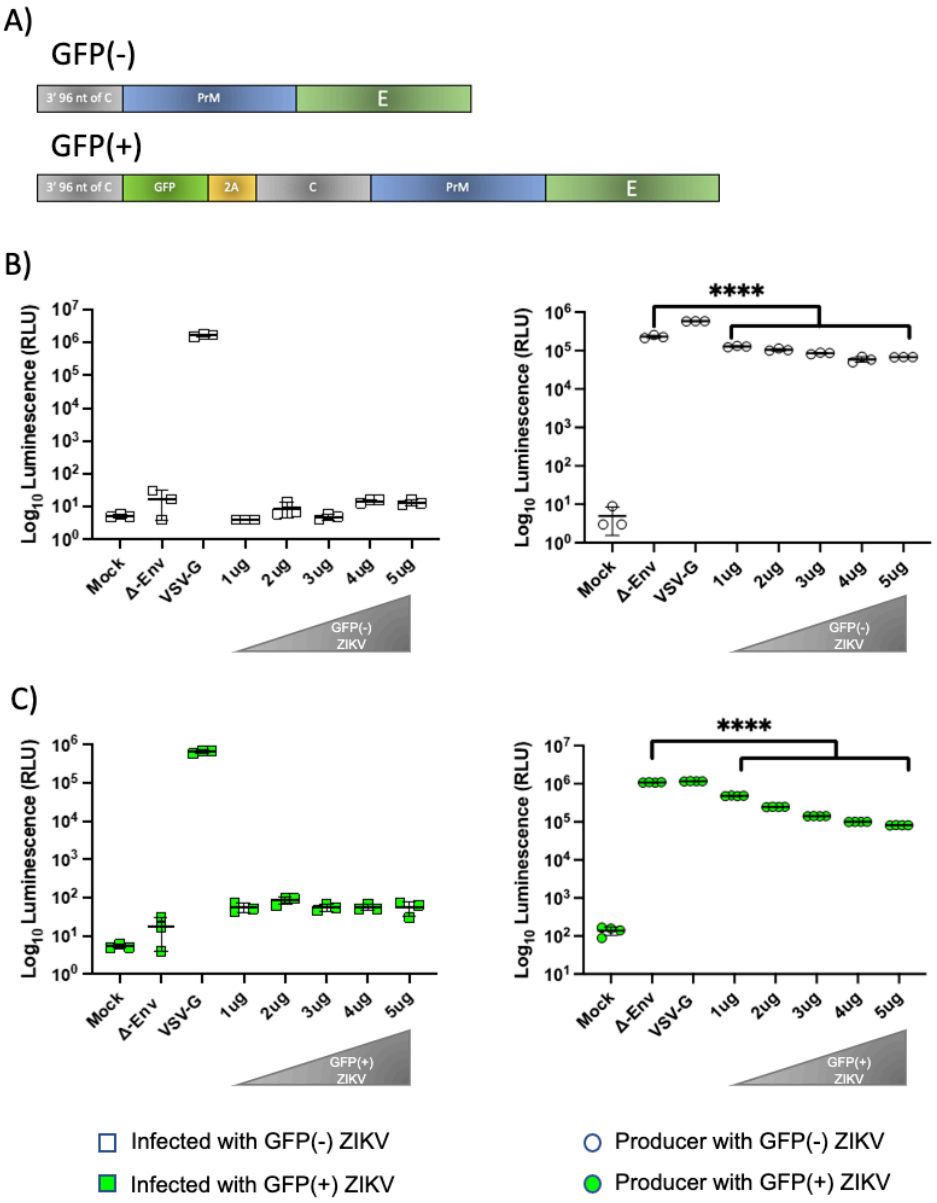

Figure 5.10. ZIKV GP sequence introduced on the plasmids and luciferase activity measured in both producer and infected cells. A) Viral proteins introduced into the plasmids to produce PPs. 293T cells were co-transfected with a fixed amount of 2 µg of the PNL 4.3 HIV based retroviral backbone and increasing amounts of **B)** GFP $^{(-)}$ ZIKV PrM and E glycoprotein plasmid or **C)** GFP $^{(+)}$ ZIKV PrM and E glycoprotein plasmid. The production of the retroviral proteins was measured using the luciferase reporter gene. Luciferase activity was expressed in relative light units (RLU). 293T cells were infected

with pseudo particles (pp) that include different viral proteins (VSV-G was used as positive control). Graphs show mean ± SEM of three independent experiments.

Due to the evidence displayed before, western blot assays were performed to detect the levels of protein expression in the producer cells and to detect the presence of the viral proteins in the supernatants. The proteins were divided between the components of the capsid (HIV-1 PrGag) and the viral glycoprotein (VSV-G and E protein). On **Figure 5.11** the WB shows the clear detection of the VSV-G band (**Figure 5.11. A**), whereas, when the ZIKV E protein was detected it shows the same effect as the cells that were measured for its luciferase activity, as the plasmid concentration increases the protein expression decreases and the band's detection goes dimmer compared to the lowest amount of plasmid (**Figure 5.11. B**). PrGag is a 55 KDa protein, and it is the precursor for the capsid when it is located within the cell, but it is processed into p24, p17 and p15 when the virion buds from the plasmatic membrane and it is a crucial step during viral maturation. WB assay was carried out looking for capsid precursor (**Figure 5.11. C**), a similar behaviour to the ZIKV GP was observed. The positive and negative control shows the expression of the HIV-1 protein; however, as the amount of the ZIKV plasmid increases the detection of the protein decreases in a dose-dependent way. Ultracentrifuged supernatants were probed against the same viral proteins, VSV-G was detected on the pelleted PPs (**Figure 5.11.D**), whereas, when the pellet was tested for ZIKV GP no band was detected. HIV p55 and p24 had similar behaviour, and the expression of the protein decreased as the amount ZIKV GP plasmid increases.

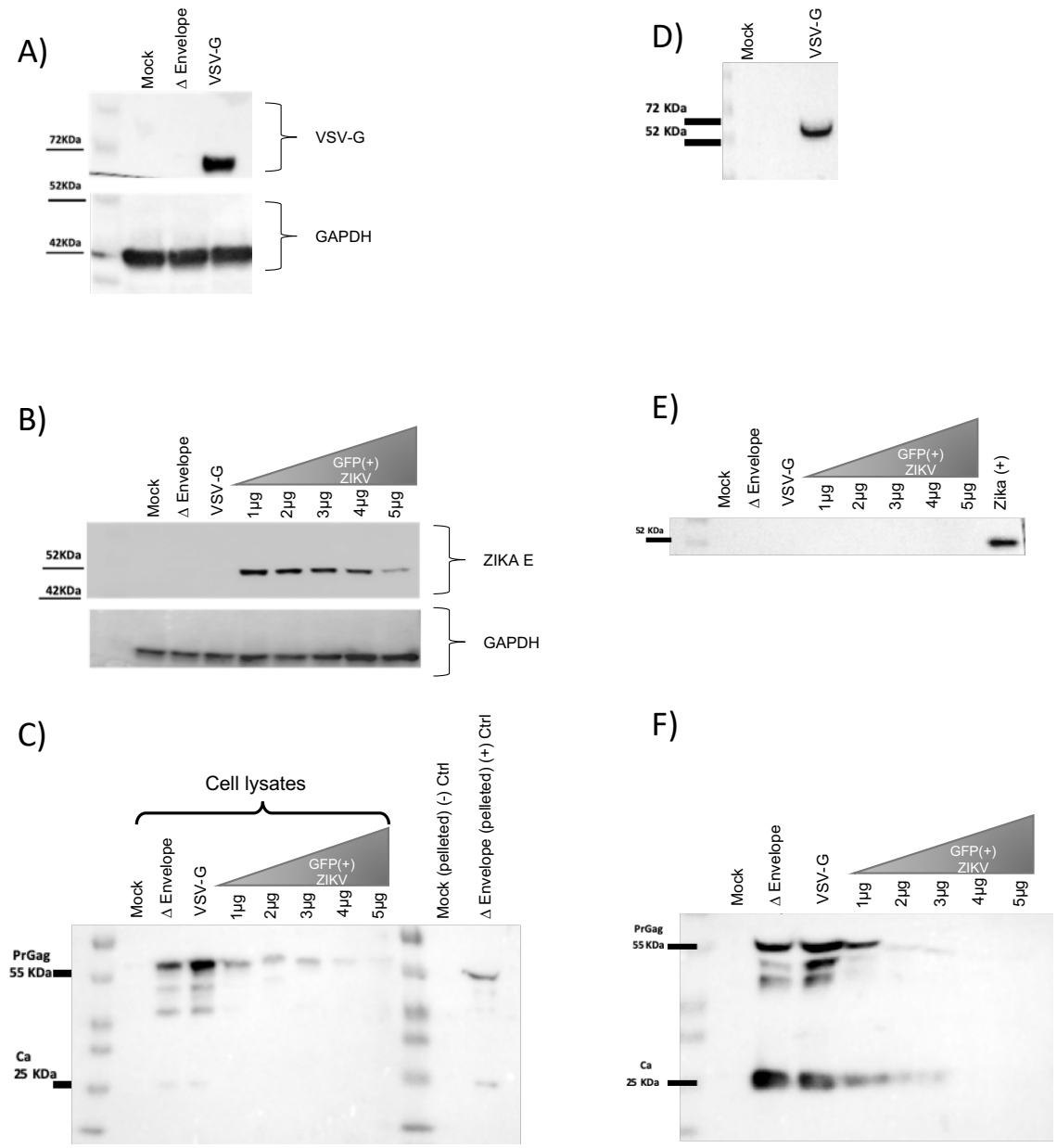

Figure 5.11. Detection of viral proteins in cell lysates and pelleted Pps by western blot assays. Cell lysates. The presence of viral proteins was measure using the anti VSV-G antibody in **A),** expression of Zika envelope protein detected using pan-flaviviral antibody **B), HIV** P55 PrGag protein and P24 **are** shown on **C)**. **Expression of the viral**

proteins was measured on pelleted PPs D) VSV-G. **E)** Zika glycoprotein. **F)** HIV PrGag and p24 were detected in supernatants.

Once the WB analysis was performed the expression of the protein within the cell was analysed using immunofluorescence. HEK293T cells were transfected with pNL4.3, and ZIKV PrM/E GFP (+) plasmid, HIV-1 p24 and E protein were probed (**Figure 5.12.**). Control cells (**Figure 5.12. A**) were mock-transfected but treated with both primary and secondary antibodies, these cells did not show any protein presence, and this corresponds to the previous experiments. ZIKV E protein was detected in the perinuclear region and the cytoplasm, GFP reporter gene was also observed (**Figure 5.12. B**). Finally, cells were co transfected with both plasmids and the viral proteins were detected along with the GFP reporter (**Figure 5.12. C**), also a colocalization analysis was performed for p-24 and E showing a moderated correlation between the two proteins (**Figure 5.12. D**)

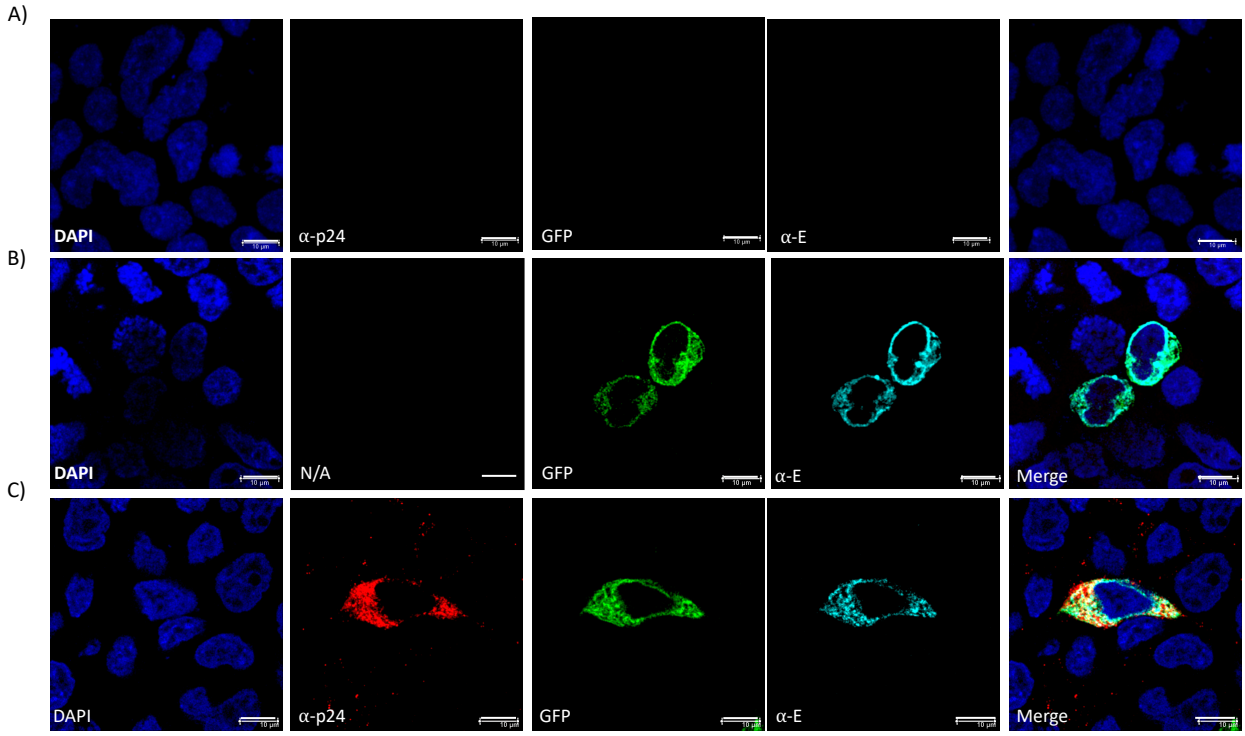

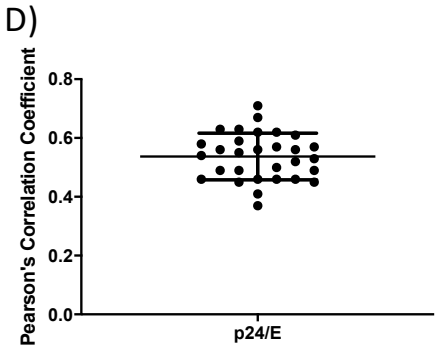

Figure 5.12. Immunofluorescence of transfected HEK293T cells against HIV-1 and ZIKV proteins. A) HEK293T control cells. B) HEK293T cells transfected with the GFP $^{(+)}$ ZIKV PrM/E glycoprotein plasmid, cell expressed both the reporter protein (green) and the viral GP/ E (cyan). C) HEK293T cells transfected with both GFP $^{(+)}$ ZIKV PrM/E glycoprotein plasmid and the pNL4.3 HIV-1 plasmid, cells expressed ZIKV E, and the capsid p24 HIV-1 protein (red). D)Pearson`s correlation coefficient graph, a moderated co-localization between ZIKV E and HIV-1 p24 was observed (co-localization= 0.53). Scale bar of 10µm , Image representative of a triplicate.

All the evidence described before suggested that a possible interaction between the plasmids may be downregulating the expression of the viral proteins. Thus, a matrix of different ratios of pNL4.3 and ZIKV PrM/E GFP (+) plasmids was tested (Figure 16). Increasing amounts of pNL4.3 (1 µg up to 5 µg) were tested against a fixed amount of ZIKV PrM/E plasmid. **Figure 5.13. A** shows the matrix of concentrations divided into five different graphs, no difference was observed on any of the samples compared with the negative control suggesting that the interference described before persisting even at lower or higher concentrations compared with the standard of 2 µg of each plasmid. Accounting the previous evidence, it was possible that the cell line was not permissive to the infection with the PPs, so CHO, BHK-21 and VERO cell lines were tested (**Figure 5.13. B**), no difference was observed between the cells infected with the ZIKV PPs compared with the negative control.

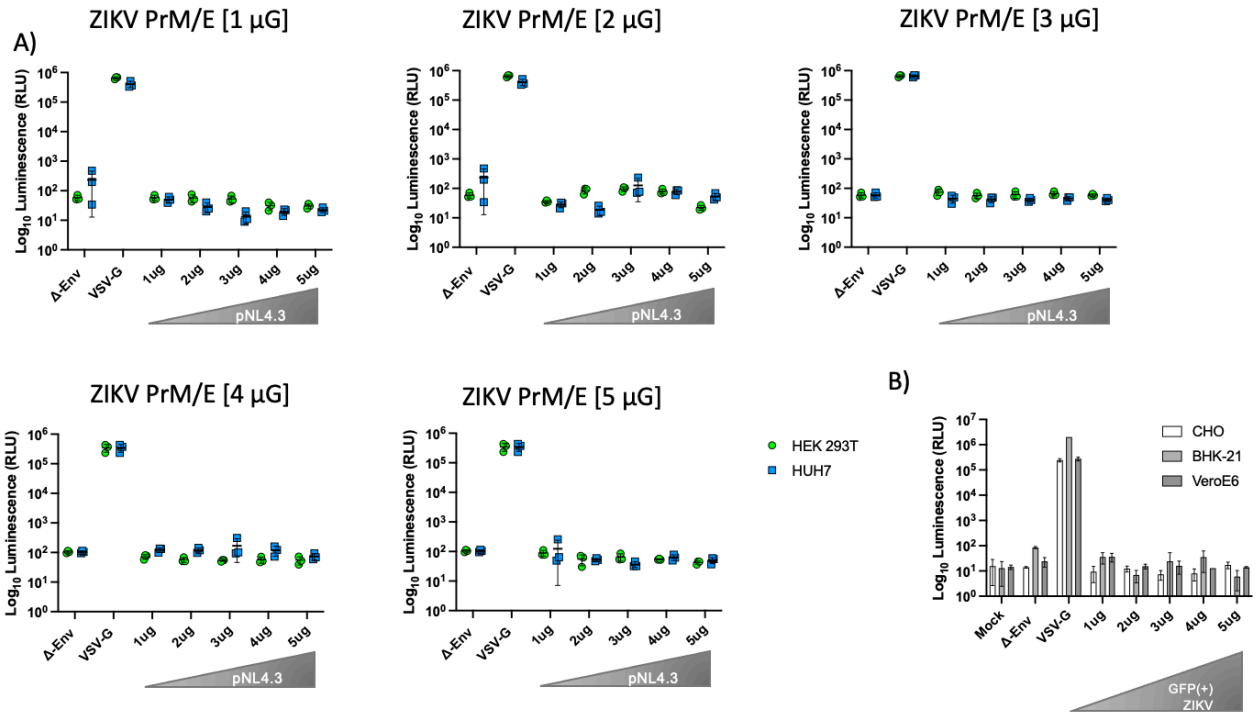

Figure 5.13. Different cell lines treated with Zika PPs. A) HEK 293T and HU7 cells treated with PP produced with different ratios of ZIKV glycoprotein and pNL4.3. A matrix of concentrations was designed to try to improve the pp production, different ratios of the plasmids were used, ranging from 1 µg to 5 µg of PNL 4.3 and 1µg to 5µg of Zika PrM/E. The PPs produced this way were used to infect HEK 293T and HUH7 cells. VSV-G was used as positive control and ∆ -Env as negative control. **B)** Mammalian cell lines VERO, BHK-21 and CHO were treated with PPs produced using increasing concentrations of Zika PrM / E plasmid (from 1 μg to 5 μg) in 293T cells. Graphs show mean ± SEM of three independent experiments.

After all the conditions tested before, three different strategies were proposed to tackle the issues discussed before: the supplementation of the viral protease NS3 and its cofactor NS2B may help in the processing of the viral glycoprotein, lower amounts of the GP plasmid may reduce the interference during co-transfection, use an MLV-based retroviral backbone may overcome the issues that occurred when using pNL4.3. First, the protease and the cofactor were cloned from the ZIKV containing plasmid (**Figure 5.14**), a product of 2.3 Kbp was inserted into pcDNA™3.1/V5-His TOPO plasmid.

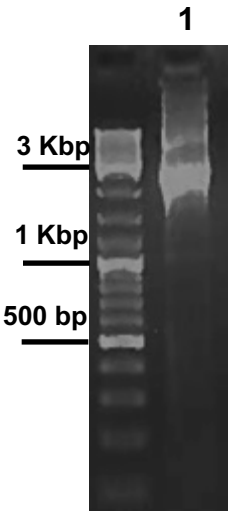

Figure 5.14. Zika protease NS2B/NS3 amplification. 1) Amplification of de ZIKV NS2B/NS3 gene from the PCCI-SP6-ZIKV plasmid,

HEK293T cells were transfected with the NS2B/NS3 and the ZIKV PrM/E GFP (+) plasmids; the protein expression was detected using IF against NS3 and E (**Figure 5.14.).**

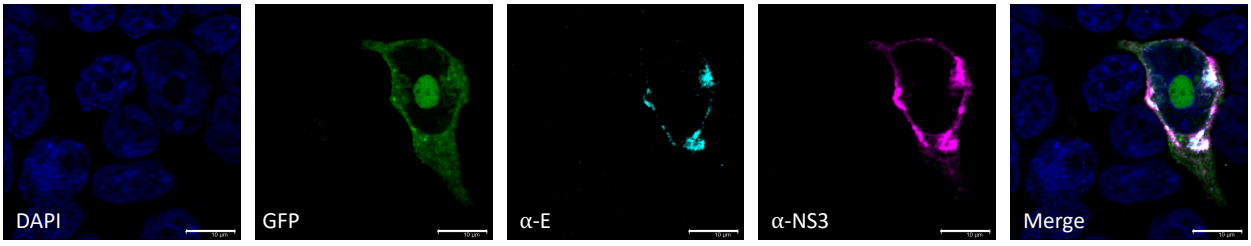

Figure 5.15 Immunofluorescence of transfected HEK293T cells against NS3 and E ZIKV proteins. HEK293T cells transfected with the ZIKV PrM/E GFP $^{(+)}$ glycoprotein plasmid, cell-expressed both the reporter protein (green) and the viral GP/ E (cyan), NS2B/NS3 (magenta) was also expressed by the cells. Scale bar of 10µm, Image representative of a triplicate.

Once the expression of the protein was detected, the infectivity assays were carried out (**Figure 5.16.**). Similar to previous experiments, enzymatic activity was measured in both the producer and the infected cells, as expected, the producer cells had detectable luciferase activity. When it came to the infected cells no difference was observed between the negative control compared with the cells treated with the PPs produced with a fixed

amount of pNL4.3 and ZIKV PrM/E GFP $^{(+)}$, supplemented with increasing amounts of the protease containing plasmid **(Figure 5.16 A)**. To test if the reduction in the amount of the PrM/E GFP $^{(+)}$ had any positive impact in the infectivity 5- fold dilutions were made (2µg,0.4 µg,0.08µg,0.016µg and 0.0032µg), this dilution had an impact slightly increasing the infectivity of the particles as the concentration decreased, however, no difference was observed when compared with the negative control (**Figure 5.16. B**). Finally, MLV backbone alternative was tested using the standard concentration 2µg for each of the plasmids, luciferase activity was detected on the producer cells and cells treated with the positive control. However, no increase on the infectivity was detected on the cells treated with the ZIKV GP PPs (**Figure 5.16. C**).

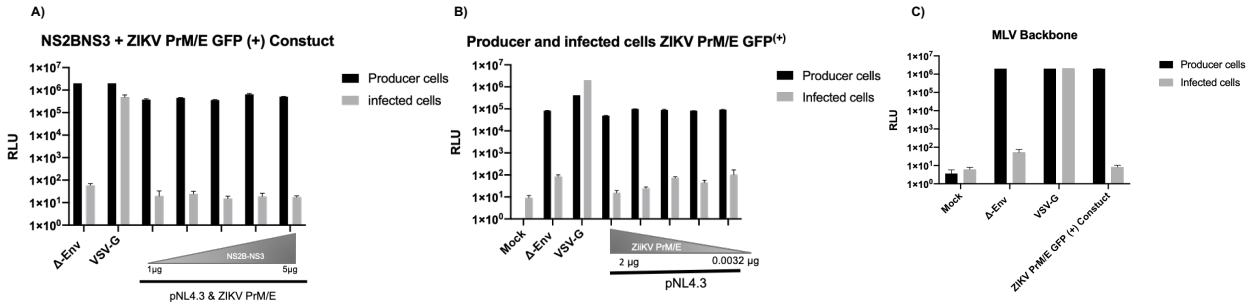

Figure 5.16. Luciferase activity measured in the producer and infected cells supplemented with viral protease plasmid. A) 293T cells were co-transfected with 2µg of the PNL 4.3 HIV based retroviral backbone and 2 µg of different viral glycoproteins (VSV-G, ZIKA). Increasing amounts (from 1 µg to 5 µg) of the NS2B/NS3 protease plasmid were added to the cells transfected with the Zika glycoprotein. B) 293T cells were transfected with a fixed pNL4.3 plasmid concentration (2µg) and with 5-fold dilutions of the ZIKV GP plasmid (2µg,0.4 µg,0.08µg,0.016µg and 0.0032µg). The production of the retroviral proteins was measured using the luciferase reporter gene, luciferase activity was expressed in relative light units (RLU). C) Murine Leukemia Virus (MLV) Backbone was tested at standard working concentrations for Zika virus glycoprotein in order to find infectivity differences between backbones. Graphs show mean ± SEM of three independent experiments.

With all the evidence gathered, it was possible that the GP was not located in the place where it can adequately interact. An IF assay was carried out to test if the ZIKV Envelope protein could be detected without permeabilization suggesting that the GP may be located in the plasmatic membrane a site that has been described as a site where the HIV buds and it incorporates the GP of interest. Cells that were not permeabilized did not emit any signal of the Envelope protein (**Figure 5.17.A**), and only the GFP reporter protein was detected, in contrast, the cells that were permeabilized did emit a signal for the Envelope protein (**Figure 5.17.B**) meaning that no detectable levels of protein were detected on the cell surface.

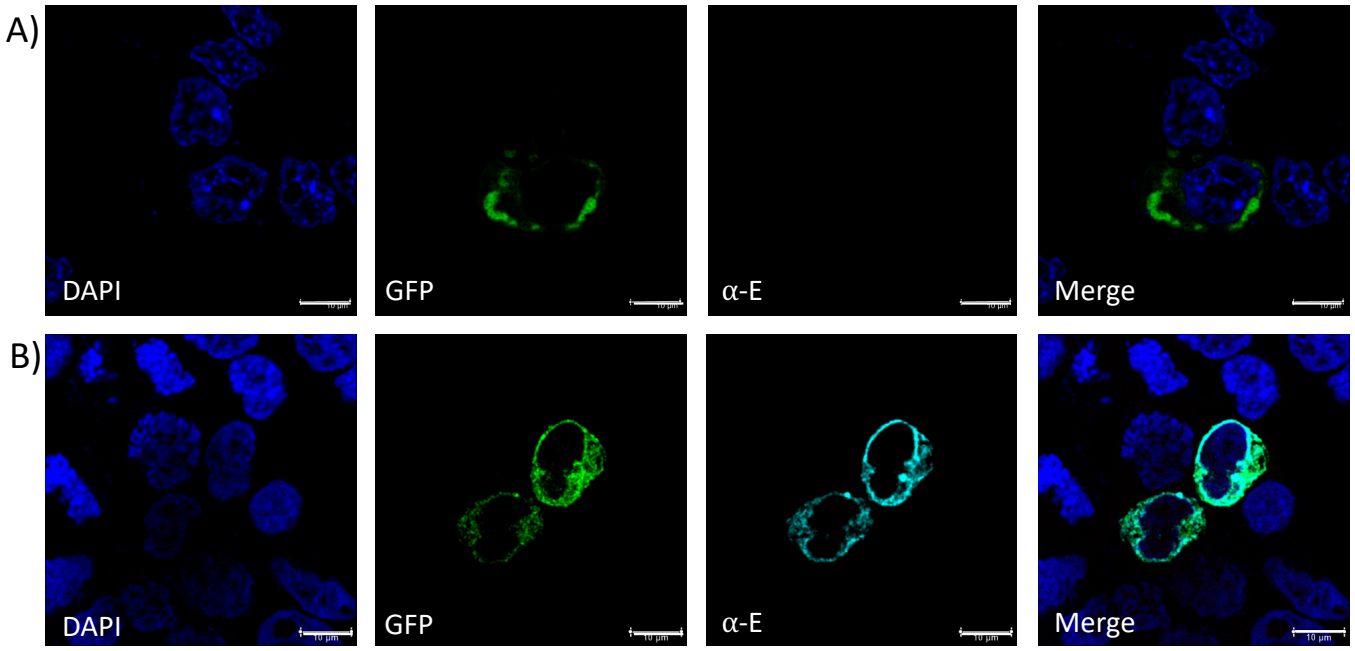

Figure 5.17. Immunofluorescence of nonpermeabilized and permeabilized HEK293T cells transfected with ZIKV PrM/E GFP (+) plasmid. A) HEK293T that were not permeabilized only emitted signal from the GFP reporter gene (green), whereas **B)** when the cells were permeabilized the antibody was able to interact with the viral protein E (cyan) and the GFP (green) was also detected. Scale bar of 10μm, Image representative of a triplicate.

Finally, since the protein degradation could be an issue during the incorporation of the heterologous glycoprotein different concentrations of the proteasomal inhibitor MG132 were tested. HEK293T cells were treated with a set of five different concentrations

(0.1μM,1 μM, 10 μM, 25 μM, 50 μM), viability was measured in cells after 72 hours of treatment (**Figure 5.18 A**), from this experiment the working concentration of 0.1μM was selected. The following experiment was to measure the viability of the cells transfected with the pNL4.3 and ZIKV PrM/E GFP (-) plasmids and treated with MG132 during the whole transfection process (**Figure 5.18 B)**, there was no evidence of an increase of mortality on the transfected cells. When the infectivity from the particles produced under the MG-132 treatment was measured (**Figure 5.18 C**), no difference was observed compared with the negative control.

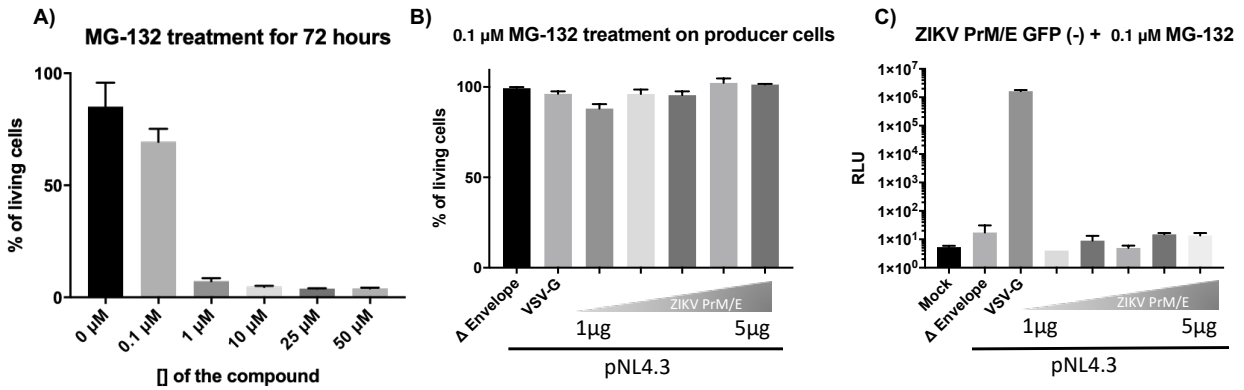

Figure 5.18. Effect of the proteasomal inhibitor MG132 on the producer cells and the impact in the infectivity of the PPs. A) Viability of HEK293T cells that were treated with increasing concentrations of MG132 (0.1μM,1 μM, 10 μM, 25 μM, 50 μM), **B)** Viability of HEK293T cells transfected with the pNL4.3 and ZIKV PrM/E GFP (-) and then treated with MG132 for 72 hours. **C)** Infectivity assay of cells exposed to the particles produced during the inhibitor treatment.

Since the pseudotyping of flaviviruses is so scarcely reported in the bibliography an in-silico analysis was carried out on about thirty sequences of the cytoplasmic tail of different viruses that had been efficiently pseudotyped, the analysis involved classifying the residues into their physicochemical properties and the spatial conformation that it adopts **(Figure 5.19)**. The objective of this analysis was to try to find common features within the CT. However, no obvious pattern was observed.

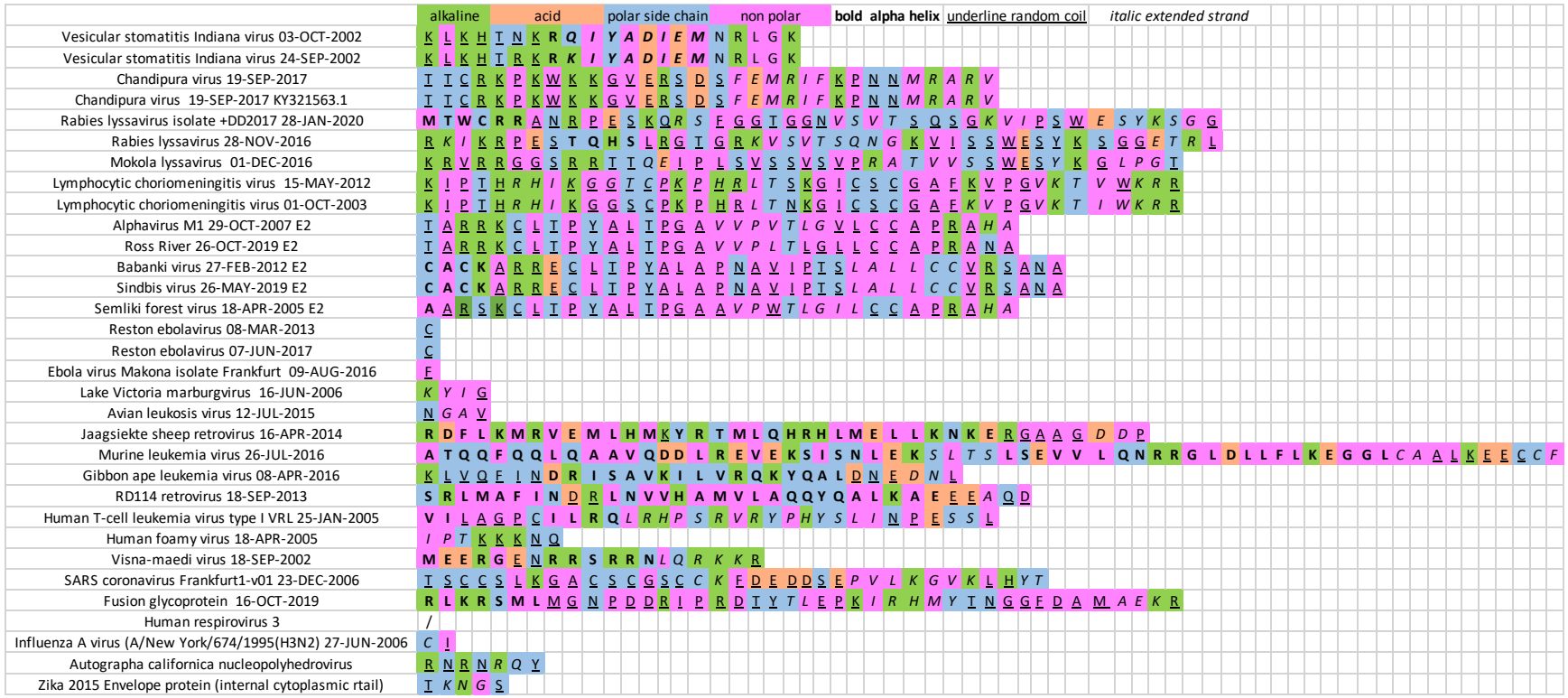

Figure 5.19. Table describing cytoplasmic tails of different viruses that were efficiently pseudotyped. The amino acid sequences are detailed highlining the nature of the residue and the spatial conformation. The code is:

alkaline (green), acid (orange), polar side chain (blue), non-polar (magenta), alpha-helix (**bold**), random coil (<u>underline</u>), extended strand (*italic*).

i

Since none of the strategies worked when trying to establish an infectivity model based on pseudotyping, different approaches were planned to create models that could be easily handled. An infectious clone of the genome was designed based on a multicopy plasmid that can be stored and amplified without much effort.

5.5. Reverse genetic system, construction of ZIKV plasmid.

The plasmid used as a template on previous experiments (pCCI-SP6-ZIKV) was a single copy plasmid with difficulties when trying to propagate it. Due to the size of the insert in the backbone and the instability of the *Flavivirus* genome in plasmids, NEB Stable Competent *E. coli* (High Efficiency) cells were used to propagate and store the pCCI SP6 ZIKV plasmid. Cells were heat-shocked and transformed using the standard protocol.

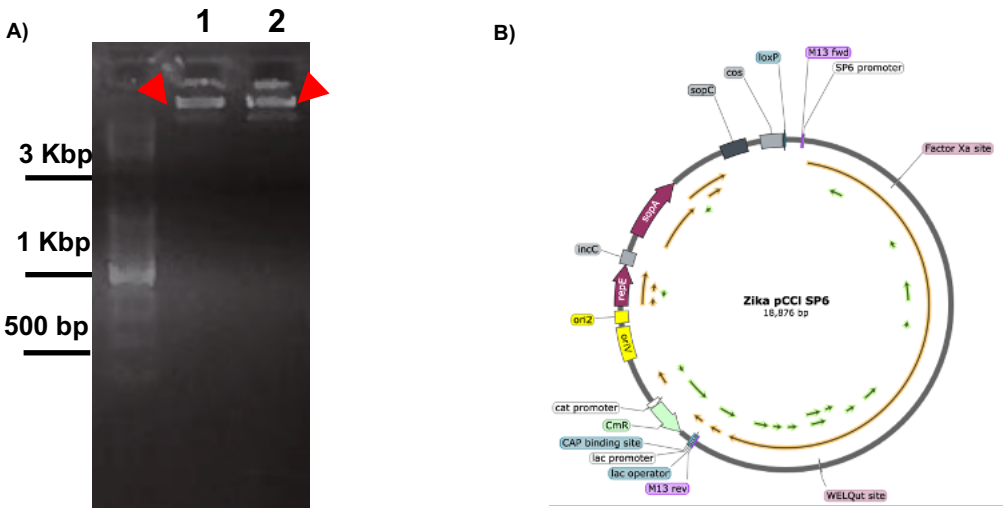

Figure 5.20. pCCI SP6 ZIKV plasmid map and transformation on NEB Stable Competent *E. coli* (High Efficiency) cells. A) 1) Plasmid purification of pCCI SP6 ZIKV WT after 24 hours incubation, 2) Plasmid purification after 48 hours incubation (bands pointed with red arrowheads), **B)** Plasmid map of pCCI-SP6-ZIKV including size and standard features.

Standardisation of the transformation process was carried out using different amounts of plasmids, increasing amounts of the ZIKV genome plasmid were used, the plates contained a fixed concentration of chloramphenicol as an antibiotic. Transformation efficiency was calculated with the formula described below.

- $\text{Transformation efficiency } \left(\frac{\text{transformants}}{\mu g}\right) = \frac{\#colonies\ on\ plate}{(ng\ of\ DNA\ plated)}\ x\ 1000\frac{ng}{\mu g}$

The transformation efficiency was calculated, considering the number of colonies and the nanograms of plasmid using during the transformation. Increasing amounts of DNA were used (50 ng, 100 ng, 250 ng, 500 ng, 750 ng), and the results are displayed in **Figure 5.21.**

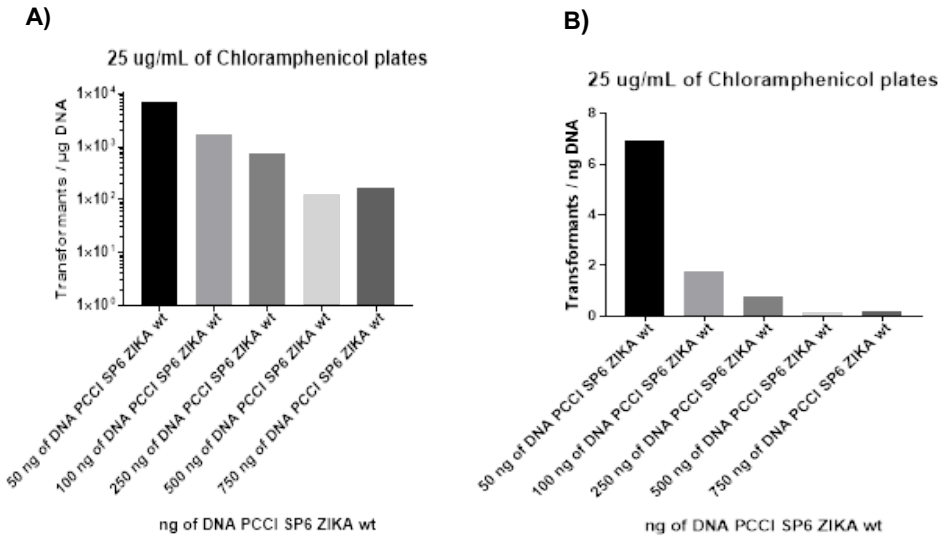

Figure 5.21. Transformation efficiency on NEB Stable Competent *E. coli* (High Efficiency) cells. A) Graph showing the number of colonies (transformants) per microgram of DNA. **B)** The number of colonies per nanogram DNA. Colonies were counted using a magnifying glass when needed.

After analysing the number of transformants per nanogram of DNA showed that at lower concentrations of plasmid, the cells had a higher uptake, and the efficiency was better overall. 50 ng of plasmid were enough to produce seven colonies per nanogram of DNA. Once the optimal amount of plasmid was established, the antibiotic concentration was modified to allow higher bacterial growth (**Figure 5.22.**), the standard concentration of 25 µg per ml was cut to 12.5 µg per ml. However, the diminishment of the antibiotic concentration increased the number of colonies in a way that it was impossible to isolate them properly.

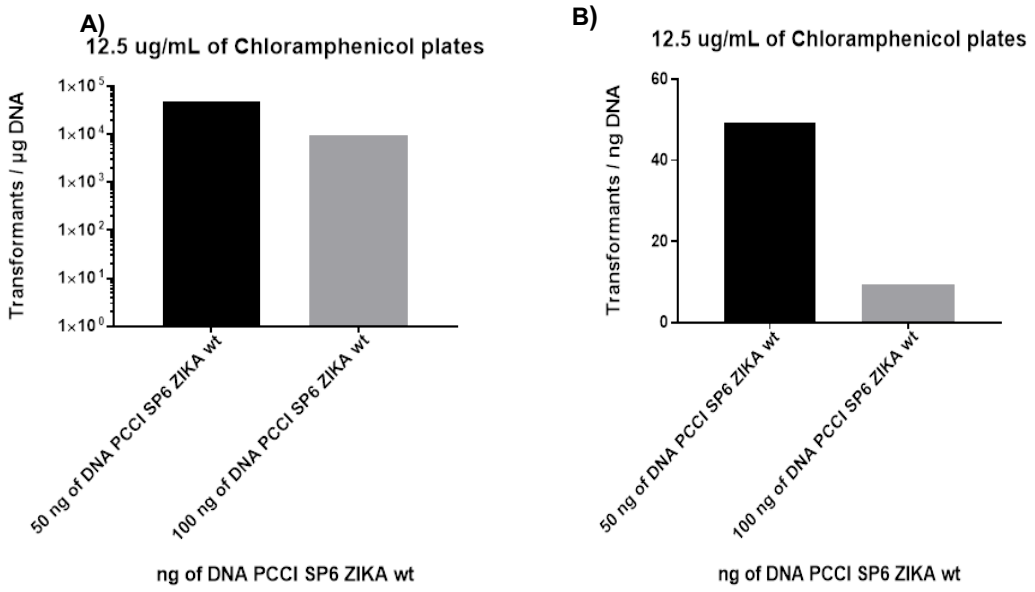

Figure 5.22. Reduction antibiotic concentration during the transformation process. A) The number of colonies per microgram of DNA when the plate contained 12.5 µg of chloramphenicol per ml, 50 and 100 ng of DNA were used during transfection. **B)** The number of colonies per nanogram of DNA.

Once the conditions for plasmid growth were established (50 ng of plasmid per aliquot and 25 µg per ml of chloramphenicol on the agar), the cells were incubated for 24 or 48 hours on Terrific broth (**Figure 5.23**).

Figure 5.23. pCCL SP6 ZIKV WT Plasmid isolation after 24 and 48 hours. 1) Plasmid isolated after 24 hours incubation on Terrific broth at 37ºC. **2)** Isolation after 48 hours incubation under same conditions (bands pointed with red arrowheads).

No difference was observed between 24 or 48 hours of incubation.

As a way to validate the presence of the ZIKV genome, a PCR was carried out with the primers used to amplify the PrM/E genes (**Figure 5.24**).

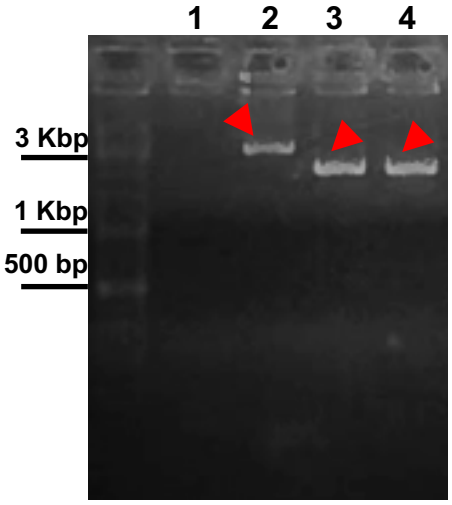

Figure 5.24 Amplification of the PrM/E genes of the plasmid using the laboratory standardised conditions.**1)** Negative Ctrl (-) water, **2)** Positive Ctrl (+) ZIKV PrM/E GFP (+) plasmid, **3)** Colony 2 NEB Stbl pCCl SP6 Zika with 24 hrs, **4)** Colony 2 NEB Stbl pCCl SP6 Zika with 48 hrs.

Once the genome containing plasmid was efficiently propagated; due the size of the insert the viral genome was divided into different fragments with overlapping ends for PCR amplification, this design gave the fragments the flexibility to be used in different techniques. The fragment containing PrM/E genes containing the GFP reporter gene was amplified using the same conditions described for generation of ZIKV PrM/E GFP (+) plasmids. The next three fragments containing the Non-Structural proteins were named NS1-F1, F1-2, F2-END. Gradient PCR was used to find the optimal temperature for amplification (**Figure 5.25**).

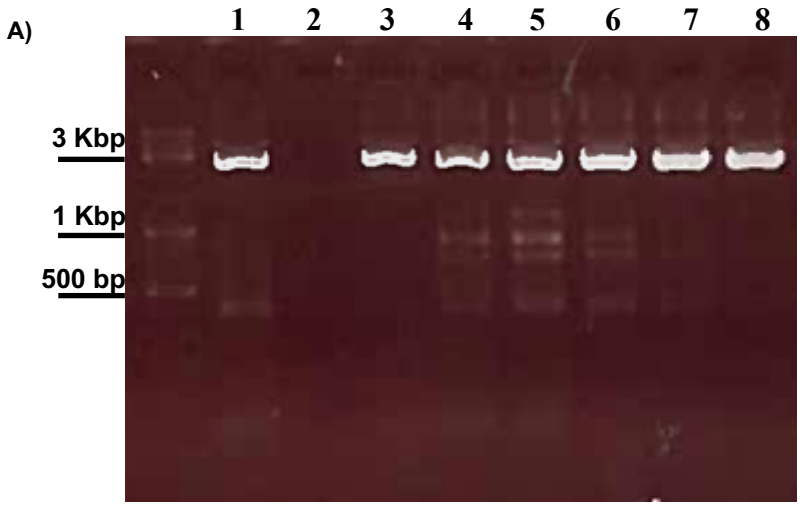

Q5 amplification fragment NS1-F1 temperature gradient. 1)T= 55.0ºc, **2**) T=55.8ºc, **3**) T=57.8ºc, **4**) T= 59.3ºc, **5**) T=62.4ºc, **6**) T=63.5ºc, **7**) T=64.3ºc, **8**) 65.0 ºc.

B)

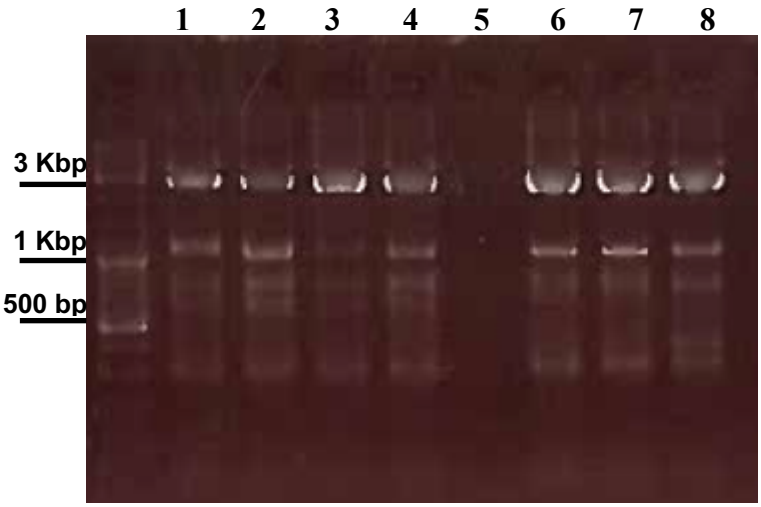

Q5 amplification fragment 1-2 temperature gradient. 1)T= 55.0ºc, **2**) T=55.8ºc, **3**) **T**=57.8ºc, **4**) T= 59.3ºc, **5**) T=62.4ºc, **6**) T=63.5ºc, **7**) T=64.3ºc, **8**) 65.0 ºc.

C)

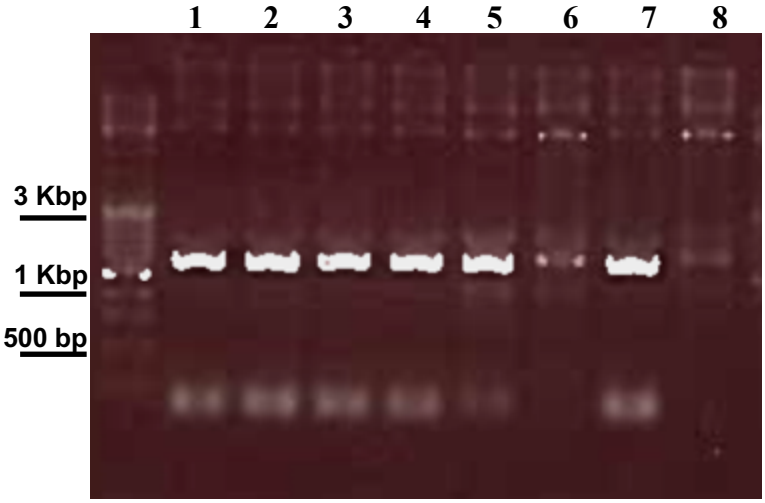

Q5 amplification fragment 2-End temperature gradient. 1)T= 55.0ºc, **2**) T=55.8ºc, **3**) T=57.8ºc, **4**) T= 59.3ºc, **5**) T=62.4ºc, **6**) T=63.5ºc, **7**) T=64.3ºc, **8**) 65.0 ºc.

Figure 5.25. Genome fragments amplification. A) The temperature gradient of the NS1-F1 fragment, **B)** Amplification of F1-F2 fragment, **C)** Temperature gradient of F2-END fragment.

To generate a new multicopy plasmid, the fragments were ligated into a pUC19 plasmid using different strategies. Gibson assembly was used to fuse the genome fragments, including the pUC19 backbone (**Figure 5.26A**). An excess of equimolar amounts of PCR products were mixed with pUC19 and the enzymatic mix. The protocol was followed as the manufacturers directed. The product of the stitching was then transformed into NEB Stable Competent *E. coli* (High Efficiency) cells. Colonies were screened looking for different genes of ZIKV, including NS2B/NS3 and NS5; a representative experiment is shown in **Figure 5.26 B**.

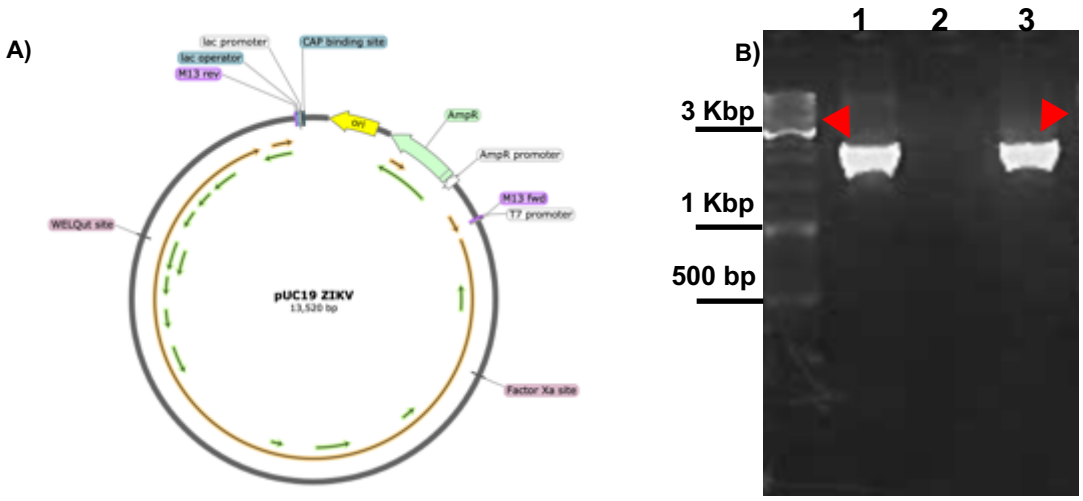

Figure 5.26. Plasmid map of pUC19 ZIKV and gene amplification. A) Plasmid map of the pUC19 ZIKV construct. **B)** Genes amplified as controls for the genome insertion. **1)** Plasmid derived positive control (NS2B/NS3) **2)** NS2B/NS3 screening pUC19 colony #5 Gibson Assembly, **3)** NS5 screening pUC19 colony #5 Gibson Assembly.

Interestingly, the colony screening showed the amplification of the non-structural gene NS5 but not the NS2B/NS3 fragment. This behaviour was conserved among the samples tested, the loss of one of the genes or the inability to amplify them was enough to discard this method; instead, the complete of amplification of genome was tested using Long Amp and Clone amp reactions. Primers were designed to amplify the whole genome with the addition of an overlap sequence to fuse the pUC19 backbone with the PCR product. No

amplification was detected when using Clone Amp, this protocol was discarded, and the Long Amp protocol was followed.

5.6. LONG AMP amplification

Amplification of the ZIKV genome (genome size ~ 11 kb) was carried out following the manufacturer's instructions. A gradient PCR was designed to find the proper temperature to amplify the genome (**Figure 5.27**).

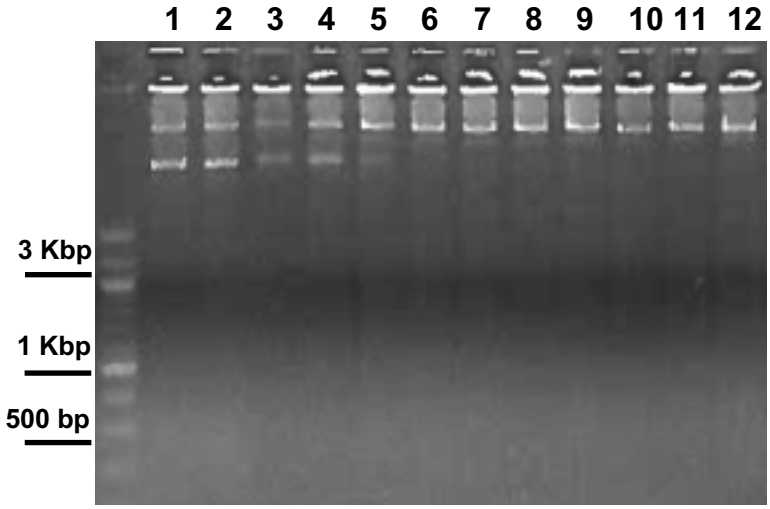

Figure 5.27 Long Amp gradient temperature. Each column shows the product of amplification obtained with different temperatures. **1)**T= 50.0ºc, **2**) T=50.5ºc, **3**) T=51.55ºc, **4**) T= 53.20ºc, **5**) T=55.5ºc, **6**) T=58.4ºc, **7**) T=61.8ºc, **8**) T=64.6 ºc, **9**) T=66.8, **10**) T=68.4 ºc, **11**) T=69.6 ºc **12**) T=70.0 ºc

The full-length genome amplicon was then inserted into digested pUC19 plasmid. However, when the bacterial colonies were screened looking for viral genes, no bands were observed **(data not shown).**

5.7. Generation of pCCl19 ZIKV Δ Env construct.

As an alternative to the previous approaches, the plasmid containing the genome without PrM/E genes was amplified, this design would help to swap glycoprotein mutants with just single digestion and ligation (**Figure 5.28.A**). Two temperatures from the previous gradient were chosen to amplify this new construct. The appearance of multiple bands may cause interference with the ligation process so temperatures where specific amplification occurred are shown in **Figure 5.28.B**.

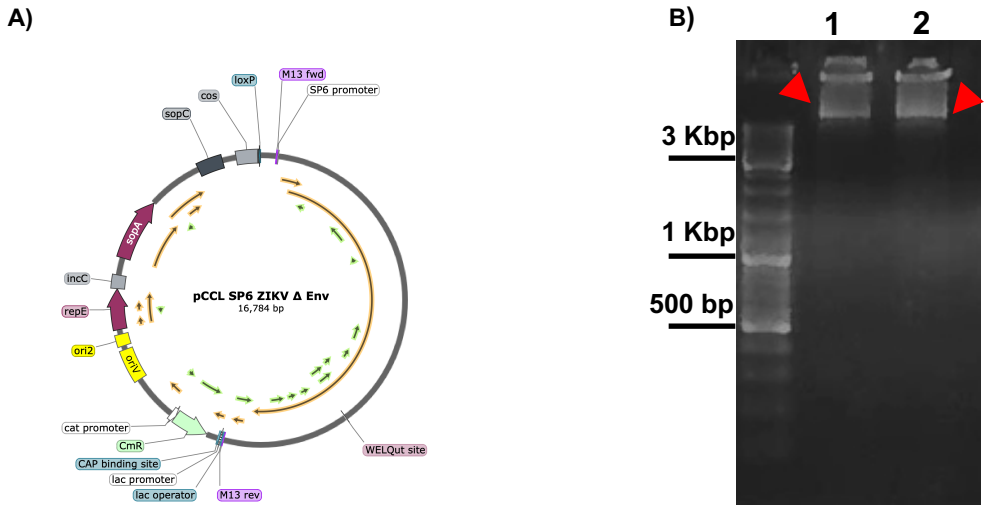

Figure 5.28. Amplification of Zika genome without PrM/E genes using Long Amp *Taq* DNA Polymerase. A) Plasmid map of pCCl19 ZIKV Δ Env **B)** Amplification of the Δ Env fragments **1**) Long amp amplification T=58.4 ,**2**) Long amp amplification T=61.8.

Once the temperature for amplification was selected (51.51ºC), KLD enzymatic mixture was used to help to produce blunt edges for the ligation process. The products treated with KLD were used to transform Stellar cells which were then incubated for 24 or 48 hours. Colonies were screened for the NS2B/NS3 gene (2380 bp); a representative image of the gel is shown in **Figure 5.29**

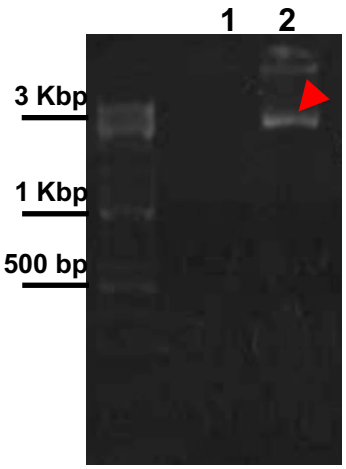

Figure 5.29. Colony screening ZIKV PrM/E (-) Plasmid. 1)pCCl SP6 ZIKV Δ PrM/E Col 1 Long Amp 24 hrs + KLD treatment, **2**) pCCl SP6 ZIKV Δ PrM/E Col 1 Long Amp 48 hrs + KLD treatment.

After 48 hours, the NS2B/NS3 gene was detected, so the colony was seeded on Terrific Broth and incubated for 24 or 48 hours again. The plasmid was then purified, and the product was loaded on an agarose gel (**Figure 5.30)**.

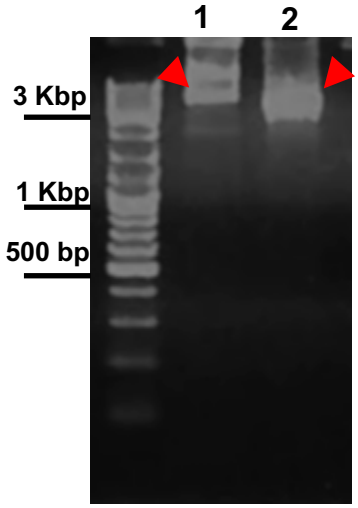

Figure 5.30. Plasmid purification of Long Amp product transformed colonies. ZIKV PrM/E (-) Plasmid produced using Long Amp amplification **1**) amplification at 51.51ºC,

transformation and incubation for 24 hours, **2**) amplification at 51.51ºC, transformation and incubation for 48 hours.

The agarose gel showed a band pattern that corresponds not to a single plasmid but a mixture of different products. To verify the identity of the plasmid, a series of PCRs looking for the plasmid backbone and various ZIKV fragments were performed (**Figure 5.31**).

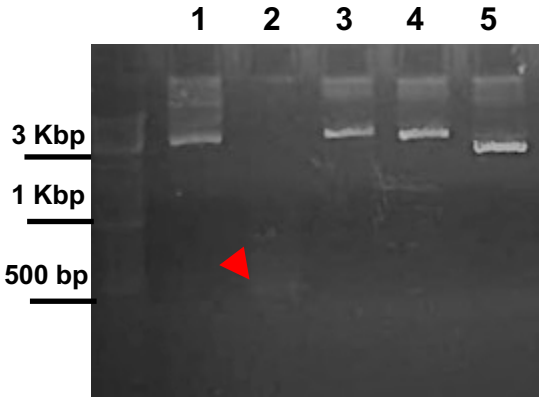

Figure 5.31.-Identification of the plasmid components using PCR. 1) pUC19 plasmid backbone (2686 bp), **2**) Sp6 promoter+5´UTR+Capsid gene minus the las 96 nt of the 3´region (red arrowhead) (440bp), **3**) Ns1-F1 fragment (3000 bp), **4**) F1-F2 fragment (3000bp), **5**) F2-end fragment (2355 bp).

The PCR products corresponded to the predicted sizes of the amplicons; however, different behaviours appeared: 1.- the sudden loss of the plasmid from the bacterial population after few generations or due the continuous passaging of the plasmids fragments of the genome were lost, this was corroborated using Sanger sequencing. Due to the previous reports of the instability of the *Flavivirus* genomes on diverse plasmid systems, an in-silico analysis was carried out to identify the possible prokaryotic sequences hidden within the viral genome. Both the 3´to 5´ and the 5´to 3´senses were analysed (**Table 5.4 and Table 5.5**).

Table 5.4. Promoter predictions for sequence ZIKV. Promoter predictions for the prokaryotic sequence with a score cut off 0.90 (transcription start shown in larger font).

Start	End	Score	Promoter Sequence	Part of the genome
21	66	0.98	TTCGAGTTTGAAGCGAAAGCTAGCAACAGTATCAACAGGT**T**TTATTTTGG	C
302	347	0.98	GGTTCAGTTGGGAAAAAAGAGGCTATGGAAATAATAAAGA**A**GTTCAAGAA	C
892	937	0.98	GCTTTTGGGAAGCTCAACGAGCCAAAAAGTCATATACTTG**G**TCATGATAC	E
1419	1464	0.97	TCGTTAATGACACAGGACATGAAACTGATGAGAATAGAGC**G**AAAGTTGAG	E
1823	1868	0.96	GGCCACTTGAAATGTCGCCTGAAAATGGATAAACTTAGAT**T**GAAGGGCGT	E
2192	2237	0.94	GCATTTGAAGCCACTGTGAGAGGTGCCAAGAGAATGGCAG**T**CTTGGGAGA	E
2328	2373	0.99	CATTGTTTGGAGGAATGTCCTGGTTCTCACAAATTCTCAT**T**GGAACGTTG	E
2659	2704	0.94	AAGAATGGAAAACATCATGTGGAGATCAGTAGAAGGGGAG**C**TCAACGCAA	NS1
2725	2770	0.9	AGTTCAACTGACGGTCGTTGTGGGATCTGTAAAAAACCCC**A**TGTGGAGAG	NS1
2932	2977	0.96	CTTTCTTGTGGAGGATCATGGGTTCGGGGTATTTCACACT**A**GTGTCTGGC	NS1
6057	6102	0.94	ACTGGCTTGAAGCAAGAATGCTCCTTGACAATATTTACCT**C**CAAGATGGC	NS3
6281	6326	0.96	TGGTGCTTTGATGGCACGACCAACAACACCATAATGGAAG**A**TAGTGTGCC	NS3
8165	8210	0.92	TGGCTTGAAAAAAGACCAGGAGCCTTTTGTATAAAAGTGT**T**GTGCCCATA	NS5
9554	9599	0.93	CAAGACTTGTGGCTGCTGCGGAGGTCAGAGAAAGTGACCA**A**CTGGTTGCA	NS5
9675	9720	0.96	ATAGGTTTGCACATGCCCTCAGGTTCTTGAATGATATGGG**A**AAAGTTAGA	NS5

Table 5.5. Predicted promoters for the reverse strand of sequence ZIKV. Sequences predicted for the prokaryotic sequence with a score cut off 0.90 (transcription start shown in larger font).

Start	End	Score	Promoter Sequence	Part of the genome
10407	10362	0.94	CCAAGCTGTGGCTGACTAGCAGGCCTGACAACATTAAGAT**T**GGTGCTTAC	NS5
9739	9694	0.98	TTCCACTCTTGTGTGTCCTTTCTAACTTTTCCCATATCAT**T**CAAGAACCT	NS5
8651	8606	0.96	ATCCCAGGGTTTTGACAGGAGCCTGACAACCCCGTTTATT**A**GAGAGGACG	NS5
6863	6818	0.96	CATGATGATGATTGCCATTTGGTTGTCCTGGGGAGATCTT**T**GCTTTTCTG	NS4B
5698	5653	0.93	TTCCTCACGCTTGGAACAAACCAAACTGTTTTTCCAGAAT**G**ATCCGTCAC	NS3
5514	5469	0.99	TCTCAACCCTTGTTGAAATGTATCCTCTTGCTGCTATACT**T**GAGGGATCT	NS3
5359	5314	0.96	GTTCCAGAGTGGGTGACATTGACTGCTGTTGTCATATAAC**G**CACTGGAAG	NS3
5078	5033	0.97	ATAACTCCCATTTTTGATCACGACCCCATTGCCATAAAGT**C**CTATCACTC	NS3
3710	3665	0.91	CATCAAAATTGCAAGCTTAGCCAGGTCACTCATTGAAAAT**C**CTCCCAGGA	NS2A
2870	2825	0.95	AAAGCTGTTATTTGTCTTTGCTGCTCTGACGAAGTACGAT**T**TCCCCCAAG	NS1
2665	2620	0.96	TTTTCCATTCTTGAAACAGAGGAGATCCCGCAGATACCAT**C**TTCCCAGGC	NS1
2363	2318	0.98	AATGAGAATTTGTGAGAACCAGGACATTCCTCCAAACAAT**G**ATTTGAAAG	E
1910	1865	0.92	GATCTTGGTGAATGTGAACGCTGCAGTACACAAGGAGTAT**G**ACACGCCCT	E
1485	1440	0.9	CTCTTGGTGAATTGGGCGTTATCTCAACTTTCGCTCTATT**C**TCATCAGTT	E
842	797	0.9	TATCCAATTTTCGACTCTAATCAAGTGCTTTGTGTATTCT**C**TTGATTCCA	M
544	499	0.97	CCCAATGTGGTTGGAAAAGATATGGCCTCCCCAGCATCGT**T**TCTGTCCAA	Pr
276	231	0.99	GTGATGGCTTGATTGCCGTGAATCTCAAAAAGGCTAGAAT**C**GCCAAGACC	C

The analysis revealed that the sequence of C, E, NS1, NS3 and NS5 genes might work as promoters for toxic peptides within the bacterial cells when the 3´to 5´sense was scanned and the NS5, NS4B, NS3, NS2A, NS1, E, M and C genes were identified in the reverse strand.

The evidence suggested that a model using an infectious clone based on a pUC19 backbone with no replicative control was not adequate to store and maintain a plasmid stock. A similar behaviour was observed when the pCCL plasmid was modified to generate a genome lacking the glycoprotein, this imperfectability led to the discarding of these strategies. Plasmid-free, Reverse genetic systems appeared as suitable candidates for the generation of viable viruses using the same primers employed on previous experiments since the fragments of the genome were produced before it was only needed to adapt the fragments to the purpose.

5.8. Plasmid-free reverse genetic system.

The plasmid-free reverse genetic systems can be divided into two different categories: a linear structure known as Infectious subgenomic amplicons (ISA) and a circular product generated by PCR or circular polymerase extension reaction (CPER). Both methodologies require the addition of the CMV promoter upstream of the 3´UTR and the HDVR sequence along with the SV40 polyadenylation signal (pA) downstream the 5´UTR region. This approach confers plasticity to the system since fragments can be swapped when needed and incorporation of mutants does not cause off-target complication since the mutation reaction can be performed on a plasmid prior the subcloning process of the fragments.

HEK293T cells were chosen for transfection and viral production. The capability of the cells to sustain Zika virus replication was confirmed using Muench and Reed assay and electron microscopy. Transmission electron microscopy was performed on Mock infected

and ZIKV infected cells; the objective was to observe the viral production and viral particles within the cells.

The cells were infected with treated with the mock or ZIKV at an MOI of 1 for 24 hours; then they were harvested, fixed, and sent for imaging (**Figure 5.32**)

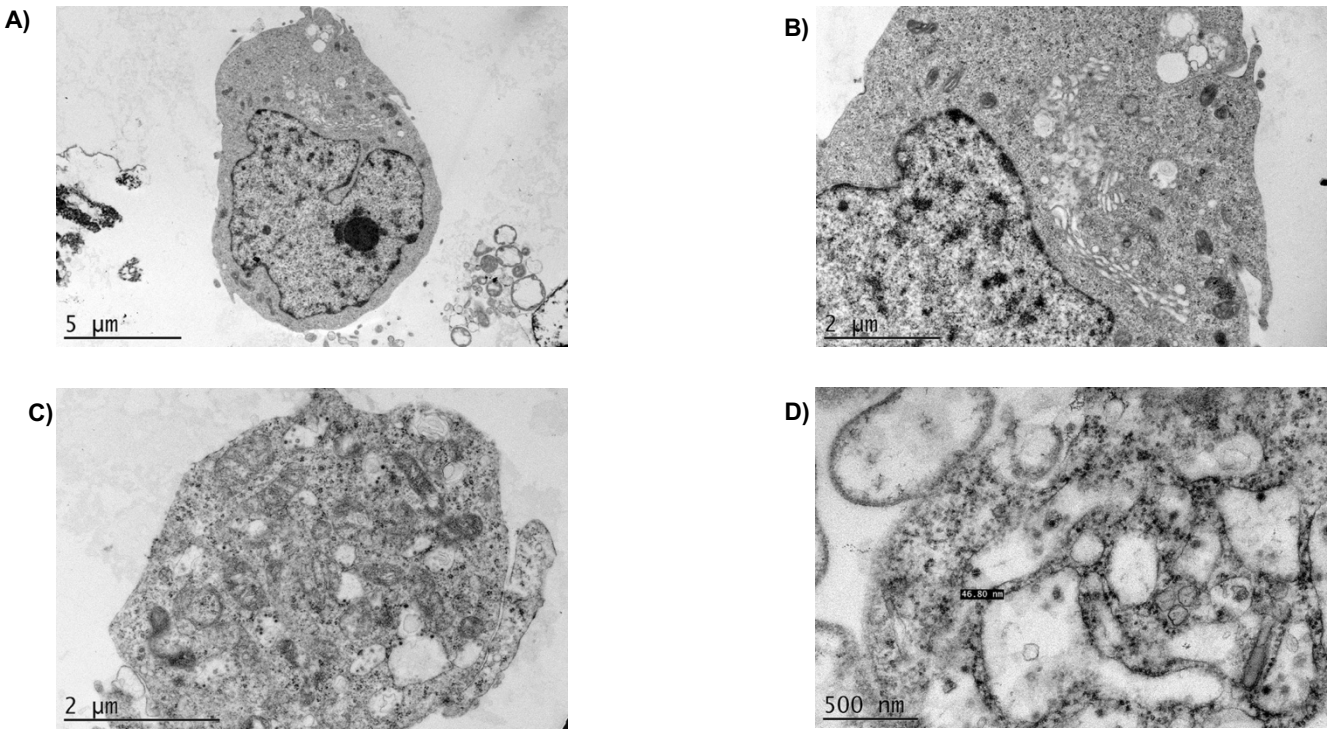

Figure 5.32. Transmission electron microscopy of Mock or ZIKV infected HEK293T cells. A) Mock cells with typical morphology without vesiculations. **B)** Close up of the cell´s interior, normal morphology of the organelles. **C)** ZIKV infected cells, electron-dense bodies can be seen within the cells and an increase in the number of vesicles. **D)** Close up of the infected cell; viral factories can be seen as membranous structures and the virus within as electron-dense bodies. A viral particle was measured; the size corresponds with previous literature reports (Electron microscopy was carried out by Dr. Bibiana Chávez Munguia on the The Center for Research and Advanced Studies of the National Polytechnic Institute (Me

xico city,Mexico)

The viral titre was measured after consecutive passages on HEK293T cells (**Figure 5.33**).

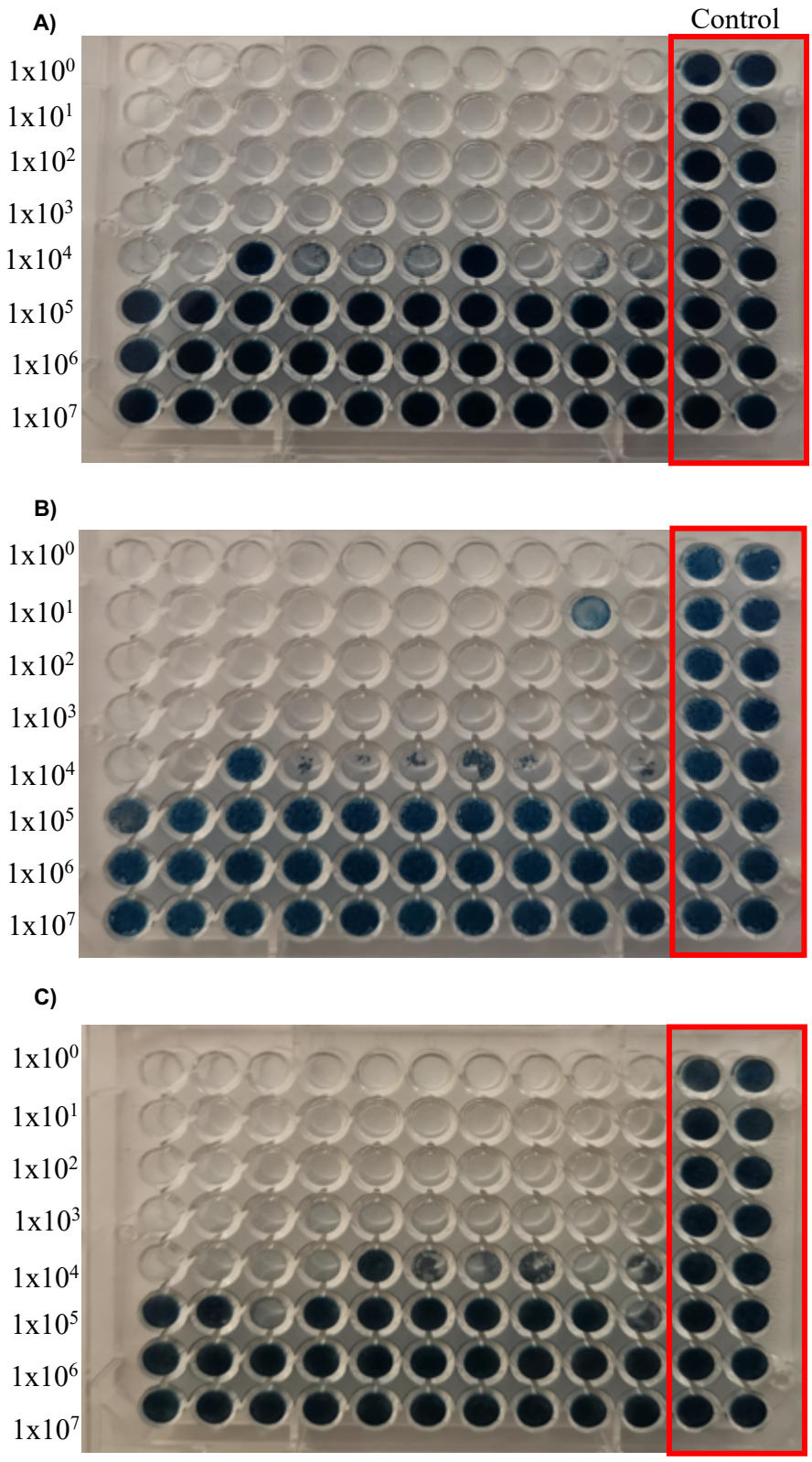

Figure 5.33. Consecutive ZIKV passaging on HEK293T cells. ZIKV containing media was harvested and 96-well plates of BHK-21 were treated with dilutions of it to calculate the viral titre. **A**) ZIKV p7 viral TCID50: 9.98x10^4 /ml- FFU: 6.88X10^4 **B**) ZIKV p8 viral TCID50: 1.26 x10^4 /ml- FFU: 8.67 X 10^4 **C**) ZIKV p9 viral TCID50: 1.26 x10^4 /ml- FFU: 8.67 X 10^4. TCID is calculated by the Spearman & Kärber algorithm. FFU approx. 0.69 x TCID50

Once the viral culturing was standardized, the next step was to amplify the fragments of the genome and were subcloned and transfected to HEK293T cells.

5.8.2. Reverse genetic system Infectious sub-genomic amplicon (ISA) and circular polymerase extension reaction (CPER).

CMV promoter and enhancer were subcloned from pcDNA 3.1 stock plasmid, Capsid gene minus the last 96 nt of the 3´ end, NS1-F1 fragment, F1-F2 fragment, F2-End Fragment were cloned from the pCCl SP6 ZIKV plasmid, Full-length PrM/E genes, and the 3′ 96-nucleotide region of the C gene GFP reporter gene from ZIKV C/GFP/PrM/E plasmid, SV40 polyadenylation signal (pA) from pcDNA 3.1 stock plasmid, Hepatitis delta virus ribozyme (HDVR) plasmid kindly donated from Dr Jordan J. Clark **(Figure 5.34).** The PCR fragments were purified with both sodium acetate and ethanol protocol or by Monarch PCR Clean-up Kit.

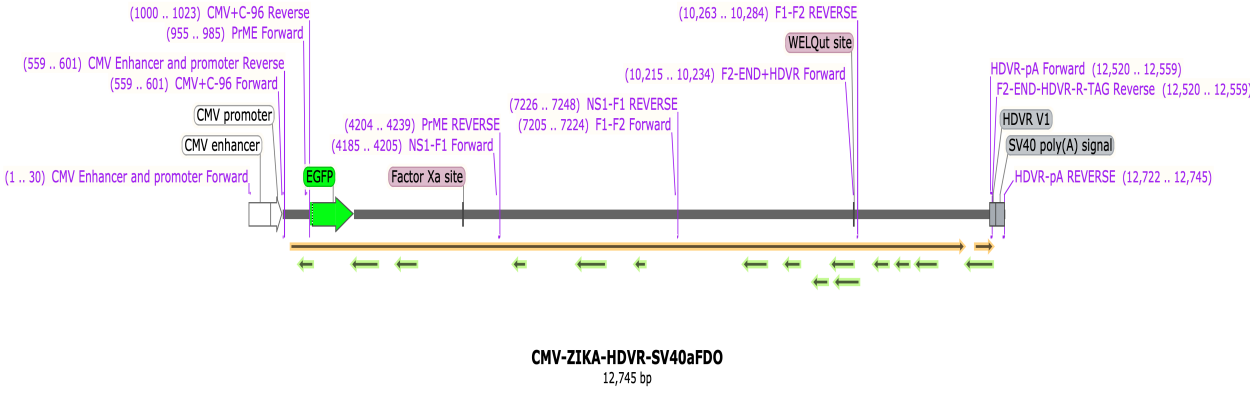

Figure 5.34. Infectious sub-genomic amplicon (ISA) structures with both HDVR versions. ISA linear product with the HDVR cloned from a plasmid kindly donated from Dr Jordan J. Clark. Primers used during the amplification are shown in purple and the common features are embedded within the structure.

The fragments were amplified and electrophered to check the proper size of the insert (**Figure 5.35 and 5.36)**, multiple bands were observed, an additional step of temperature optimization was carried out.

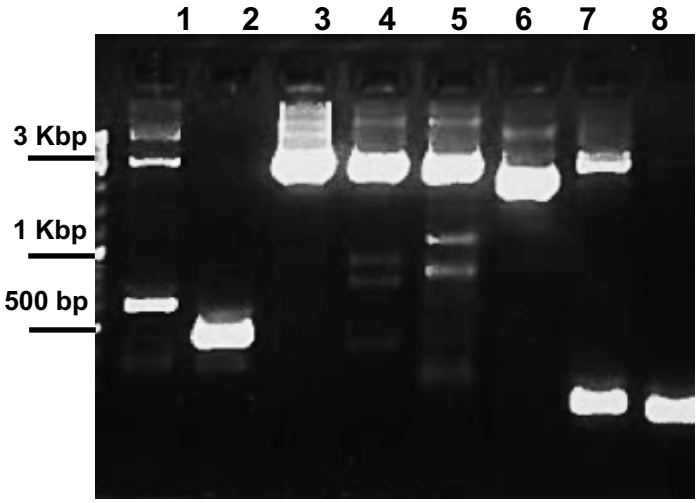

Figure 5.35 Infectious sub-genomic amplicon (ISA) initial approach. 1) CMV promoter and enhancer subcloned from pcDNA3.1 plasmid (727 bp), **2)** Capsid gene minus the last 96 nt of the 3´ end (400bp), **3)** Full-length PrM/E genes and the 3′ 96-nucleotide region of the C gene with GFP (3285 bp), **4)** NS1-F1 fragment (3000 bp), **5)** F1-F2 fragment (3000 bp), **6)** F2-End Fragmen t(2300 bp), **7)** SV40 polyadenylation signal (pA) (150 bp), **8)** Hepatitis delta virus ribozyme (HDVR)(100 bp).

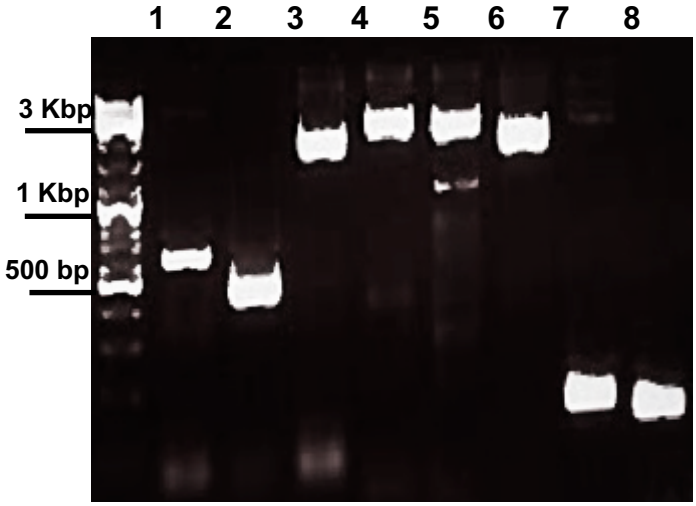

Figure 5.36. Infectious sub-genomic amplicon (ISA) optimization. 1) CMV promoter and enhancer subcloned from pcDNA3.1 plasmid, 2) Capsid gene minus the last 96 nt on 3´, 3) Full-length PrM/E genes and the 3′ 96-nucleotide region of the C gene with GFP, 4) NS1-F1 fragment, 5) F1-F2 fragment, 6) F2-End Fragment, 7) SV40 polyadenylation signal (pA), 8) Hepatitis delta virus ribozyme (HDVR).

The PCR products treated with Dpn1 enzyme and then column purified, HEK293T cells were transfected with these products using a 3 to 1 molar radio of PCR products. The PrM/E GFP fragment was taken as reference and the rest of the fragment were added accordingly. A GFP containing plasmid was used as control for transfection, after 72 hours both the control and triplicates of the infected cells were observed on the Epifluorescence microscope (**Figure 5.37**).

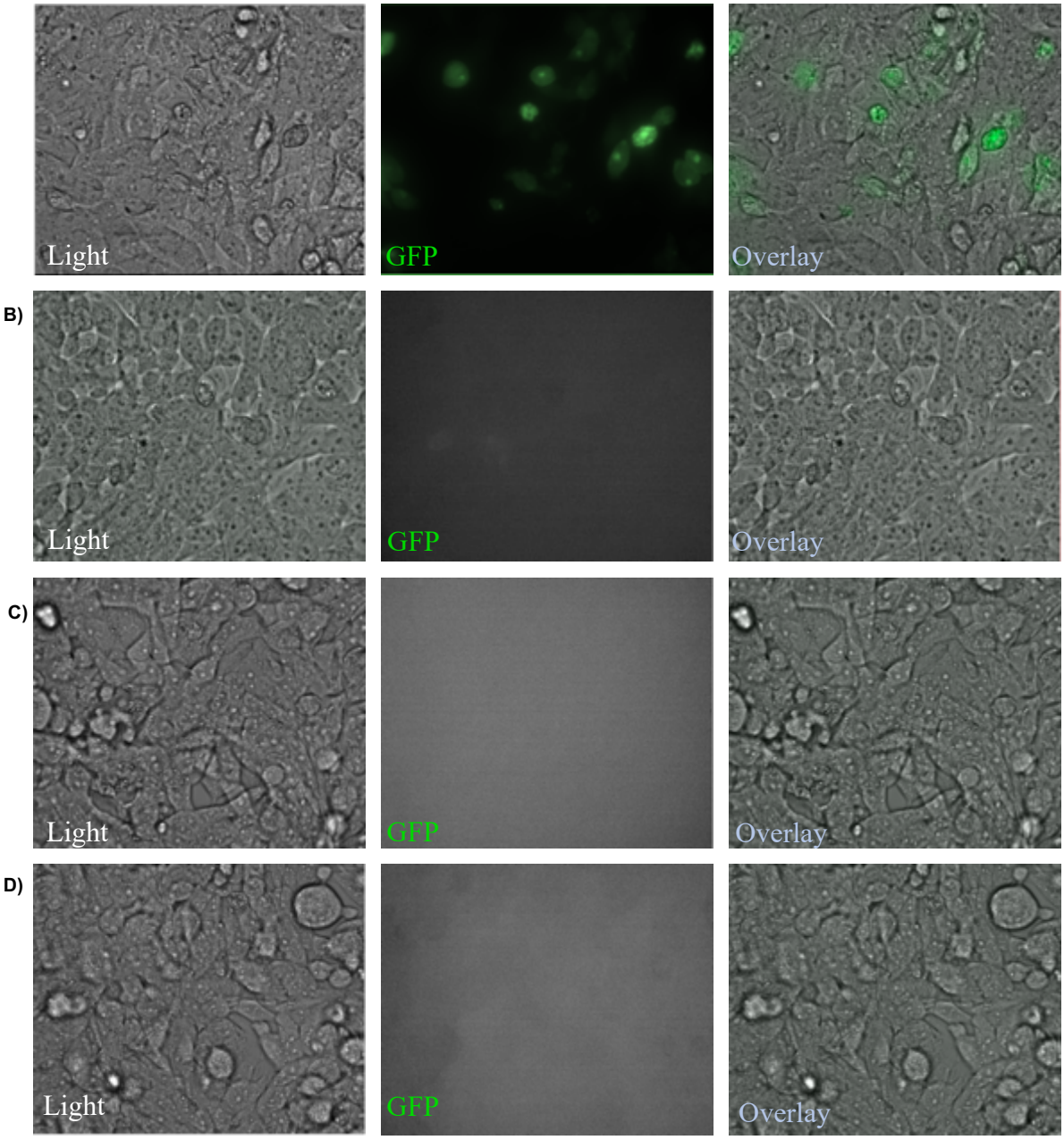

Figure 5.37 HEK293T cells transfected with ISA products. A) Cells transfected with GFP positive plasmid. **B)** Cells transfected with linear ISA products. **C)** Duplicate of cells transfected with ISA products. **D)** Duplicate of cells transfected with ISA products.

No fluorescence was detected on the HEK293T cells transfected with ISA products (**Figure 5.37 B, C, D**). VERO cells were used as an alternative for the transfection and electroporation was carried out to transfect the fragments of the genome. Control cells

were checked before (**Figure 5.38 A**), after 24 hours (**Figure 5.38 B**), 48 hours (**Figure 5.38 C**), and after 72 hours (**Figure 5.38 D**).

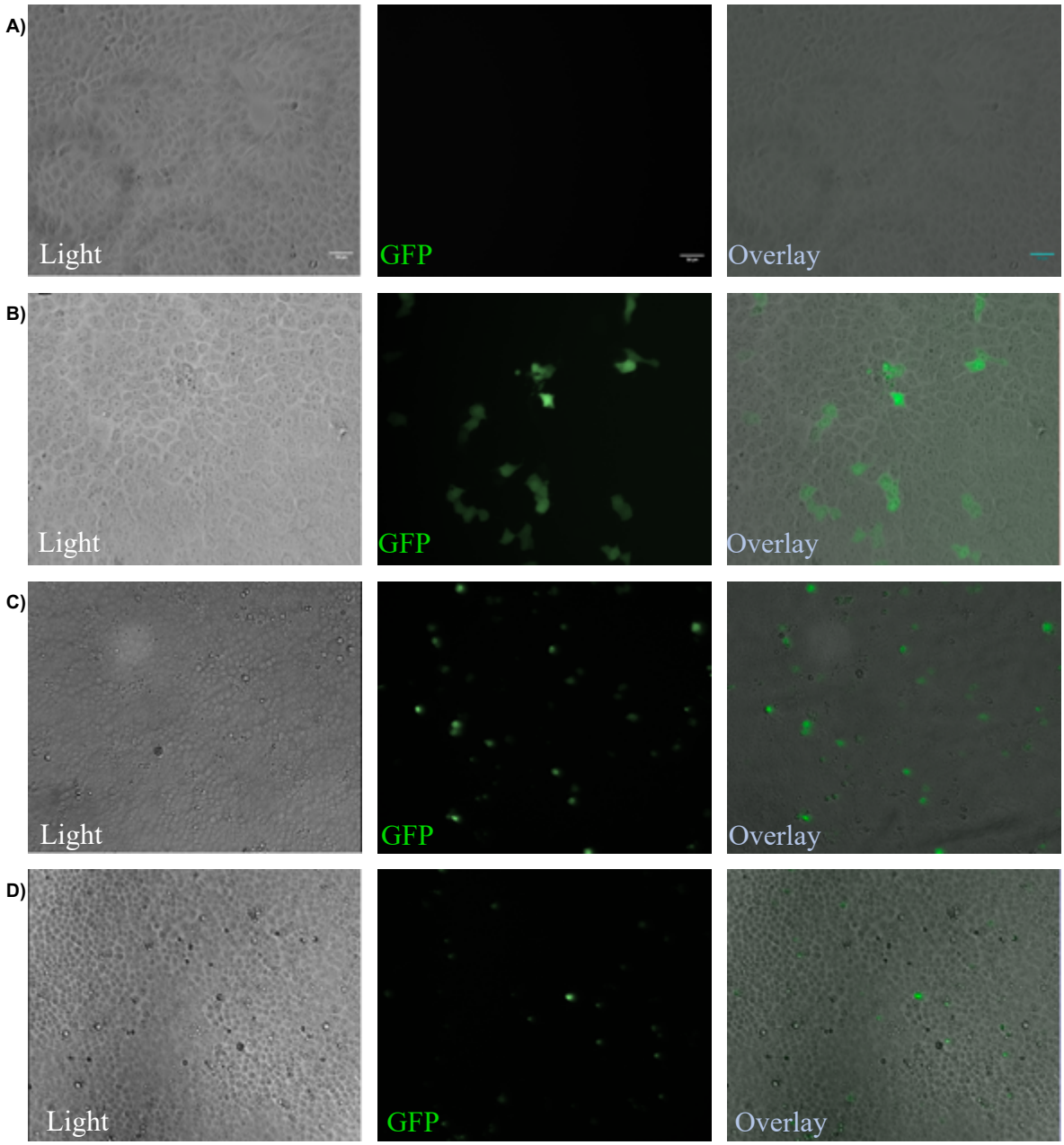

Figure 5.38 VERO cells electroporated with GFP positive plasmid. A) Cells observed before electroporation, **B)** GFP expression after 24 hours of transfection, **C)** GFP expression after 48 hours, **D)** Cells checked after 72 hours of the GFP positive plasmid.

VERO cells transfected with the ISA products were checked before the procedure (**Figure 5.39 A**), after 24 hours (**Figure 5.39 B**), and after 72 hours (**Figure 5.39 C**).

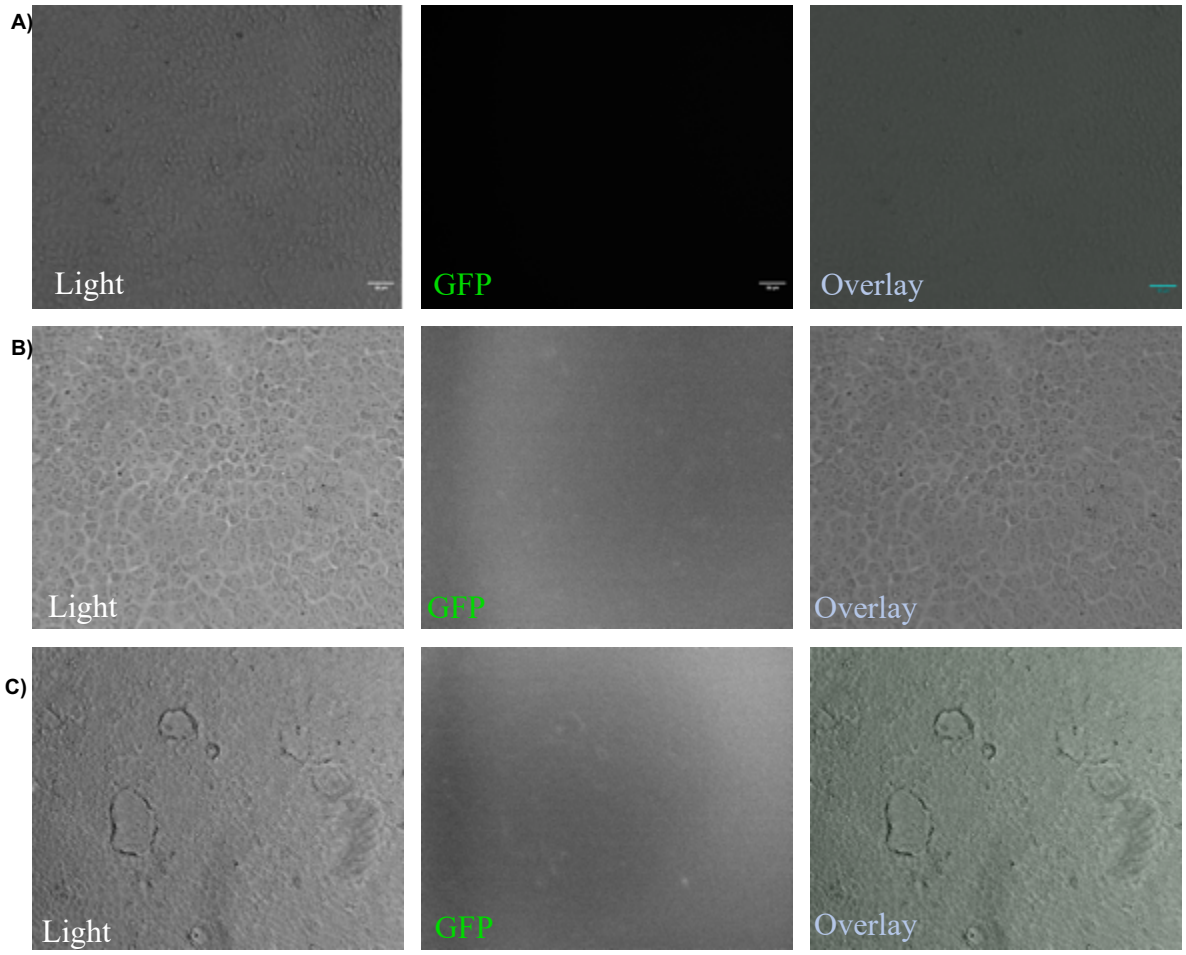

Figure 5.39 VERO cells electroporated with the ISA products. A) Cells observed before electroporation, **B)** GFP expression after 24 hours of transfection, **C)** Cells checked after 72 hours of the ISA products.

After the experiments with both HEK293T and VERO cells using different methodologies expression of the GFP reporter gene was not detected, ISA method is based on the notion that the transfected cell performs a recombination event where the fragments are fused together into a single DNA strain, however this process seems to be inefficient under the conditions tested, although CPER has a similar approach in this case after the initial

cloning a second PCR step was carried to fuse the fragments together and form a circular structure that facilitates the translation and replication (**Figure 5.40**).

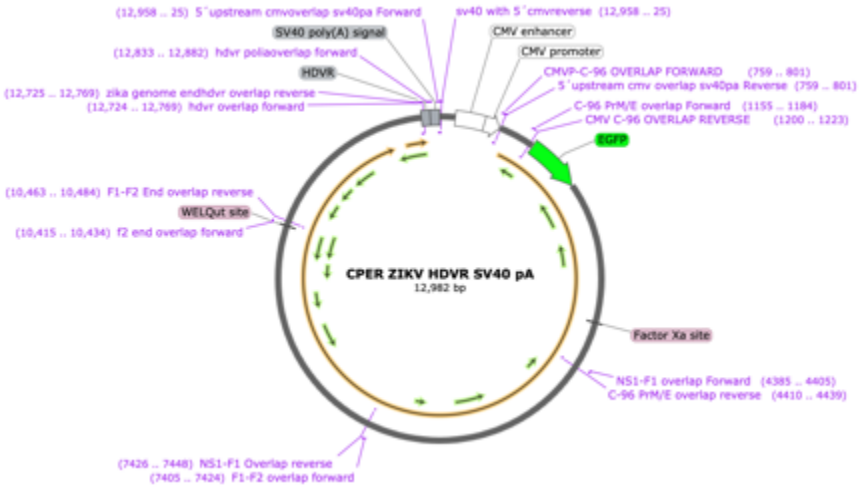

Figure 5.40. Map of the ZIKV CPER structure including common features. The map displays the features included in the structure including CMV promoter and enhancer, GFP reporter gene (green), the translated protein (orange), pA signal and HDVR. The primers used to clone the fragments and the position of these are shown in purple.

The fragments were cloned and electrophered on an agarose gel to check the size of the products (**Figure 5.41**).

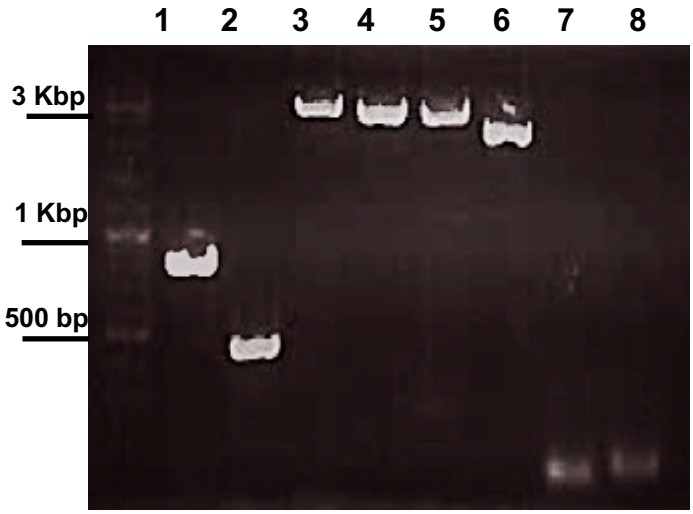

Figure 5.41. Circular polymerase extension reaction (CPER) optimization. 1) CMV promoter and enhancer subcloned from pcDNA3.1 plasmid (900bp), **2)** Capsid gene minus the last 96 nt on 3´, **3)** Full-length PrM/E genes and the 3′ 96-nucleotide region of the C gene, **4)** NS1-F1 fragment, **5)** F1-F2 fragment, **6)** F2-End Fragment, **7)** Hepatitis delta virus ribozyme (HDVR), **8)** SV40 polyadenylation signal (pA).

Once the products were identified by size the second PCR was carried out to fuse the fragments together and the whole reaction was transfected into HEK293T cells, due the length of the process and difficulties that carry the transfection and translation process, the cells were observed 96 hours post transfection (**Figure 5.42**) and the supernatant was harvested to calculate the viral titer (**Figure 5.43.**).

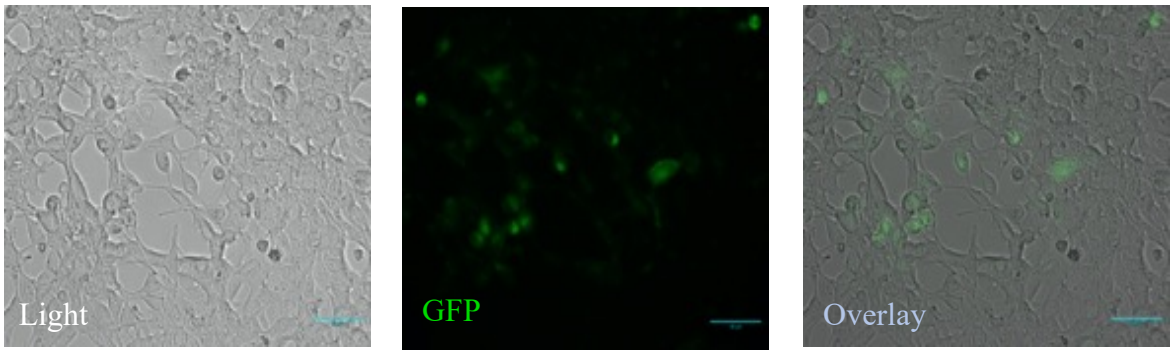

Figure 5.42 GFP⁺ HEK293T cells 96 hours after being transfected with the CPER structure. H93T cells were incubated for 96-hours after transfection, then were observed under an epifluorescence microscope. The cells that displayed green fluorescence were taken as positive for the transfection of the circular structure.

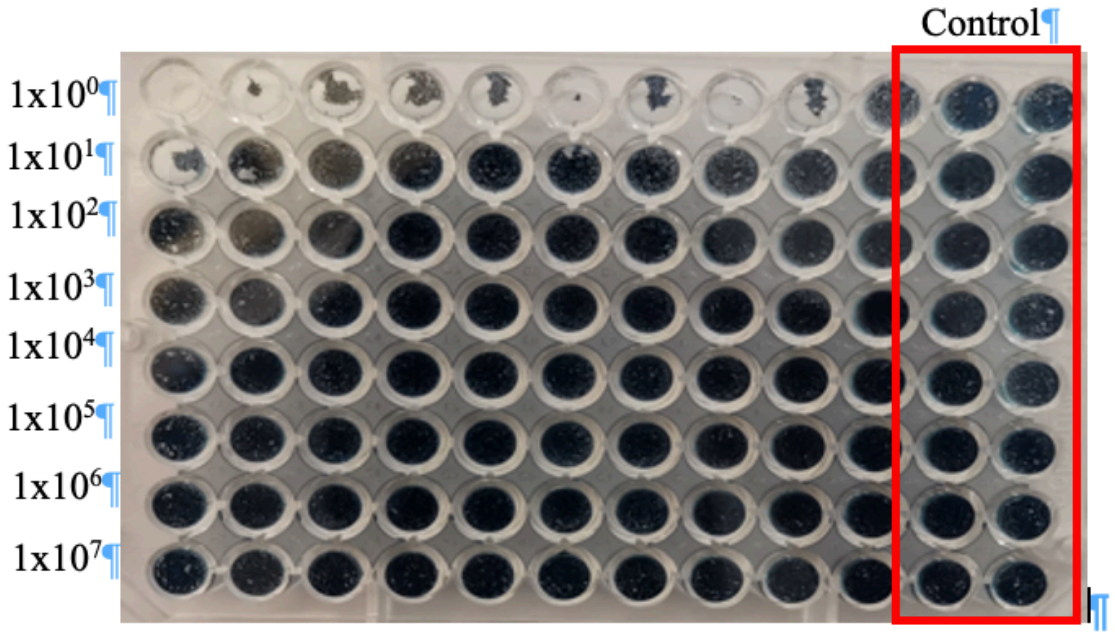

Figure 5.43. Supernatant collected from HEK293T cells after 4 days of transfection. ZIKV containing media was harvested and 96-well plates of BHK-21 were treated with dilutions of it to calculate the viral titre. **A**) ZIKV TCID50: $1.58x10^1$ /ml- FFU: $1.09X10^1$.

As a final experiment, HEK293T cells were transfected with a control of a mixture of products for CPER but without 2 fragments thus inhibiting the formation of the circular structure, wild type ZIKA with GFP reporter, and the mutants produced in the previous sections, Mutant N132S, **4**) Mutant H691Y, **5**) Mutant M763V **6**) Mutant M777T. Cells were incubated 96 hours post transfection, after the time concluded the cells were harvested and lysed for WB analysis against ZIKV E protein (Experiment was repeated twice) (**Figure 5.44.**).

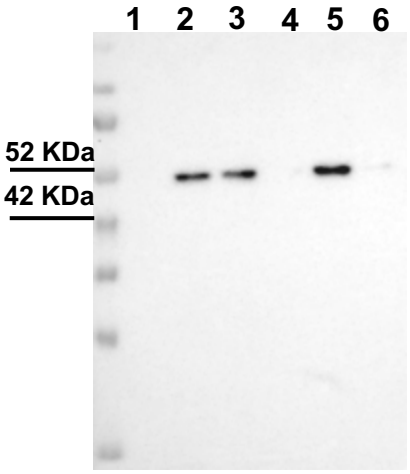

Figure 5.44. Western blot against ZIKV E protein on the CPER transfected 293T cells extracts. 1) Control cells without 2 fragments of the genome.**2**) Wild type ZIKV,**3**) Mutant N132S, **4**) Mutant H691Y, **5**) Mutant M763V **6**) Mutant M777T (Experiment was repeated twice).

ZIKV E protein was detected on the cells transfected with the wild-type construct, interestingly two out of the four mutants were positive for the viral glycoprotein. Mutant N132S and Mutant M763V produced a strong signal, whereas Mutant M777T only produced a faint band and Mutant H691Y did not produce any signal. These results suggest that it may be a difference between the production of this viruses and the mutation may have an influence in this process more experiments are required to verify this behaviour and if it is a result of the differences in capability to infect new cells within the population (infectivity) or is due the plasmid construct itself.

6. Discussion.

Since it is within the scope of this project to evaluate if the genetic changes that occurred to ZIKV during the different outbreaks had any impact in the tropism and pathogeny it is advantageous to recapitulate the natural history of the virus. ZIKV introduction into the American continent during 2015 was first reported as a Dengue-like syndrome in Natal, state of Rio Grande do Norte, Brazil. The patients that attended the health services displayed symptoms including arthralgia, oedema of extremities, mild fever, maculopapular rashes, frequently pruritic, headaches, retroorbital pain, etc. However, when the patients were screened the lab results indicated a non-DENV non-CHIKV disease [75], as described before the initial clinical manifestations did not differ from other febrile illnesses. Although ZIKV arrival to the American continent occurred within the last decade, it was initially discovered on the Zika Forest in Uganda during 1947 [4]. Previous collections of mosquitoes in the country allowed the identification of different viral agents such as Yellow Fever virus (YFV), Rift valley fever virus (RVF), Mengo encephalomyelitis virus, later known as Encephalomyocarditisvirus (EMCV), Semiliki forest virus (SFV), Bunyamwera orthobunyavirus (BUNV) and Ntaya virus (NTAV) [76]. The virus caused an acute febrile episode on a sentinel rhesus monkey (Rhesus 766) with no further symptomatology; the serum from this specimen was inoculated on another rhesus monkey (Rhesus 771), producing slight pyrexia, the serum from 766 was also inoculated either intraperitoneal or intracerebrally to mice with no observable symptoms, the virus was subsequently passaged until it was isolated again from mosquitoes of the Aedes africanus species on the Zika forest on 1948 when searching for Yellow Fever. The virus went mostly unnoticed with evidence of circulation within the human population until 1954 were during a jaundice outbreak, three patients were attended to a dispensary with fever ranging from 37.3 to 38.2, other diseases that cause fever such as malaria and yellow fever were discarded [4]. The evidence gathered from the rhesus macaques, the mosquitoes, and the patients showed that the virus caused a self-resolving disease characterised by febrile episodes, headaches and retroorbital pain.

After discrete epidemics within the African continent, cases of ZIKV related fever were reported in Asia, specifically in Indonesia, between 1977 and 1978. After three days,

patients with a persistent fever were screened for viral agents using anti-flaviviral and anti-alphaviral antibodies; patients positive against ZIKV reported rash as a symptom of the disease; this new symptom was added to high fever, malaise, stomachache, dizziness, and anorexia [77]. In 2010 ZIKV was detected in Cambodia from a sample of a three-year-old patient with fever and sore throat but no maculopapular rash; the general symptomatology was similar to other flaviviruses endemic to the region (DENV and JEV) [78]. The outbreaks that preceded the arrival to the American continent were crucial due to the number of infected patients and the apparition of neurological symptoms. On the Yap Islands, 73% of the population older than three years were infected during the 2007 outbreak. On the outbreak that occurred on French Polynesia between 2013 and 2014, a clear association between the ZIKV infection and microcephaly was established [6][79]. During the passage of the virus across the African and the Asiatic continent, new symptoms were added to the clinical profile of the ZIKV infection; however, since most of the cases coursed through a mild fever disease, the total circulation of the virus could be underestimated.

In **Figure 5.1**, a phylogenetic tree was constructed using the sequences of 59 different ZIKV genome samples collected from Africa, Asia, and America; the samples were selected from viruses isolated from biological fluids and were not passage through cells cultures. The selection aimed to discard sequences that have passed through cell culture adaptation, thus adding variants that are not present in nature. The tree clearly shows the two different lineages known up to date; 66.9% of the Asiatic lineage samples were isolated from the north, central and south America,26.1% of Asian lineage isolates were collected from the Asian and Oceania continents [80]. It is worth noting an underrepresentation of the African lineage with only 7% of the total isolates published. In an effort to refine the number of samples, an alignment of the ZIKV glycoprotein sequences from representative isolates of the outbreaks before the 2015 Brazilian outbreak were included being Yap Island and French Polynesia the most important ones. In **Figure 5.2**, a second phylogenetic tree was constructed using the representative sequences of outbreaks that preceded the Brazilian pandemic and samples from diverse countries of the south, central, and north America. The samples used were isolated from

either blood, saliva, urine, amniotic fluid, and breast milk. Two different clusters were formed, one comprising the American and Polynesian samples and another one with the Micronesia (Yap Island) sample. It is worth noting that the oldest sequence corresponding to Yap Island has the highest difference between the samples creating its clade; the reason for this was the accumulation of different mutations during its travel across the pacific in the period between 2007 and 2014. Previous reports cite two different disseminations from Southeast Asia into the Pacific region, the first one correlates with the Micronesian outbreak in 2007, with no further spread, and the second originated the South Pacific-American lineage that started the epidemics between 2013-2016 in the South Pacific and the Americas [81]. The phylogenetic data from the French Polynesian sample suggests that it was the probable source of the American epidemic, and most importantly, the first reported cases of microcephaly and Guillain-Barre syndrome appeared during this period [81][82][83].

The multiple sequence alignment analysis between the parental sequence provided by Dr Andres Merits (Brazil 2015) and sequences retrieved from Genbank identified 49 mutations; 41 were synonymous and did not have any impact. However, the remaining eight mutations impacted the aminoacidic sequence, changing either the charge, polarity, or size of the amino acids residues. These mutations were found either in the Pr/M protein or in the domains DI, DII or the DIII of E protein. However, no mutations were found within the fusion loop of DII of the E protein. The mutants are located on the PrM protein and DI of E protein are displayed in **Table 5.2**; no mutations were detected on the DII that is in charge of the dimerization, which contains the fusion loop, on **Table 5.3** are listed the mutations found on the DIII (receptor-binding domain (RBD)). The importance of the mutation in the E protein comes from the pivotal role of this structural protein during the infection; this protein directly interacts with the cellular receptor and orchestrates the membrane fusion between the viral and the plasmatic membranes, changes in the aminoacidic sequence may confer the capability to infect new cell types or hosts causing the neurological symptoms associated to the Polynesian and American outbreaks [51].
Nevertheless, this process is only possible with the proper processing of M protein and the Pr peptide cleavage to produce mature virions. Previous experiments comparing

Cambodian 2010 and Venezuelan 2016 isolates correlated the mutation S139N in the Pr/M protein to a boost of neurovirulence in neonatal mice and NPCs models, S139N referred to as residue 17 of prM protein, is fully exposed on the surface of prM-E heterodimers or immature particles [84]. Further evidence regarding the comparison between the African historic strain MR766 and the American epidemic strain BR15 showed a contrast in the levels of virus attachment to human brain glial SNB-19 cells, viral replication, and cell cytotoxicity measured by cell proliferation and apoptosis.

To test if the strains' differences could be attributed to the GP's changes, the C-prM and E regions of the structural proteins were swapped between the MR766 and the BR15 viral genomes. The experiments showed that the E protein was associated with viral attachment to host cells, the C-PrM region oversaw the permissiveness and ZIKV-induced cytotoxicity, and the Pr peptide is responsible for the PrM associated cytotoxicity [85]. All this evidence suggested that during its travel across the Pacific and its subsequential arrival to the American continent, the virus accumulated mutations that alter the cellular tropism favouring its neuroinvasiveness; these changes led to the apparition of new symptoms raising the public health alarms across the continent. The notion that few mutations can alter the tropism and host interaction has much backup from other viral species. A study addressing the role of spike protein differences between SARS-CoV and palm civet-CoVs and its impact on viral entry and cross-neutralisation found that amino acid changes in the RBD of SARS-CoV which resemble naturally occurring civet-CoVs, reduce the level of viral entry into human ACE2 cells significantly, but not only that, these changes confer resistance to neutralising antibodies generated by S glycoprotein-based SARS-CoV vaccines [86].

Mutations located far from the RBD may impact the viral tropism; for example, changes in the spike protein subunit S2 of Coronaviruses have been associated with changes in the cell tropism even though there are no recognisable RBD motifs on this protein, some of these changes are directly involved on the cleavage sites of the S protein and are located at the S1/S2 boundary or immediately upstream of the fusion peptide (S2-0 cleavage site). This protein processing appears to be crucial for virus-cell fusion, the

access to host proteases that process the S protein is pivotal for the viral tropism; the significance of S protein cleavage at the S1/S2 boundary comes clear in the case of Bat Coronavirus (BtCoV) HKU4, which is closely related to the MERS-CoV [87]. HKU4 S glycoprotein can interact with bot bat and human Dipeptidyl peptidase IV (DPP4). However, only in the context of bat cells and not in human cells, the virus can use it as an entry receptor [88].

In contrast, the Middle East Respiratory Syndrome Coronavirus (MERS-CoV) can infect both human and bat cells using DPP4 orthologues, this capability is related to two-amino acid substitutions (S746R and N762A) in the S1/S2 boundary of the S protein that allowed bat MERS-like CoV to resist the proteolytic environment of the human cells. As described before, changes within the RBD or in the proteolytic sites significantly impact the virus tropism and interaction with cellular receptors. There is evidence that ZIKV mutations could have an impact on the neurological symptoms. The real outcome of a single mutation in the ZIKV GP still needs to be evaluated due the fact that even if there is a positive impact in the infectivity , an i*n-vitro* model may be too limited to describe the process that occurs in nature and mutations in other structural or non-structural proteins may have a bigger impact in viral fitness, we have to be extremely cautions when it comes to interpretation of the results. However, methods like pseudotyping help to pinpoint what elements are important during entry and if changes within the protein sequence have a direct repercussion in the interaction between the cell and the virus.

To dissect the entry process and the influence of the GP mutants, the first step was to clone the 3′ 96-nucleotide region of the C gene (corresponding to amino acid residues 101 to 114, which encode the signal peptide) and full-length PrM/E genes and a reporter gene version 3′ 96-nucleotide region of the C gene, GFP, Foot-and-mouth disease virus 2A protease full-length C/PrM/E genes. The fragments were amplified from plasmids containing the infectious clones of ZIKV WT and ZIKV GFP+; **Figure 5.4** shows the two different fragments amplified using the plasmids templates, the size of the products corresponded to the one predicted from the in-silico PCR. Once the products were purified (**Figure 5.5**), duplicates were prepared and then introduced into the pcDNA3.1

plasmid with the help of the TOPO directional cloning system, the addition of the CACC tag at the 5'end establish the sense of the insertion without any further steps. The ligated plasmids pcDNA3.1 ZIKV C/GFP/PrM/E and pcDNA3.1 ZIKV PrM/E were then propagated into *E.coli* cells, colony screening (**Figure 5.6** and **Figure 5.7**), the low efficiency of the transformation may be due to the total size of the plasmid being about 8 KDa in the case of the GFP+ and around 7 KDa in the case of the WT [89]. Once the plasmids were purified and identified using sanger sequencing (data not shown), they were used as templates for SDM (**Figure 5.8**). This strategy was chosen due to the ease of working with a pair of proteins within a plasmid instead of introducing a mutation into the whole viral genome that may cause off-target mutations that may impact the viral fitness masking the real impact of the planned changes. The identity of the mutations was corroborated by sanger sequencing. Before testing the mutants' infectivity and the wild-type glycoprotein, a quick receptor screening on HEK293T and HUH7 cells was carried out; TIM-1, TYRO3 and AXL are described as the possible receptors for the virus. However, evidence suggests that in the absence of one or more of them, the virus can still infect the cells; CD 299 was added to the receptor screening due to its role as a cellular receptor on other flaviviruses such as DENV. mRNA was isolated from both cell lines, and cDNA was synthesised; an approach to the abundance of the receptor was stated using base-ten dilutions of the products. HUH7 cells were positive for TYRO3 and TIM-1, however, although AXL bands were detected, they had a bigger size than expected when designing the primers (considering intron-exon borders) and it could be due the presence of genomic DNA on the samples that interfere with the PCR reaction giving a false positive to further confirm this result addition of DNAse can be added to the mixture after the RNA isolation process and discard any possible contamination (**Figure 5.9 A**). HEK293T cells were also positive for AXL, TYRO3 and TIM1 proteins (**Figure 5.9 B**); this may explain both cell lines' permissiveness to ZIKV infection.

Interestingly neither HEK293T nor HUH7 cells were positive for CD299. Nonetheless, CD299 also known as L-SIGN, a transmembrane receptor expressed in the endothelial cells of the lymph nodes and liver, neither of the cell lines shares these characteristics. Further experiments are needed to completely discard the absence of CD299 on the

HEK293T and HUH7s, which include the selection of a proper positive control for the gene, choosing a cell line that has been reported to express the protein will validate the results and discard the possibility that the primers had a faulty design. Validation of the PCR results is also imperative to corelate the presence of the receptor to the permissiveness to the infection, immunoblotting against the protein is essential in these cases due the fact that not always the presence of mRNA is translated to protein expression, mechanisms of translational repression may be active, lessening specific protein production. It is also worth noting that even though AXL seems to be necessary in some tissues, cells, or cell lines to be infected by ZIKV [90][91], the virus has the capability to infect cells that do not express this molecule [13].

Since the objective of this thesis was to test if the mutations on the glycoprotein had any impact on the tropism exhibited during the American pandemic, a model that dissect the entry process needed to be employed, the use of pseudotypes or PPs was the best option due to the plasticity of the methodology. Pseudotypes were prepared by transfecting HEK293T cells with a pair of plasmids, an HIV-1 backbone, and a heterologous glycoprotein. The particles produced were not replicative competent but can introduce a reporter gene into the recipient cell. During the first approach, the glycoproteins were VSV-G (as a positive control) and ZIKA GP (a scheme of the two plasmid versions of ZIKA GP is displayed in **Figure 15.10 A**). Considering that there was no available protocol to pseudotype ZIKV GP, the laboratory standard protocol was used, starting with 2 µg of pNL4.3 HIV-1 backbone and 2 µg of GP plasmid. However, there was no evidence of infectivity (measured by luciferase activity) under this condition. Since the standard parameters did not work, five different GP plasmid concentrations were tested, starting with 1 µg and increasing one by one until reaching 5 µg. The PPs produced using the pcDNA3.1 ZIKV PrM/E plasmids were used to infect HEK293T cells (**Figure 5.10 B**). Luciferase activity was measured in both the infected and the producer cells; there was no evidence that the pseudo particles infected the HEK293T cells to test if the producer cells were translating the components needed to assemble the PPs, luciferase activity was measured as well.

Interestingly, there was a significative decrease (**p<0.001**) in the luciferase activity as the plasmid concentration used for transfection increases. The pcDNA3.1 ZIKV C/GFP/PrM/E plasmid was also tested (**Figure 5.10 C)** with similar results; no difference in the luciferase activity was observed when the samples were compared with the negative control (PPs without viral GP). Similarly, when de luciferase activity was measured on the producer cells showed the same behaviour as with the transfection of the pcDNA3.1 ZIKV PrM/E construct, as the plasmid concentration increased, the enzymatic activity diminished significatively (**p<0.001).** VSV-G was used as a positive control for both constructs. The luciferase activity of both the producer and the infected cells displayed on both graphs demonstrated that the cells could translate the backbone genes and assemble the PPs efficiently.

Since no evidence of infectivity was found when the cells were treated with ZIKV PPs, the next step was to look for protein expression of viral proteins from both the backbone and the heterologous glycoprotein. **Figure 5.11** shows the proteins detected from cell lysates and pelleted PPs. VSV-G glycoprotein was detected from both the producer cells and the pelleted PPs (at the weight reported previously on the bibliography) (**Figure 5.11 A and 5.11 D**), the expression of the GP correlated with the results observed on the infectivity assays [92]. However, when ZIKV GP was blotted, the band corresponding to the protein went dimmer as the plasmid concentration increased (**Figure 5.11 B);** this behaviour was similar to the observed on the luciferase activity of the producer cells, interestingly, when looking for ZIKV GP on the pelleted PPs, no signal was detected partially explaining why the particles were not infectious (**Figure 5.11 E**). Finally, when the HIV-1 p55 gag and p24 capsid proteins were blotted, the same phenomenon was observed, as the amount of plasmid increased, the expression of P55 gag protein decreased on the producer cells (**Figure 5.11 C**) and when the pellets were analysed only faint bands were detected at the lowest concentrations of ZIKV GP transfection (**Figure 5.11 F**). These results back up the data gathered from the infectivity assays; there is a direct effect on the protein expression as a direct result of the increasing plasmid concentrations.

The formation of infectious particles not only depends on the expression of viral proteins but the proper localisation of these to try to elucidate if the components of the particles

shared the same space during translation immunofluorescence was performed **(Figure 5.12)**. Plasmid pcDNA3.1 ZIKV C/GFP/PrM/E was used to track the transfection process, mock-treated cells (**Figure 5.12 A**) were used as fluorescence control, the expression of the GFP (green) and ZIKV envelope protein (cyan) was found on the cytoplasm, and the perinuclear area (**Figure 5.12 B**) since the assembly of the ZIKV virion takes place on replicative complexes (modifications of the ER) the distribution of the fluorescence labels corresponds to the previous bibliographic reports which include the perinuclear region and the centrosome [93][94][95]. A co-transfection was carried out using the standard 2 µg of pNL4.3 HIV-1 backbone and 2 µg of GP plasmid; proteins are displayed as GFP (green), ZIKV envelope protein (cyan) and p55/p24 HIV-1 capsid protein (red), all three proteins had similar cytoplasmic distribution (**Figure 5.12 C**). Co-localisation analysis was performed (**Figure 5.12 D**), Pearson's correlation coefficient graph. A moderated co-localisation between ZIKV E and HIV-1 p24 was observed (co-localization= 0.53); this interaction may not be enough to form the infectious particles due to the intimate contact needed during GP incorporation. One explanation for the particles' defective formation was that the ratio between the retroviral backbone and the glycoprotein was not ideal for translating both proteins; a matrix of twenty-five different combinations was designed to eliminate the interference between the plasmids. **Figure 5.13 A** displays a set of five graphs that correspond to the treatment of HEK293T and HUH7 cells with PPs produced using the plasmid combination. To generate the infectious particles, fixed concentrations of ZIKV GP and increasing concentrations from 1 µg to 5 µg of pNL4.3 HIV-1 were used. As in the previous experiments, there was no difference between the negative control and the PPs produced using the concentrations matrix. As another way to tackle the lack of evidence about the infectivity, different mammalian cell lines were tested (**Figure 5.13 B**), CHO, VERO and BHK-21 were used since previous reports showed that VERO and BHK-21 were permissive to the viral infection and CHO cells were refractive to this [96].

Luciferase activity did not show any infection sign by the PPs; VSV-G was used as a positive control since this viral GP's broad tropism. Another strategy implemented to boost the particles' infectivity was to clone the NS2B-NS3 protease and its cofactor (**Figure 5.14**). Previous reports linked the presence of the viral protease to increased

processing by the signal peptidase of the NH2 terminus of prM during expression of the structural region of the Murray Valley encephalitis polyprotein; this protease cleaves the COOH terminus of C protein, this behaviour is shared between members of the Flavivirus family [97][98] [99]. The cells were co-transfected with the pcDNA3.1 ZIKV C/GFP/PrM/E and the NS2B-NS3 plasmids; the protein expression was estimated using IF (**Figure 5.15**), the two proteins were located on the cytoplasm and the perinuclear region, when the signals were merged a certain level of overlap was observed, suggesting that both share the same cellular localisation at some extent. However, no increase of infectivity was observed when the producer cells were transfected with fixed concentrations (2 µg) of the pcDNA3.1 ZIKV C/GFP/PrM/E and pNL4.3 HIV-1 plasmids and increasing concentrations of the NS2B-NS3 plasmid (1 µg and an increasing one by one until reaching 5 µg) (**Figure 5.16 A**). Other strategies were designed to boost the infectivity of the particles, including transfecting 5-fold dilutions of the ZIKV GP plasmid (2µg,0.4 µg,0.08µg,0.016µg and 0.0032µg) (**Figure 5.16B**) with no positive results. Finally, the MLV backbone was tested since there was a chance that a different backbone may induce the proper incorporation of the glycoprotein (**Figure 5.16 C)**; when the luciferase of the producer cells was measured, the positive control and the ZIKV GP transfected cells had similar levels of enzymatic activity. Nonetheless, this substitution on the backbone plasmid did not confer any advantage in terms of infectivity.

Since one of the proposed mechanisms for the pseudo particles production involves the presence of the heterologous GP on the plasmatic membrane [63][64], two sets of HEK293T cells were transfected with pcDNA3.1 ZIKV C/GFP/PrM/E plasmid and treated or not with permeabilization solution (**Figure 17**).

The transfected cells that were not treated with the permeabilization solution only displayed the GFP's signal reported protein (green). However, no signal of the Env protein was detected (**Figure 17 A**), which suggests that the Env protein was not present on the plasmatic membrane or not in enough concentration to be recognised by the antibody. These results are backed up by the fact that by treating the cells with the permeabilization solution, the Env protein signal (cyan) was detected within the cells (**Figure 17 B**). One

of the proposed explanations for the lack of infectivity is that since the protein is not present on the PM, the HIV-1 virion cannot incorporate it into its membrane as it exists in the producer cell.

Finally, to increase the amount of viral protein available within the cell and favour the spill over of these proteins into other cellular compartments, the protease inhibitor MG132 was used (**Figure 5.18.)**. Cell viability was evaluated using increasing concentrations of the inhibitor since most of the concentrations were lethal due to induction of apoptosis after 72 hours (1 μM, 10 μM, 25 μM, 50 μM) the lower concentration of 0.1μM was used since it had the lowest impact on cell viability (**Figure 5.18 A**) [100] [101] [102]. HEK293T cells were transfected with increasing amounts of the GP plasmid a fixed amount of pNL4.3 and treated with MG132 mimicking the PP production process; the viability was evaluated after 72 hours with no negative impact (**Figure 5.18B).** The luciferase activity assay did not show any change in the particles' infectivity produced by the cells treated with the proteasome inhibitor (**Figure 5.18 C**).

The production of PPs is an intricate process that involves not only the plasmids used during the transfection but the nature of the heterologous GP; there are common traits among the proteins that have been efficiently pseudotyped, including the length of the cytoplasmic tail and its capability to interact with the pockets formed during the capsid formation and the cellular localisation. However, not all the GP have the same length or residues (**Figure 5.19**). It is worth noting that most of the GPs have at least 20 residues on the cytoplasmic tail with few notable exceptions like the Ebola virus and members of the same family, which have just a couple of amino acids, no apparent similarity was noticeable after the analysis of the sequences except by the proportion of polar and non-polar residues which seems to be the most abundant between the four types of amino acids analysed.

Not only the nature of the GP is involved in the formation of the PPs, but the origin of the backbone will determine how does this interacts with the host cell; a clear example is the difference between the MLV and the HIV-1 backbones; each of them have different

efficiencies depending on the stage of the cell cycle. Finally, the efficiency of transfection and protein production is a limiting step when it comes to viral assembly; PEI is a common choice of a transfection reagent due to its easy preparation, cost, and safety. However, factors such as the plasmid size, the nature of the protein, and the amount used for the transfection limit or enhance the protein expression [103].

The latest experiments reported by *Kretschmer et al.* showed that they could produce infective PPs that incorporated the ZIKV glycoprotein. However, the methodology differed from the one exposed in this thesis on the amount of genetic material used during the transfection (8 µg of the HIV backbone (pNL Luc AM) + 37 µg of the ZIKV GP(pME-Z1 plasmid), although they used the same cell line as us (HEK293T) the format were the cells were seeded, transfected and incubated was a six-well plate, contrasting with the 10 cm dish used during the experiments presented before [104]. The authors reported that under these conditions, the cells could produce particles that infected other cell lines. The explanation for these results involved the presence of the HIV-1 protein *Nef,* contained on the backbone plasmid pNL Luc AM which helps during the particle formation process and that is absent on the pNL4.3 plasmid, but not only this when higher amounts of the GP plasmid were used during the transfection process the cells were able to incorporate the protein into the PPs efficiently. Altogether the information mentioned before differs from the approaches exposed during the development of our experiments performed to try to produce PPs; the amounts of plasmids used by *Kretschmer et al.* exceeds the range used in our experiments by several micrograms, by using these quantities overflows the system and the viral proteins may spill over into other cellular compartments favouring the incorporation into the HIV-1 capsid.

Since the parameters tested during the pseudotype production did not work, an infectious clone system was tested. This approach began with amplification of the original plasmid provided by Dr Merits; since the plasmid size was about 18 Kb standard, Stellar E. coli cells had problems with its maintenance and propagation of NEB Stable cells. After the transformation, 24 hours and 48 hours incubation were tested, the plasmids were then purified and electrophered with noticeable bands (**Figure 5.21 A and B**). This experiment

was followed by the elucidation of the optimal concentration of plasmid that was going to be used during the transformation step (**Figure 5.222**). Increasing amounts of plasmid were used for transformation (50 ng, 100 ng, 250 ng, 500 ng, 750 ng), being 50 ng, the optimal concentration producing $7x10^3$ colonies per microgram of DNA or seven colonies per nanogram of DNA, the approach that followed was the reduction of the antibiotic concentration, this leaded to a notable increase on the number of colonies. However, this increment in the number of colonies made it almost impossible to properly isolate a single colony (**Figure 5.23 A and B**). The optimisation concluded with the substitution of LB media with Terrific broth to improve the plasmid production (**Figure 5.24)**; gathering all these data, the best strategy was to transform Stable cells with 50 ng of plasmid, incubate them on Terrific broth for 24 hours.

To validate the isolated plasmids' identity, a PCR was carried out, amplifying the PrM/ E genes; plasmids isolated from 24 and 48 hours were positive for the envelope genes confirming the identity (**Figure 5.25).** Once the plasmids were amplified, a reverse genetic system was designed to introduce the mutations on the envelope protein and then reintroduce it into the infectious clone; the genome was divided into different fragments and amplified (**Figure 5.26**). The main reason behind this design was to produce a plasmid that could be readily amplified; genome fragments could be swap just with one digestion and ligation step; pUC19 was selected as plasmid backbone due to its small size and plasticity (**Figure 5.26 A**). The fragments were fused with Gibson assembly's help; colonies were screened with positives results (**Figure 5.26 B**); this method was used before producing infectious DENV viruses [105] efficiently. Nevertheless, when the cells were evaluated against two different non-structural proteins, mixed results were obtained.

Interestingly, the cells tested negative for the NS5 gene but not for the NS2B/NS3 gene suggesting the loss of viral genes during either the assembly or plasmid replication process. To circumvent this issue, the whole genome was amplified using the LongAmp reaction with positive results; the optimal temperature was determined using a temperature gradient (**Figure 5.27**). When this product was transformed, no positive colonies were observed, a possible explanation was that the fragments used to construct

the plasmid were cleaved during the replication process; this may be in part due to the inherent instability that the Flavivirus genomes display when they are introduced into multicopy plasmids [106][107].

As an alternative, the genome and the plasmid backbone were amplified without the envelope genes (**Figure 5.28 A and B**); the product of this amplification was treated with KLD as preparation for ligation and transformed. The colonies were screened against the NS2B-NS3 protease (**Figure 5.29)**, the positive colonies were seeded on terrific broth, and the plasmid was isolated (**Figure 5.3o**) to confirm the identity of the plasmid genome fragments were amplified with positive results (**Figure 5.31**). Interestingly, when the plasmids were amplified, the cell lost it after a couple of passages; previous reports showed that a model using an infectious clone based on a pUC19 backbone with no replicative control was not adequate to store and maintain a plasmid stock, the production of toxic products is linked to cryptic promoters present on the genome (**Table 5.4 and 5.5**), it is worth noting that the genes that encode for C, E, NS1, NS3 and NS5 genes might work as promoters for toxic peptides within the bacterial cells when the 3'to 5'sense was scanned and the NS5, NS4B, NS3, NS2A, NS1, E, M and C genes were identified in the reverse strand [69][70].

Lastly, in order to produce infectious virus, a plasmid-free system was designed. To test if the HEK293T cells could produce live virus efficiently, the cells were infected with ZIKV. They were then imaged by electron microscopy (**Figure 5.32**), the infected cells showed electron-dense bodies in vesicles, a morphology typically associated with viral particles [108]. Viral titration assays later confirmed the viral particles' production on BHK-21 cells; as the virus was passaged, the titre stabilised (**Figure 5.33;** this knowledge was used for later viral passaging and storage. Two different methodologies were used to try to produce live virus ISA (infectious subgenomic amplicons) and CPER (Circular Polymerase Extension Reaction); the first one relays on a yet to be described *in cellular* recombination event that fuses different fragments of a viral genome into a single-stranded molecule that can be translated by the cell, the second one need to create a circular structure similar to a plasmid that drives the production of the viral particles

[71][72][73]. The ISA construct was designed with the addition of CMV promoter and enhancer sequence at the 5'region to drive the expression of the viral sequence, the sv40 pA signal and the HDV ribozyme was added downstream the genome on the 3'end, these sequences contribute to the stability and the processing of the viral RNA (**Figure 5.34**). The genome was divided into different fragments, including the GFP reporter gene that was later amplified (**Figure 5.35 and 5.36)**; the fragments were transfected into HEL293T cells, a plasmid containing GFP was used as a positive control. No positive cells were observed under an epifluorescence microscope (**Figure 5.37**). As an alternative, VERO cells were electroporated with both the positive control (**Figure 5.38**) and the ISA products (**Figure 5.39)**; again, no positive cells were observed under the microscope. The possible explanation was that the cells could not recombine the fragments, even if this method has been used before to produce full viruses [109], the determinants and conditions required to propagate the virus efficiently. The CPER approach had a similar design that adds the CMV promoter, SV40 pA and HDVR sequences; however, in this case, to produce the circular structure, a linker region needs to be added (**Figure 5.40)**, the fragments were amplified following the same approximation as with the ISA method (**Figure 5.41)**. When the cells were transfected using this circular molecule, they efficiently produced the reporter protein (**Figure 5.42**), the viral production was later confirmed by the titration assay (**Figure 5.43**), as expected the TCID50 was low after four days of incubation ($1.58x10^1$ /ml- FFU: $1.09X10^1$), the viral titre could be increased by extending the incubation time, the main problem of this was the cell death and medium acidification after the fourth day. Finally, since the system plasticity allows to swap viral genes at will and the cells could produce infectious virus, the wild type prM/E genes were exchanged with the Mutants N132S, H691Y, M763V, M777T. The cells were transfected with these different structures (**Figure 5.44**, WB of the Envelope protein was used to analyse protein expression.

Interestingly, the different mutations have different band intensities; this may suggest that there is either a difference in viral production and replication leading to are higher or lower levels of infection to the nearby cells or that the antibody is not able to properly recognize the protein due the changes produced by the mutation this still needs to be elucidated

and it's a good to topic to follow-up. When comparing ISA vs CPER methods, CPER seemed to be the ideal method to produce infectious virus, this due the fact that ISA relays on a yet to be described mechanism of *in-cellulo* recombination mechanism that may not be as efficient under the circumstances tested in this thesis, both methods have the advantage of being able to swap genes with mutations of interest so the election of the methodology will depend of the reproducibility of the results [110][111][112]. Further experiments are needed to produce the viral particles homogeneously and with a stable viral titer; however, due to the ongoing SARS-CoV-2, the access to the laboratory that was going to host these experiments (Virology Lab of the Infectomics and Molecular Pathogenesis department at the Center for Research and Advanced Studies of the National Polytechnic Institute, Mexico) restricting the access only to essential personal limiting the capability to perform experiments and discarding the chance to carry out any further tests.

7. Future work.

Evidence that mutations accumulated across the time on the envelope protein of different viruses including ZIKV have an impact on the development of the infection keeps piling up; different models have been used to dissect the entry process and the influence of the changes on the amino acid sequence on the infectivity of the virus. Pseudotyping was used efficiently before with different viruses, the difficulties that arose during the development of this project suggests that other not all viral proteins can be pseudotyped using the typical approaches, previous experiments showed that adding tags that target the plasmatic membrane had little to no impact in the infectivity of particles that tried to incorporate Flaviviral proteins. However, other pathways could be used, such as creating chimeric proteins with longer cytoplasmatic tails, with these modifications, the protein could interact with the structure formed by the capsid protein of the backbone.

The plasmid-free system seems to be more promising to test the mutations; this system could be replicated using clinical samples or swapping other structural and non-structural proteins. Future experiments are required to validate the efficient production of infectious viruses (**Table 19);** however, it was impossible to carry on with this process due to the ongoing SARS-CoV-2 pandemic. Phenotyping ZIKV has a huge impact in our understanding of the pathological process and the effects that point mutations have on overall picture, this could help identifying mutant that escape neutralization or that have increased viral fitness that confers them an advantage against other viral populations.

Table 7.1- Future work timeline.

Future work timeline	
Action	Time
Purification, and validation of viral genome cloning	3 weeks
Transfection and harvest of Viral particles	1 month
Viral titer and stock creation	1 month
Test wilt type and mutant viruses' infectivity	3 months
Validation of viral particle production	1 month

Antibody neutralization tests	2 weeks
Test the viruses on different cell lines and assess the differences on infectivity	3 months

8. Bibliography:

[1] Wang, A., Thurmond, S., Islas, L., Hui, K., & Hai, R. (2017). Zika virus genome biology and molecular pathogenesis. Emerging Microbes & Infections, 6(3), e13. http://doi.org/10.1038/emi.2016.141

[2] Heinz, F. X., & Stiasny, K. (2017). The Antigenic Structure of Zika Virus and Its Relation to Other Flaviviruses: Implications for Infection and Immunoprophylaxis. Microbiology and Molecular Biology Reviews, 81(1), e00055-16. http://doi.org/10.1128/MMBR.00055-16

[3] Imperato, P. J. (2016). The Convergence of a Virus, Mosquitoes, and Human Travel in Globalizing the Zika Epidemic. Journal of Community Health, 41(3), 674–679. http://doi.org/10.1007/s10900-016-0177-7

[4] MacNamara, F. N. (1954). Zika virus: A report on three cases of human infection during an epidemic of jaundice in Nigeria. *Transactions of the Royal Society of Tropical Medicine and Hygiene*, *48*(2), 139–145. https://doi.org/10.1016/0035-9203(54)90006-1

[5] Gebre, Y., Forbes, N., & Gebre, T. (2016). Zika virus infection, transmission, associated neurological disorders and birth abnormalities: A review of progress in research, priorities and knowledge gaps. Asian Pacific Journal of Tropical Biomedicine, 6(10), 815–824. http://doi.org/10.1016/j.apjtb.2016.08.008

[6] Cauchemez, S., Besnard, M., Bompard, P., Dub, T., Guillemette-Artur, P., Eyrolle-Guignot, D., … Mallet, H. P. (2016). Association between Zika virus and microcephaly in French Polynesia, 2013-15: A retrospective study. The Lancet, 387(10033), 2125–2132. http://doi.org/10.1016/S0140-6736(16)00651-6

[7] Faye, O., Freire, C. C. M., Iamarino, A., Faye, O., de Oliveira, J. V. C., Diallo, M., … Sall, A. A. (2014). Molecular Evolution of Zika Virus during Its Emergence in the 20th Century. PLoS Neglected Tropical Diseases, 8(1), 36. http://doi.org/10.1371/journal.pntd.0002636

[8] ANDERSON, C. R., DOWNS, W. G., & THEILER, M. (1956). Neutralizing antibodies against certain viruses in the sera of residents of Trinidad, B.W.I. *The American Journal of Tropical Medicine and Hygiene*, *5*(4), 626–641. https://doi.org/10.4269/ajtmh.1956.5.626

[9] Smithburn, K. C. (1954). Neutralizing antibodies against arthropod-borne viruses in the sera of long-time residents of Malaya and borneo. *American Journal of Epidemiology*, *59*(2), 157–163. https://doi.org/10.1093/oxfordjournals.aje.a119630

[10] HAMMON, W. M., SCHRACK, W. D., & SATHER, G. E. (1958). Serological survey for a arthropod-borne virus infections in the Philippines. *The American Journal of Tropical Medicine and Hygiene*, *7*(3), 323–328. https://doi.org/10.4269/ajtmh.1958.7.323

[11] Kindhauser, M. K., Allen, T., Frank, V., Santhana, R. S., & Dye, C. (2016). Zika: Origine et propagation d'un virus transmis par des moustiques. *Bulletin of the World Health Organization*, *94*(9), 675-686C. https://doi.org/10.2471/BLT.16.171082

[12] Travelers' Health. (2020, May 4). Retrieved May 04, 2020, from https://wwwnc.cdc.gov/travel/page/world-map-areas-with-zika

[13] Current Zika transmission. (n.d.). Retrieved May 04, 2017, from http://ecdc.europa.eu/en/healthtopics/zika_virus_infection/zika-outbreak/Pages/Zika-countries-with-transmission.aspx

[14 Mossenta, M., Marchese, S., Poggianella, M., Slon Campos, J. L., & Burrone, O. R. (2017). Role of N-glycosylation on Zika virus E protein secretion, viral assembly, and infectivity. Biochemical and Biophysical Research Communications, 1–8. http://doi.org/10.1016/j.bbrc.2017.01.022

[15] Hamel, R., Dejarnac, O., Wichit, S., Ekchariyawat, P., Neyret, A., Luplertlop, N., … Misse, D. (2015). Biology of Zika Virus Infection in Human Skin Cells. J Virol, 89(17), 8880–8896. http://doi.org/10.1128/jvi.00354-15

[16] Fleming, I. (2003). Endothelial Cell Infection by the Zika Virus, 1149–1151. http://doi.org/10.1038/nm1267.

[17] Wells, M. F., Salick, M. R., Wiskow, O., Ho, D. J., Worringer, K. A., Ihry, R. J., … Eggan, K. (2016). Genetic Ablation of AXL Does Not Protect Human Neural Progenitor Cells and Cerebral Organoids from Zika Virus Infection. Cell Stem Cell, 19(6), 703–708. http://doi.org/10.1016/j.stem.2016.11.011

[18] Mukhopadhyay, S., Kuhn, R. J., & Rossmann, M. G. (2005). A structural perspective of the flavivirus life cycle. Nature Reviews Microbiology, 3(1), 13–22. http://doi.org/10.1038/nrmicro1067

[19] Rodenhuis-Zybert, I. A., Wilschut, J., & Smit, J. M. (2010). Dengue virus life cycle: Viral and host factors modulating infectivity. Cellular and Molecular Life Sciences, 67(16), 2773–2786. http://doi.org/10.1007/s00018-010-0357-z

[20] Smit, J. M., Moesker, B., Rodenhuis-Zybert, I., & Wilschut, J. (2011). Flavivirus cell entry and membrane fusion. Viruses, 3(2), 160–171. http://doi.org/10.3390/v3020160

[21] Ming, G., Tang, H., & Song, H. (2016). Advances in Zika Virus Research: Stem Cell Models, Challenges, and Opportunities. Cell Stem Cell, 19(6), 690–702. http://doi.org/10.1016/j.stem.2016.11.014

[22] Kostyuchenko, V. A., Lim, E. X. Y., Zhang, S., Fibriansah, G., Ng, T.-S., Ooi, J. S. G., … Lok, S.-M. (2016). Structure of the thermally stable Zika virus. Nature, 533(7603), 425–428. http://doi.org/10.1038/nature17994

[23] Soares, C. N., Brasil, P., Carrera, R. M., Sequeira, P., de Filippis, A. B., Borges, V. A., … Solomon, T. (2016). Fatal encephalitis associated with Zika virus infection in an adult. Journal of Clinical Virology, 83(January), 63–65. http://doi.org/10.1016/j.jcv.2016.08.297

[24] Araujo, A. Q. C., Silva, M. T. T., & Araujo, A. P. Q. C. (2016). Zika virus-associated neurological disorders: A review. Brain, 139(8), 2122–2130. http://doi.org/10.1093/brain/aww158

[25] Perera-Lecoin, M., Meertens, L., Carnec, X., & Amara, A. (2013). Flavivirus entry receptors: An update. Viruses, 6(1), 69–88. http://doi.org/10.3390/v6010069

[26] Simoni, M. K., Jurado, K. A., Abrahams, V. M., Fikrig, E., & Guller, S. (2016). Zika virus infection of Hofbauer cells. American Journal of Reproductive Immunology, (October), 1–4. http://doi.org/10.1111/aji.12613

[27] Chan, J. F.-W., Yip, C. C.-Y., Tsang, J. O.-L., Tee, K.-M., Cai, J.-P., Chik, K. K.-H., … Yuen, K.-Y. (2016). Differential cell line susceptibility to the emerging Zika virus: implications for disease pathogenesis, non-vector-borne human transmission, and animal reservoirs. Emerging Microbes & Infections, 5(August), e93. http://doi.org/10.1038/emi.2016.99

[28] Brault, J. B., Khou, C., Basset, J., Coquand, L., Fraisier, V., Frenkiel, M. P., … Baffet, A. D. (2016). Comparative Analysis Between Flaviviruses Reveals Specific Neural Stem Cell Tropism for Zika Virus in the Mouse Developing Neocortex. EBioMedicine, pp. 71–76. The Ohio State University Wexner Medical Center. http://doi.org/10.1016/j.ebiom.2016.07.018

[29] Fernandez-Garcia, M. D., Mazzon, M., Jacobs, M., & Amara, A. (2009). Pathogenesis of Flavivirus Infections: Using and Abusing the Host Cell. Cell Host and Microbe, 5(4), 318–328. http://doi.org/10.1016/j.chom.2009.04.001

[30] Morrison, J., & García-Sastre, A. (2014). STAT2 signaling and dengue virus infection. Jak-Stat, 3(1), e27715. http://doi.org/10.4161/jkst.27715

[31] Xie, X., Shan, C., & Shi, P.-Y. (2016). Restriction of Zika Virus by Host Innate Immunity. Cell Host & Microbe, 19(5), 566–567. http://doi.org/10.1016/j.chom.2016.04.019

[32] Wang, Q., Yang, H., Liu, X., Dai, L., Ma, T., Qi, J., … Gao, G. F. (2016). Molecular determinants of human neutralizing antibodies isolated from a patient infected with Zika virus. Science Translational Medicine, 8(369), 1–11. http://doi.org/10.1126/scitranslmed.aai8336

[33] Zika virus information for clinicians Retrieved May 04, 2017, from https://www.cdc.gov/zika/pdfs/clinicianppt.pdf

[34] Jaeger, A. S., Weiler, A. M., Moriarty, R. V., Rybarczyk, S., O'Connor, S. L., O'Connor, D. H., Seelig, D. M., Fritsch, M. K., Friedrich, T. C., & Aliota, M. T. (2020). Spondweni virus causes fetal harm in Ifnar1−/− mice and is transmitted by Aedes aegypti mosquitoes. *Virology*, *547*, 35–46. https://doi.org/10.1016/j.virol.2020.05.005

[35] Salazar, V., Jagger, B. W., Mongkolsapaya, J., Burgomaster, K. E., Dejnirattisai, W., Winkler, E. S., Fernandez, E., Nelson, C. A., Fremont, D. H., Pierson, T. C., Crowe, J. E., Screaton, G. R., & Diamond, M. S. (2019). Dengue and Zika Virus Cross-Reactive Human Monoclonal Antibodies Protect against Spondweni Virus Infection and Pathogenesis in Mice. *Cell Reports*, *26*(6), 1585-1597.e4. https://doi.org/10.1016/j.celrep.2019.01.052

[36] Retallack, H., Di Lullo, E., Arias, C., Knopp, K. A., Laurie, M. T., Sandoval-Espinosa, C., … DeRisi, J. L. (2016). Zika virus cell tropism in the developing human brain and inhibition by azithromycin. Proceedings of the National Academy of Sciences of the United States of America, 201618029. http://doi.org/10.1073/pnas.1618029113

[37] McCarthy, M. (2016). Zika related microcephaly may appear after birth, study finds. Bmj, 355(i6333), 1–1. http://doi.org/10.1136/bmj.i6333

[38] Mécharles, S., Herrmann, C., Poullain, P., Tran, T. H., Deschamps, N., Mathon, G., … Lannuzel, A. (2016). Acute myelitis due to Zika virus infection. The Lancet. http://doi.org/10.1016/S0140-6736(16)00644-9

[38] Moore, C. A., Staples, J. E., Dobyns, W. B., Pessoa, A., Ventura, C. V., Fonseca, E. B. da, Ribeiro, E. M., Ventura, L. O., Neto, N. N., Arena, J. F., & Rasmussen, S. A. (2017). Congenital Zika syndrome: Characterizing the pattern of anomalies for pediatric healthcare providers. *JAMA Pediatr*, *171*(3), 288–295. https://doi.org/10.1001/jamapediatrics.2016.3982.

[36] Parmar, H., & Ibrahim, M. (2012). Pediatric Intracranial Infections. *Neuroimaging Clinics of North America*, *22*(4), 707–725. https://doi.org/10.1016/j.nic.2012.05.016

[41] Chan, J. F. W., Choi, G. K. Y., Yip, C. C. Y., Cheng, V. C. C., & Yuen, K. Y. (2016). Zika fever and congenital Zika syndrome: An unexpected emerging arboviral disease. *Journal of Infection*, *72*(5), 507–524. https://doi.org/10.1016/j.jinf.2016.02.011

[42] Wheeler, A. C. (2018). Development of infants with congenital zika syndrome: What do we know and what can we expect? *Pediatrics*, *141*(February 2018), S154–S160. https://doi.org/10.1542/peds.2017-2038D

[43] Ma, W., Li, S., Ma, S., Jia, L., Zhang, F., Zhang, Y., … Gao, G. F. (2016). Zika Virus Causes Testis Damage and Leads to Male Infertility in Mice. Cell, 1511–1524. http://doi.org/10.1016/j.cell.2016.11.016

[44] Pardi, N., Hogan, M. J., Pelc, R. S., Muramatsu, H., Andersen, H., DeMaso, C. R., … Weissman, D. (2017). Zika virus protection by a single low-dose nucleoside-modified mRNA vaccination. Nature, 543(7644), 248–251. http://doi.org/10.1038/nature21428

[45] Enfissi, A., Codrington, J., Roosblad, J., Kazanji, M., & Rousset, D. (2015). Zika virus genome from the Americas. The Lancet, (December 2013), 227–228. http://doi.org/10.1016/S0140-6736(16)00003-9

[46]. - Joglekar, A. V., & Sandoval, S. (2017). Pseudotyped Lentiviral Vectors: One Vector, Many Guises. *Human Gene Therapy Methods*, *28*(6), 291–301. https://doi.org/10.1089/hgtb.2017.084

[47] Burns, J. C., Friedmann, T., Driever, W., Burrascano, M., & Yee, J. K. (1993). Vesicular stomatitis virus G glycoprotein pseudotyped retroviral vectors: concentration to very high titer and efficient gene transfer into mammalian and nonmammalian cells. *Proceedings of the National Academy of Sciences*, *90*(17), 8033–8037. https://doi.org/10.1073/pnas.90.17.8033

[48] Finkelshtein, D., Werman, A., Novick, D., Barak, S., & Rubinstein, M. (2013). LDL receptor and its family members serve as the cellular receptors for vesicular stomatitis virus. *Proceedings of the National Academy of Sciences of the United States of America*, *110*(18), 7306–7311. https://doi.org/10.1073/pnas.1214441110

[49] Naldini, L., Blömer, U., Gallay, P., Ory, D., Mulligan, R., Gage, F. H., … Trono, D. (1996). In vivo gene delivery and stable transduction of nondividing cells by a lentiviral vector. *Science*, *272*(5259), 263–267. https://doi.org/10.1126/science.272.5259.263

[50] Tani, H., Morikawa, S., & Matsuura, Y. (2012). Development and Applications of VSV Vectors Based on Cell Tropism. Frontiers in Microbiology, 0(JAN), 272. https://doi.org/10.3389/FMICB.2011.00272

[51] Carroll, R., Lin, J. T., Dacquel, E. J., Mosca, J. D., Burke, D. S., & St Louis, D. C. (1994). A human immunodeficiency virus type 1 (HIV-1)-based retroviral vector system utilizing stable HIV-1 packaging cell lines. Journal of Virology, 68(9), 6047–6051. https://doi.org/10.1128/jvi.68.9.6047-6051.1994

[52] Whitt, M. A. (2010). Generation of VSV pseudotypes using recombinant ΔG-VSV for studies on virus entry, identification of entry inhibitors, and immune responses to vaccines. *Journal of Virological Methods*. https://doi.org/10.1016/j.jviromet.2010.08.006

[53].-Giroglou, T., Cinatl, J., Rabenau, H., Drosten, C., Schwalbe, H., Doerr, H. W., & von Laer, D. (2004). Retroviral Vectors Pseudotyped with Severe Acute Respiratory Syndrome Coronavirus S Protein. *Journal of Virology*, *78*(17), 9007–9015. https://doi.org/10.1128/jvi.78.17.9007-9015.2004

[54].- Hu, D., Zhang, J., Wang, H., Liu, S., Yu, L., Sun, L., & Qu, Y. (2014). Chikungunya virus glycoproteins pseudotype with lentiviral vectors and reveal a broad spectrum of cellular tropism. *PLoS ONE*, *9*(10), 1–5. https://doi.org/10.1371/journal.pone.0110893

[55]. Hu, H. P., Hsieh, S. C., King, C. C., & Wang, W. K. (2007). Characterization of retrovirus-based reporter viruses pseudotyped with the precursor membrane and envelope glycoproteins of four serotypes of dengue viruses. Virology, 368(2), 376–387. http://doi.org/10.1016/j.virol.2007.06.0

[56] Ho, M. R., Tsai, T. T., Chen, C. L., Jhan, M. K., Tsai, C. C., Lee, Y. C., Chen, C. H., & Lin, C. F. (2017). Blockade of dengue virus infection and viral cytotoxicity in neuronal

cells in vitro and in vivo by targeting endocytic pathways. Scientific Reports, 7(1), 1–11. https://doi.org/10.1038/s41598-017-07023-z

[-6] Chavali, P. L., Stojic, L., Meredith, L. W., Joseph, N., Nahorski, M. S., Sanford, T. J., Sweeney, T. R., Krishna, B. A., Hosmillo, M., Firth, A. E., Bayliss, R., Marcelis, C. L., Lindsay, S., Goodfellow, I., Woods, C. G., & Gergely, F. (2017). Neurodevelopmental protein Musashi-1 interacts with the Zika genome and promotes viral replication. *Science*, *357*(6346), 83–88. https://doi.org/10.1126/science.aam9243

[50] Yonezawa, A., Cavrois, M., & Greene, W. C. (2005). Studies of Ebola Virus Glycoprotein-Mediated Entry and Fusion by Using Pseudotyped Human Immunodeficiency Virus Type 1 Virions: Involvement of Cytoskeletal Proteins and Enhancement by Tumor Necrosis Factor Alpha. *Journal of Virology*, *79*(2), 918–926. https://doi.org/10.1128/jvi.79.2.918-926.2005

[51] Urbanowicz, R. A., McClure, C. P., Sakuntabhai, A., Sall, A. A., Kobinger, G., Müller, M. A., Holmes, E. C., Rey, F. A., Simon-Loriere, E., & Ball, J. K. (2016). Human Adaptation of Ebola Virus during the West African Outbreak. *Cell*, *167*(4), 1079-1087.e5. https://doi.org/10.1016/j.cell.2016.10.013

[52] Kobinger, G. P., Weiner, D. J., Yu, Q. C., & Wilson, J. M. (2001). Filovirus-pseudotyped lentiviral vector can efficiently and stably transduce airway epithelia in vivo. *Nature Biotechnology*, *19*(3), 225–230. https://doi.org/10.1038/85664

[53] Akkina, R. K., Walton, R. M., Chen, M. L., Li, Q. X., Planelles, V., & Chen, I. S. (1996). High-efficiency gene transfer into CD34+ cells with a human immunodeficiency virus type 1-based retroviral vector pseudotyped with vesicular stomatitis virus envelope glycoprotein G. *Journal of Virology*, *70*(4), 2581–2585. https://doi.org/10.1128/jvi.70.4.2581-2585.1996

[54] Chen, S. T., Iida, A., Guo, L., Friedmann, T., & Yee, J. K. (1996). Generation of packaging cell lines for pseudotyped retroviral vectors of the G protein of vesicular

stomatitis virus by using a modified tetracycline inducible system. *Proceedings of the National Academy of Sciences of the United States of America*, *93*(19), 10057–10062. https://doi.org/10.1073/pnas.93.19.10057

[55] Borok, Z., Harboe-Schmidt, J. E., Brody, S. L., You, Y., Zhou, B., Li, X., Cannon, P. M., Kim, K.-J., Crandall, E. D., & Kasahara, N. (2001). Vesicular Stomatitis Virus G-Pseudotyped Lentivirus Vectors Mediate Efficient Apical Transduction of Polarized Quiescent Primary Alveolar Epithelial Cells. *Journal of Virology*, *75*(23), 11747–11754. https://doi.org/10.1128/jvi.75.23.11747-11754.2001

[56] Pan, D., Gunther, R., Duan, W., Wendell, S., Kaemmerer, W., Kafri, T., Verma, I. M., & Whitley, C. B. (2002). Biodistribution and toxicity studies of VSVG-pseudotyped lentiviral vector after intravenous administration in mice with the observation of in vivo transduction of bone marrow. Molecular Therapy, 6(1), 19–29. https://doi.org/10.1006/mthe.2002.0630

[57] DePolo, N. J., Reed, J. D., Sheridan, P. L., Townsend, K., Sauter, S. L., Jolly, D. J., & Dubensky, T. W. (2000). VSV-G pseudotyped lentiviral vector particles produced in human cells are inactivated by human serum. *Molecular Therapy*, *2*(3), 218–222. https://doi.org/10.1006/mthe.2000.0116

[58] Saad, J. S., Miller, J., Tai, J., Kim, A., Ghanam, R. H., & Summers, M. F. (2006). Structural basis for targeting HIV-1 Gag proteins to the plasma membrane for virus assembly. *Proceedings of the National Academy of Sciences of the United States of America*, *103*(30), 11364–11369. https://doi.org/10.1073/pnas.0602818103

[59] Checkley, M. A., Luttge, B. G., & Freed, E. O. (2011). HIV-1 envelope glycoprotein biosynthesis, trafficking, and incorporation. In *Journal of Molecular Biology* (Vol. 410, Issue 4, pp. 582–608). Academic Press. https://doi.org/10.1016/j.jmb.2011.04.042

[60] Hallenberger, S., Bosch, V., Angliker, H., Shaw, E., Klenk, H. D., & Garten, W. (1992). Inhibition of furin-mediated cleavage activation of HIV-1 glycoprotein gpl60. Nature, 360(6402), 358–361. https://doi.org/10.1038/360358a0

[61] Ono, A., & Freed, E. O. (2001). Plasma membrane rafts play a critical role in HIV-1 assembly and release. Proceedings of the National Academy of Sciences of the United States of America, 98(24), 13925–13930. https://doi.org/10.1073/pnas.241320298

[62] Postler, T. S., & Desrosiers, R. C. (2013). The Tale of the Long Tail: the Cytoplasmic Domain of HIV-1 gp41. *Journal of Virology*, *87*(1), 2–15. https://doi.org/10.1128/jvi.02053-12

[63] Dorfman, T., Mammano, F., Haseltine, W. A., & Göttlinger, H. G. (1994). Role of the matrix protein in the virion association of the human immunodeficiency virus type 1 envelope glycoprotein. *Journal of Virology*, *68*(3), 1689–1696. https://doi.org/10.1128/jvi.68.3.1689-1696.1994

[64] Manrique, J. M., Celma, C. C. P., Hunter, E., Affranchino, J. L., & González, S. A. (2003). Positive and Negative Modulation of Virus Infectivity and Envelope Glycoprotein Incorporation into Virions by Amino Acid Substitutions at the N Terminus of the Simian Immunodeficiency Virus Matrix Protein. *Journal of Virology*, *77*(20), 10881–10888. https://doi.org/10.1128/jvi.77.20.10881-10888.2003

[65] Rao, Z., Belyaev, A. S., Fry, E., Roy, P., Jones, I. M., & Stuart, D. I. (1995). Crystal structure of SIV matrix antigen and implications for virus assembly. *Nature*, *378*(6558), 743–747. https://doi.org/10.1038/378743a0

[66] Mercier-Delarue, S., Durier, C., Verdière, N. C. de, Poveda, J.-D., Meiffrédy, V., Garcia, M. D. F., Lastère, S., Césaire, R., Manuggera, J.-C., Molina, J.-M., Amara, A., & Simon, F. (2017). Screening test for neutralizing antibodies against yellow fever virus, based on a flavivirus pseudotype. *PLoS ONE*, *12*(5). https://doi.org/10.1371/JOURNAL.PONE.0177882

[67] Matsuda, M., Yamanaka, A., Yato, K., Yoshii, K., Watashi, K., Aizaki, H., Konishi, E., Takasaki, T., Kato, T., Muramatsu, M., Wakita, T., & Suzuki, R. (2018). High-throughput neutralization assay for multiple flaviviruses based on single-round infectious particles using dengue virus type 1 reporter replicon. *Scientific Reports*, *8*(1). https://doi.org/10.1038/S41598-018-34865-Y

[68] Zibert, A., Maass, G., Strebel, K., Falk, M. M., & Beck, E. (1990). Infectious foot-and-mouth disease virus derived from a cloned full-length cDNA. Journal of Virology, 64(6), 2467–2473. http://www.ncbi.nlm.nih.gov/pubmed/2159523

[69] Almazán, F., González, J. M., Pénzes, Z., Izeta, A., Calvo, E., Plana-Durán, J., & Enjuanes, L. (2000). Engineering the largest RNA virus genome as an infectious bacterial artificial chromosome. *Proceedings of the National Academy of Sciences of the United States of America*, *97*(10), 5516–5521. https://doi.org/10.1073/pnas.97.10.5516

[70] Mishin, V. P., Cominelli, F., & Yamshchikov, V. F. (2001). A “minimal” approach in design of flavivirus infectious DNA. *Virus Research*, *81*(1–2), 113–123. https://doi.org/10.1016/S0168-1702(01)00371-9

[71] Pu, S.-Y., Wu, R.-H., Yang, C.-C., Jao, T.-M., Tsai, M.-H., Wang, J.-C., Lin, H.-M., Chao, Y.-S., & Yueh, A. (2011). Successful Propagation of Flavivirus Infectious cDNAs by a Novel Method To Reduce the Cryptic Bacterial Promoter Activity of Virus Genomes. Journal of Virology, 85(6), 2927–2941. https://doi.org/10.1128/jvi.01986-10

[72] Li, D., Aaskov, J., & Lott, W. B. (2011). Identification of a Cryptic Prokaryotic Promoter within the cDNA Encoding the 5′ End of Dengue Virus RNA Genome. *PLoS ONE*, *6*(3), e18197. https://doi.org/10.1371/journal.pone.0018197

[73] Atieh, T., El Ayoubi, M. D., Aubry, F., Priet, S., De Lamballerie, X., & Nougairède, A. (2018). Haiku: New paradigm for the reverse genetics of emerging RNA viruses. PLoS ONE, 13(2), 1–10. https://doi.org/10.1371/journal.pone.0193069

[74] Aubry, F., Nougairède, A., de Fabritus, L., Querat, G., Gould, E. A., & de Lamballerie, X. (2014). Single-stranded positive-sense RNA viruses generated in days using infectious subgenomic amplicons. Journal of General Virology, 95(Pt 11), 2462–2467. https://doi.org/10.1099/vir.0.068023-0

[75] Setoh, Y. X., Prow, N. A., Peng, N., Hugo, L. E., Devine, G., Hazlewood, J. E., Suhrbier, A., & Khromykh, A. A. (2017). De Novo Generation and Characterization of New

Zika Virus Isolate Using Sequence Data from a Microcephaly Case. *MSphere*, *2*(3), e00190-17. https://doi.org/10.1128/mspheredirect.00190-17

[76] NPS@: Network Protein Sequence Analysis TIBS 2000 March Vol. 25, No 3 [291]:147-150 Combet C., Blanchet C., Geourjon C. and Deléage G.

[77] Zanluca, C., De Melo, V. C. A., Mosimann, A. L. P., Dos Santos, G. I. V., dos Santos, C. N. D., & Luz, K. (2015). First report of autochthonous transmission of Zika virus in Brazil. *Memorias Do Instituto Oswaldo Cruz*, *110*(4), 569–572. https://doi.org/10.1590/0074-02760150192

[78] Dick G. (1952). Zika isolation and serological specificity. *Trans Royal Soc Trop Med Hyg*, *46*(5), 509–520.

[79] Olson, J. G., Ksiazek, T. G., Suhandiman, G., & Triwibowo, V. (1981). Zika virus, a cause of fever in central java, indonesia. *Transactions of the Royal Society of Tropical Medicine and Hygiene*, *75*(3), 389–393. https://doi.org/10.1016/0035-9203(81)90100-0

[80] Heang, V., Yasuda, C. Y., Sovann, L., Haddow, A. D., da Rosa, A. P. T., Tesh, R. B., & Kasper, M. R. (2012). Zika virus infection, Cambodia, 2010. Emerging Infectious Diseases, 18(2), 349–351. https://doi.org/10.3201/eid1802.111224

[81] Duffy, M. R., Chen, T.-H., Hancock, W. T., Powers, A. M., Kool, J. L., Lanciotti, R. S., Pretrick, M., Marfel, M., Holzbauer, S., Dubray, C., Guillaumot, L., Griggs, A., Bel, M., Lambert, A. J., Laven, J., Kosoy, O., Panella, A., Biggerstaff, B. J., Fischer, M., & Hayes, E. B. (2009). Zika Virus Outbreak on Yap Island, Federated States of Micronesia. New England Journal of Medicine, 360(24), 2536–2543. https://doi.org/10.1056/nejmoa0805715

[82] Beaver, J. T., Lelutiu, N., Habib, R., & Skountzou, I. (2018). Evolution of two major Zika virus lineages: Implications for pathology, immune response, and vaccine

development. Frontiers in Immunology, 9(JUL). https://doi.org/10.3389/fimmu.2018.01640

[83] Delatorre, E., Fernández, J., & Bello, G. (2018). Investigating the role of easter island in migration of Zika virus from south pacific to Americas. In Emerging Infectious Diseases (Vol. 24, Issue 11, pp. 2119–2121). Centers for Disease Control and Prevention (CDC). https://doi.org/10.3201/eid2411.180586

[84] Pettersson, J. H. O., Eldholm, V., Seligman, S. J., Lundkvist, Å., Falconar, A. K., Gaunt, M. W., Musso, D., Nougairède, A., Charrel, R., Gould, E. A., & de Lamballerie, X. (2018). Erratum for Pettersson et al., "How Did Zika Virus Emerge in the Pacific Islands and Latin America?" MBio, 9(2), 1–6. https://doi.org/10.1128/mBio.00386-18

[85] Faria, N. R., Do Socorro Da Silva Azevedo, R., Kraemer, M. U. G., Souza, R., Cunha, M. S., Hill, S. C., Thézé, J., Bonsall, M. B., Bowden, T. A., Rissanen, I., Rocco, I. M., Nogueira, J. S., Maeda, A. Y., Da Silva Vasami, F. G., De Lima Macedo, F. L., Suzuki, A., Rodrigues, S. G., Cruz, A. C. R., Nunes, B. T., … Vasconcelos, P. F. C. (2016). Zika virus in the Americas: Early epidemiological and genetic findings. Science, 352(6283), 345–349. https://doi.org/10.1126/science.aaf5036

[86] Yuan, L., Huang, X. Y., Liu, Z. Y., Zhang, F., Zhu, X. L., Yu, J. Y., Ji, X., Xu, Y. P., Li, G., Li, C., Wang, H. J., Deng, Y. Q., Wu, M., Cheng, M. L., Ye, Q., Xie, D. Y., Li, X. F., Wang, X., Shi, W., … Qin, C. F. (2017). A single mutation in the prM protein of Zika virus contributes to fetal microcephaly. Science, 358(6365), 933–936. https://doi.org/10.1126/science.aam7120

[87] Li, G., Bos, S., Tsetsarkin, K. A., Pletnev, A. G., Desprès, P., Gadea, G., & Zhao, R. Y. (2019). The roles of prM-E proteins in historical and epidemic zika virus-mediated infection and neurocytotoxicity. Viruses, 11(2). https://doi.org/10.3390/v11020157

[88] Liu, L., Fang, Q., Deng, F., Wang, H., Yi, C. E., Ba, L., Yu, W., Lin, R. D., Li, T., Hu, Z., Ho, D. D., Zhang, L., & Chen, Z. (2007). Natural Mutations in the Receptor Binding Domain of Spike Glycoprotein Determine the Reactivity of Cross-Neutralization between Palm Civet Coronavirus and Severe Acute Respiratory Syndrome Coronavirus. Journal of Virology, 81(9), 4694–4700. https://doi.org/10.1128/jvi.02389-06

[89] Hulswit, R. J. G., de Haan, C. A. M., & Bosch, B. J. (2016). Coronavirus Spike Protein and Tropism Changes. In Advances in Virus Research (Vol. 96, pp. 29–57). https://doi.org/10.1016/bs.aivir.2016.08.004

[90] Yang, Y., Du, L., Liu, C., Wang, L., Ma, C., Tang, J., Baric, R. S., Jiang, S., & Li, F. (2014). Receptor usage and cell entry of bat coronavirus HKU4 provide insight into bat-to-human transmission of MERS coronavirus. Proceedings of the National Academy of Sciences of the United States of America, 111(34), 12516–12521. https://doi.org/10.1073/pnas.1405889111

[91] Chan, V., Dreolini, L., Flintoff, K.A., Lloyd, S.J., & Mattenley, A.A. (2002). The Effect of Increasing Plasmid Size on Transformation Efficiency in Escherichia coli.

[92] Richard, A. S., Shim, B. S., Kwon, Y. C., Zhang, R., Otsuka, Y., Schmitt, K., Berri, F., Diamond, M. S., & Choe, H. (2017). AXL-dependent infection of human fetal endothelial cells distinguishes Zika virus from other pathogenic flaviviruses. *Proceedings of the National Academy of Sciences of the United States of America*, *114*(8), 2024–2029. https://doi.org/10.1073/pnas.1620558114

[93] Nobrega, G. M., Samogim, A. P., Parise, P. L., Venceslau, E. M., Guida, J. P. S., Japecanga, R. R., Amorim, M. R., Toledo-Teixeira, D. A., Forato, J., Consonni, S. R., Costa, M. L., Proenca-Modena, J. L., Amaral, E., Besteti Pires Mayer-Milanez, H. M., Ribeiro-do-Valle, C. C., Calil, R., Bennini Junior, J. R., Lajos, G. J., Altemani, A., … Muraro, S. P. (2020). TAM and TIM receptors mRNA expression in Zika virus infected

placentas. *Placenta*, *101*(September), 204–207. https://doi.org/10.1016/j.placenta.2020.09.062

[94] Mangor, J. T., Monsma, S. A., Johnson, M. C., & Blissard, G. W. (2001). A GP64-Null Baculovirus Pseudotyped with Vesicular Stomatitis Virus G Protein. *Journal of Virology*, *75*(6), 2544–2556. https://doi.org/10.1128/jvi.75.6.2544-2556.2001

[95] Hou, W., Cruz-cosme, R., Armstrong, N., Obwolo, L. A., Wen, F., Hu, W., Luo, M. H., & Tang, Q. (2017). Molecular cloning and characterization of the genes encoding the proteins of Zika virus. *Gene*, *628*, 117–128. https://doi.org/10.1016/j.gene.2017.07.049

[96] Cortese, M., Goellner, S., Acosta, E. G., Neufeldt, C. J., Oleksiuk, O., Lampe, M., Haselmann, U., Funaya, C., Schieber, N., Ronchi, P., Schorb, M., Pruunsild, P., Schwab, Y., Chatel-Chaix, L., Ruggieri, A., & Bartenschlager, R. (2017). Ultrastructural Characterization of Zika Virus Replication Factories. *Cell Reports*, *18*(9), 2113–2123. https://doi.org/10.1016/j.celrep.2017.02.014

[97] Royle, J., Ramírez-Santana, C., Akpunarlieva, S., Donald, C. L., Gestuveo, R. J., Anaya, J. M., Merits, A., Burchmore, R., Kohl, A., & Varjak, M. (2020). Glucose-regulated protein 78 interacts with zika virus envelope protein and contributes to a productive infection. *Viruses*, *12*(5). https://doi.org/10.3390/v12050524

[98] Himmelsbach, K., & Hildt, E. (2018). Identification of various cell culture models for the study of Zika virus. *World Journal of Virology*, *7*(1), 10–20. https://doi.org/10.5501/wjv.v7.i1.10

[99] Tan, T. Y., Fibriansah, G., Kostyuchenko, V. A., Ng, T. S., Lim, X. X., Zhang, S., Lim, X. N., Wang, J., Shi, J., Morais, M. C., Corti, D., & Lok, S. M. (2020). Capsid protein structure in Zika virus reveals the flavivirus assembly process. *Nature Communications*, *11*(1), 1–13. https://doi.org/10.1038/s41467-020-14647-9

[110] Stocks, C. E., & Lobigs, M. (1998). Signal Peptidase Cleavage at the Flavivirus C-prM Junction: Dependence on the Viral NS2B-3 Protease for Efficient Processing Requires Determinants in C, the Signal Peptide, and prM. *Journal of Virology*, *72*(3), 2141–2149. https://doi.org/10.1128/jvi.72.3.2141-2149.1998

[101] Amberg, S. M., Nestorowicz, A., McCourt, D. W., & Rice, C. M. (1994). NS2B-3 proteinase-mediated processing in the yellow fever virus structural region: in vitro and in vivo studies. *Journal of Virology*, *68*(6), 3794–3802. https://doi.org/10.1128/jvi.68.6.3794-3802.1994

[102] Guo, N., & Peng, Z. (2013). MG132, a proteasome inhibitor, induces apoptosis in tumor cells. In *Asia-Pacific Journal of Clinical Oncology* (Vol. 9, Issue 1, pp. 6–11). John Wiley & Sons, Ltd. https://doi.org/10.1111/j.1743-7563.2012.01535.x

[103] Meiners, S., Laule, M., Rother, W., Guenther, C., Prauka, I., Muschick, P., Baumann, G., Kloetzel, P. M., & Stangl, K. (2002). Ubiquitin-proteasome pathway as a new target for the prevention of restenosis. *Circulation*, *105*(4), 483–489. https://doi.org/10.1161/hc0402.102951

[104] Han, Y. H., & Park, W. H. (2010). MG132 as a proteasome inhibitor induces cell growth inhibition and cell death in A549 lung cancer cells via influencing reactive oxygen species and GSH level. *Human and Experimental Toxicology*, *29*(7), 607–614. https://doi.org/10.1177/0960327109358733

[105] Carpentier, E., Paris, S., Kamen, A. A., & Durocher, Y. (2007). Limiting factors governing protein expression following polyethylenimine-mediated gene transfer in HEK293-EBNA1 cells. *Journal of Biotechnology*, *128*(2), 268–280. https://doi.org/10.1016/j.jbiotec.2006.10.014

[106] Kretschmer, M., Kadlubowska, P., Hoffmann, D., Schwalbe, B., Auerswald, H., & Schreiber, M. (2020). Zikavirus prme envelope pseudotyped human immunodeficiency

virus type-1 as a novel tool for glioblastoma-directed virotherapy. *Cancers*, *12*(4). https://doi.org/10.3390/cancers12041000

[107] Siridechadilok, B., Gomutsukhavadee, M., Sawaengpol, T., Sangiambut, S., Puttikhunt, C., Chin-inmanu, K., Suriyaphol, P., Malasit, P., Screaton, G., & Mongkolsapaya, J. (2013). A Simplified Positive-Sense-RNA Virus Construction Approach That Enhances Analysis Throughput. *Journal of Virology*, *87*(23), 12667–12674. https://doi.org/10.1128/jvi.02261-13

[108] Bredenbeek, P. J., Kooi, E. A., Lindenbach, B., Huijkman, N., Rice, C. M., & Spaan, W. J. M. (2003). A stable full-length yellow fever virus cDNA clone and the role of conserved RNA elements in flavivirus replication. *Journal of General Virology*, *84*(5), 1261–1268. https://doi.org/10.1099/vir.0.18860-0

[109] Mishin, V. P., Cominelli, F., & Yamshchikov, V. F. (2001). A “minimal” approach in design of flavivirus infectious DNA. *Virus Research*, *81*(1–2), 113–123. https://doi.org/10.1016/S0168-1702(01)00371-9

[110] Caldas, L. A., Azevedo, R. C., da Silva, J. L., & de Souza, W. (2020). Microscopy analysis of Zika virus morphogenesis in mammalian cells. *Scientific Reports*, *10*(1), 1–11. https://doi.org/10.1038/s41598-020-65409-y

[111] Ali, S. M., Vega-Rúa, A., Driouich, J. S., De Lamballerie, X., Failloux, A. B., & Nougairède, A. (2018). Comparison of chikungunya viruses generated using infectious clone or the infectious subgenomic amplicons (isa) method in aedes mosquitoes. *PLoS ONE*, *13*(6). https://doi.org/10.1371/journal.pone.0199494

[112] Edmonds, J., van Grinsven, E., Prow, N., Bosco-Lauth, A., Brault, A. C., Bowen, R. A., Hall, R. A., & Khromykh, A. A. (2013). A Novel Bacterium-Free Method for Generation of Flavivirus Infectious DNA by Circular Polymerase Extension Reaction Allows Accurate

Recapitulation of Viral Heterogeneity. *Journal of Virology*, *87*(4), 2367–2372. https://doi.org/10.1128/jvi.03162-12

[113] Tamura, T., Fukuhara, T., Uchida, T., Ono, C., Mori, H., Sato, A., Fauzyah, Y., Okamoto, T., Kurosu, T., Setoh, Y. X., Imamura, M., Tautz, N., Sakoda, Y., Khromykh, A. A., Chayama, K., & Matsuura, Y. (2017). Characterization of Recombinant Flaviviridae Viruses Possessing a Small Reporter Tag. *Journal of Virology*, *92*(2). https://doi.org/10.1128/jvi.01582-17

[114] Piyasena, T. B. H., Newton, N. D., Hobson-Peters, J., Vet, L. J., Setoh, Y. X., Bielefeldt-Ohmann, H., Khromykh, A. A., & Hall, R. A. (2019). Chimeric viruses of the insect-specific flavivirus Palm Creek with structural proteins of vertebrate-infecting flaviviruses identify barriers to replication of insect-specific flaviviruses in vertebrate cells. *The Journal of General Virology*, *100*(11), 1580–1586. https://doi.org/10.1099/jgv.0.001326